893/30-8-2
ltr dtd 6/28/

MASTER

PRE-TEST PREDICTIONS OF LLTR SERIES II, SWR A2 TEST RESULTS

TABLE OF CONTENTS

TABLE OF CONTENTS (con't)

LIST OF ILLUSTRATIONS

AC03-76SF00700

I. INTRODUCTION

A series of experiments (Series II) will be run in the Large Leak Test Rig (LLTR) at the Energy Technology Engineering Center (ETEC) to study the transient effects of a Sodium-Water Reaction (SWR) in a steam generator of an LMFBR. One of the prime purposes of the experimental program is the further verification of the analytical accuracy of the SWR design codes, RELAP and TRANSWRAP. The first test of this Series consists of two parts, SWR-A1a and A1b which are scheduled to be run in mid 1979. Pre-test predictions of the expected results of the first experiments have been given in References 1 and 2. This report focuses on the second test of Series II, SWR-A2, and gives the expected time response of the various LLTR pressure and velocity sensors to the simulated SWR. This report gives the RELAP and TRANSWRAP pre-test predictions of the expected results of the SWR-A2 test based on the system configuration and test procedures as presently planned.

II. BACKGROUND

One of the objectives of the LLTR program is the verification of analytical methods for the prediction of large leak transient events. A prime tool presently available for such analyses is the TRANSWRAP II code. Extensive development effort has been directed at TRANSWRAP to check the operational status and sensitivity of its various modelling options (References 3 and 4). TRANSWRAP has also been applied to the analysis of several sodium steam generation systems including CRBRP. These system analyses have been performed with very conservative modelling assumptions to insure a safe design in the face of somewhat limited knowledge of large leak phenomena. Among these assumptions have been:

1. A complete, instantaneous, double ended guillotine break of a single tube.

2. Complete instantaneous reaction of all injected water to evolve the maximum possible amount of hydrogen gas.

3. No heat transfer from the reaction bubble to the surrounding piping.

The pre-test analyses of the LLTR Series I and II tests have the following general goals:

1. To produce a realistic prediction of the test results before the test is run and before experimental feedback is available for analytical refinement.

2. To provide a basis for the removal of some of the conservatism used in previous design analysis efforts and produce a more realistic prediction of large leak effects.

Pre- and post-test analysis of the LLTR Series I tests are reported in References 5, 6 and 7.

Pre-test predictions of Series II tests SWR-A1a and A1b are given in References 1 and 2. This report presents the pre-test predictions for Series II test SWR-A2. Post-test analysis will be performed after the tests are completed.

III. SUMMARY

The Series II SWR-A2 pre-test predictions were made using the basic methodology developed from the evaluations of Series I tests with the objective of matching the test results. Because of conservatisms inherent in this methodology, it is anticipated that the experimental results will generally be somewhat lower than these pre-test predictions of system pressures and velocities. The principal exceptions anticipated are the relief system pressure spikes, during the period the rupture discs are collapsing, which may be higher then predicted by the analysis. This difference results from the absence of a realistic rupture disc model in TRANSWRAP.

The significant results of this analysis are:

1. The pressure sent into the system following tube rupture, modified by flow cross-sectional area changes and reinforced by reflections from the system boundaries, was high enough to burst the rupture disc at approximately 10.8 milliseconds.

2. The sodium slug arrived at the reaction products separation tank (RPST) at approximately 500 milliseconds, with completion of relief system blow-down occuring at about 1150 milliseconds.

3. Pressures and velocities appear within the ranges of the Series I test results.

The pressure and velocity time traces at all sensor locations are found on Figures 15-L through 46-S of this report.

IV. FACILITY DESCRIPTION

The LLTR consists of a test article having representative steam generator geometry and those systems required to prepare for, conduct, and recover from large sodium-water reaction tests. These systems are the sodium system, the water/steam injection system, the reaction relief system, and the instrumentation and control system. Each is briefly described in the following sections.

A. Sodium System

The main sodium system piping is fabricated from 304 stainless steel. The system is designed for normal operation between 600°F and 900°F. The upper sodium line (Figure 1) is 10 in. Schedule 80 pipe and has a total length of approximately 40 ft. An upper header is 18 in. Schedule 100 pipe and is approximately 25 ft. in length. Nozzles to the rupture disc attachment flanges are 18 in. diameter. The system includes provisions for sodium filling from a 10,000 gal. surge tank, and for rapid sodium drain to the Reaction Products Tank (RPT) through a 2 1/4 Cr-1Mo, 8 in. drain line and valve. The drain valve is pneumatically operated and is automatically opened shortly after a large leak event to facilitate drainage of residual sodium and reaction products while still fluid.

The principal sodium system instrumentation consists of thermocouples for measurement of temperature, fast-response pressure transducers (Figure 1), a low-level pressure transducer to provide an accurate measure of initial sodium pressure, strain gages, and three drag-disc flowmeters (located in the relief lines and designated as sensors F506, F511, and F510 on Figure 1) to provide information to determine sodium ejection velocities and bubble growth at the rupture site. Spark plug type flow meters (sensors F508A to F508H on Figure 1) provide information to calculate the location and velocity of the fluid slug in the relief line.

B. Water Injection System

The water injection system (Figure 2) consists of water supply tanks and piping to and from the test article, the Large Leak Injection Device (LLID) which is used to induce tube rupture, and a downstream flow control valve and

condenser tank which can be used to initiate and control pretest water flow-rate. The main water supply tanks, the interconnecting piping, and the LLID are electrically heated to condition water temperatures and pressures to required test levels. Piping and components are fabricated of 2-1/4 Cr-1Mo material and are designed for operating temperatures between 550°F and 925°F.

The water injection system contains pressure and temperature instrumentation similar to that described for the sodium systems. In addition, it contains a number of flowmeters of several types and sizes to permit accurate determinations of water flow both before (low flow) and after (high flow) tube rupture. The feedwater inlet line contains both high- and low-rate flowmeters of the volumetric type (turbine meters); the steam outlet line contains one high-rate volumetric meter and a drag disc meter.

The system contains two 25 ft^3 water supply tanks: Tank T-1 provides feedwater to the normal water inlet at the bottom of the LLTV and Tank T-2 supplies the upper section of the primary rupture tube after failure. Tank T-2 also serves as a reservoir for water leaving the primary rupture tube during flow initiation prior to rupture. The water tanks are designed for a maximum operating pressure of 2050 psia and are protected by rupture discs.

The LLID (Reference 8) is a piston-cylinder device (Figure 3). It is used to apply an axial load that causes separation of the notched rupture tube to which it is attached. The cylindrical part of the mechanism is rigidly attached to the shell of the LLTV via a series of mounting flanges; the piston rod extension is welded directly to the rupture tube. A bellows seal between the fixed mechanism and the piston rod maintains the integrity of the sodium boundary during the piston stroke. The piston rod is tubular and serves an an extension of the rupture tube. Water flows through the rod in the normal flow direction prior to rupture. After rupture, the water/steam mixture reverses direction and supplies the upper segment of the rupture tube from the second water supply tank (T-2). The lower segment of the tube continues to receive feedwater flow from its normal supply (T-1). This arrangement facilitates realization of prototypic water-side conditions at the leaksite. This constitutes a significant improvement over leak injection devices used in other large leak test programs (References 9 and 10). The LLID is pressurized with

nitrogen gas to initiate tube rupture. Gas pressures between 1600 and 1800 psig (which yield forces of 7000 to 8000 lb) will be utilized for the LLTV installation to assure proper activation. A crushable structure is included at the top of the cylinder to absorb the kinetic energy of the piston rod and attached tube segment after rupture occurs. Pressure and displacement information from the LLID are monitored.

C. Reaction Relief System

The reaction relief system (Figure 1) starts at the two 18 in. reverse buckling rupture discs, which protect the sodium system, and consists of the downstream piping, a large reaction products tank to which the sodium and reaction products are relieved after a SWR event, and a stack, with igniter, for the safe elimination of hydrogen evolved during the SWR. A blind flange will replace the upper rupture disc (Figure 1) during Series II Test SWR-A2. Thus, the only relief path during this test will be through the lower rupture disc (Figure 1). The relief system line is approximately 53 ft. in length and is 16 inches in diameter. A particulate collection tank which communicates directly with the stack is used during tests to obtain samples from which evaluations can be made of the separation efficiency of the RPT. Before each test, the reaction relief system is maintained under inert gas (nitrogen), utilizing a low-pressure rupture disc in the stack to prevent air in-leakage. The stack is equipped with a hinged safety cover which is closed to effect reasonable system isolation after a SWR test has caused rupture of the stack disc. A small nitrogen purge is maintained in the system prior to test (flowing through a bypass around the rupture disc) and a larger purge is initiated after the test to sweep out hydrogen and minimize air in-leakage.

The relief system in the LLTR is thoroughly instrumented. Spark plug detectors (sensors F508A to F508H on Figure 1) are located in the piping downstream of the rupture discs to monitor sodium velocities and bubble growth. Piping wall temperatures are monitored, as are inlet and outlet pressures. Contact-type sensors are provided downstream of each rupture disc to determine the timing of disc actuation. High-speed motion picture cameras record the movement of targets mounted on the piping. Motion pictures also are obtained on stack effluents following tube rupture. Temperature and pressure measurements are obtained in the RPT and stack, and the system is monitored continuously for oxygen and hydrogen concentrations.

The RPT is a large, carbon steel tank with a 304 SS liner. The tank is 9 ft. in diameter, has an overall length of 26.5 ft., and has an internal volume of 1700 ft^3. The inlet nozzle from the relief system header has an internal diameter of 14.3 in. and is located to provide tangential entry. The exhaust gas stack nozzle at the top of the tank has an internal diameter of 17.0 in. Exhaust gases are released directly from the stack with no additional provision for particulate separation. The downwind ground deposition rates and airborne particulate levels were very low during the Series I tests.

D. Instrumentation and Control System

The LLTR instrumentation subsystem provides the necessary capabilities for acquiring, displaying, and recording all of the process and test variables required to set up, conduct, and interpret the results of a SWR test. This subsystem includes sensors, signal conditioning, and conventional display and recording equipment, a 144-channel programmable digital data acquisition system (DDAS) and seven 14-channel FM tape recorders. The DDAS is used to record, and in some cases to perform on-line processing of data from test variables which are not subject to the extreme transients of the SWR. All major transient information is recorded on FM tapes which are digitized after the test to produce data at 10,000 samples/s. An accurate time basis (IRIG A) is recorded on one channel of each tape recorder to assure precise interpretation of time relationships.

The control subsystem provides for all normal process controls (e.g., preheating, filling, pressurization) and also for automatic control of all test related functions which must be accomplished in precise order and within short periods of time. These latter activities are handled by an automatic sequencer which initiates the required operations at preselected times, with a time resolution of 100 microseconds.

V. ANALYTICAL MODELS

The approach applied to the pre-test analysis of Series II SWR-A2 pressures and velocities is similar to that employed in the analysis of the Series I tests (Reference 7). The RELAP code (RELAP/MOD5, Reference 11) was used to predict the water injection flowrate histories using water system geometry and initial condition input data from the test request (Reference 12) and ETEC drawings, numbers DS051E-B01-PG016 through DS051E-B01-PG029, numbers DS051E-B01-PG101, DH051E-B01-PI009 and PN07433006 (Rev. D). An assumed back pressure downstream of the break was also input into RELAP. The computed flow histories were then input as boundary conditions, along with sodium and relief system geometry from the above ETEC drawings, into the TRANSWRAP Code, which calculated sodium system pressure and velocity data. The ideal code modelling technique for the analysis would be to couple the RELAP and TRANSWRAP Codes through the TRANSWRAP calculated back pressure. However, except for very early times (within about 1 1/2 ms) and for long term (after about 3 or 4 seconds), the RELAP calculated flow is choked and analysis indicates that, for the SWR-A2 Test, imposition of the TRANSWRAP calculated source pressure as the RELAP back pressure would not result in sub-sonic flow. Hence, the assumption of RELAP/TRANSWRAP code decoupling is valid.

A desription of these two codes, along with pertinent descriptions of the various code input data, follows:

A) RELAP Code Model

The RELAP code was chosen to model the water-side transients primarily because of availability and widespread use in Light Water Reactor (LWR) safety analysis involving dynamic water flow problems. The RELAP code is a computer program written in FORTRAN IV for the digital computer analysis of nuclear reactors and related systems. It is primarily applied in the study of system transient response to postulated perturbations such as coolant loop rupture, circulation pump failure and power excursions. Additional versatility extends its usefulness to related applications, such as containment analyses or general two-phase flow analyses. RELAP can be used to model system fluid conditions including flow, pressure, mass inventory, fluid quality, and heat transfer. A subroutine provides water property tables. Component thermal conditions and energy

transfers are modeled. The system being modeled is subdivided into discrete volumes which, with interconnecting junctions (flow paths), are treated as one dimensional homogeneous elements. RELAP solves an integral form of fluid conservation and state equations for each user-defined volume and generates a time history of system conditions. Data are recorded for fluid volume, component heat, and juncture flow characteristics.

The water injection histories for SWR-A2 were computed with two RELAP models specific to that test. Each model represented the segment of the injection circuit from either Tank T1 or Tank T2 (Figure 2) to the leak site. Each RELAP model consisted of the maximum possible number (75) of control volumes with relatively coarse noding upstream and relatively fine noding downstream of the controlling resistances. The tube opening history as computed with the NONSAP computer code (Reference 20) was included as a time-dependent boundary condition in each RELAP model.

The RELAP models for SWR-A2 are depicted in Figures 4 and 5. Code volumes 1 through 24 (Figure 4) represent the segment of the injection circuit from tank T1 to just upstream of the 0.141 inch diameter, square-edged orifice which was located in the three-quarter inch diameter line at the connection with the LLTV prototypic tube.

Volumes 25 through 74 represent the prototypic tube from the area change to the leaksite at the mid-zone of the LLTV. This results in a control volume length of 4 in. across the span of prototypic tube. In all the RELAP models of the LLTR tests, Volume 75 represents the gas bubble at the leak site. Initial conditions incorporated in the T1 side of the SWR-A2 model were:

1. Pressure of 1700 psia throughout.

2. Temperature of 580°F (32°F subcooled) uniform throughout corresponding to the specified test condition.

3. Zero flow rate throughout the tube (any pre-break setup flow rate is negligible).

Boundary conditions incorporated in the model were:

1. Pressure in Tank T1 constant at 1700 psia.

2. Leaksite pressure history in Volume 75 rising to 370 psi at 2.5 msec then falling to 80 psia. The RELAP calculated flow was found to be choked, thus independent of the back pressure until the back pressure rises to approximately 700 psi which is well above TRANSWRAP calculated source pressures.

3. A tube break opening time of 1.6 msec.

4. A break discharge coefficient, based on results of the Series I tests (Reference 7), of 0.6 was used.

5. Heat transfer from the surrounding sodium and structure to the water injection circuit was ignored since it had a negligible effect on computed water injection flow and quality histories.

Figure 5 represents the RELAP model of the Tank T2 side of the SWR-A2 water injection circuit. Volumes 1 through 18 represent the segment from Tank T2 to the point inside the LLID at which prototypic tube dimensions apply (upper end of piston rod). Volumes 19 through 74 represent the prototypic tube run to the leak site, again at the mid-plane of the LLTV. This results in a control volume length of 4.3 in. across the span of prototypic tube. The initial conditions (system pressures, temperatures, flows, discharge coefficient, etc.) were identical to those described above for the Tank T1 side of the break.

The system pressure drops associated with pipe friction are internally calculated by RELAP, with appropriate models for such effects as laminar flow, two-phase flow, etc. Form loss coefficients for such things as system valves, orifices, cross-sectional area changes, etc. are input to the code. The input values were taken from standard sources (Reference 13) and implicitly assumed that the form loss coefficient for the fitting was applicable to both sonic and sub-sonic flow conditions. The coefficients were based on sub-sonic flow.

In actuality, pressure losses are expected to be higher at sonic conditions, resulting in anticipated lower discharge flows and corresponding lower SWR related sodium pressures in the SWR-A2 tests. The form loss coefficients actually used in the analyses are noted at the junctions shown on Figures 4 and 5.

The two RELAP cases (one each for the Tank T1 and Tank T2 side of the break) were then run separately (since the assumption is made that the results were independent of the other under the definition of a DEG tube break). The resultant calculated mass flowrates were then combined and input, as a time varying boundary condition, into the TRANSWRAP code.

B) TRANSWRAP Code Model

The basic TRANSWRAP model (Figure 7) is similar to that used in a previous analysis of Series I data, accounting for the differences in the test rig. Referring to Figures 1 and 7, pipes 1 through 5 and 7 through 12 in the TRANSWRAP model represent the sodium-side of the LLTV. Pipe 13 represents the flow path from the centerline of the LLTV upper windows through the upper nozzle to the area change in the upper sodium line. Pipes 14 through 18 represent the upper sodium line to the upper header. The upper header is represented by pipes 19, 20, 22, and 23. Pipe 21 represents the short run of pipe between the upper header and the upper rupture disc. Pipes 24 and 25 represent the line connecting the upper header to the expansion tank while the expansion tank is modeled as pipe 26. Pipe 27 represents the flow path from the centerline of the LLTV lower window through the lower nozzle to the reducing fitting. Pipes 28 through 31 represent both the lower sodium tee to the standpipe and the standpipe itself. Pipes 46 through 58 represent the lower relief line. Pipe 6 represents the drain line from the lower end of the LLTV to the closed drain valve, while pipes 32 through 34 reflect the 4 inch drain line leading from the standpipe to the freeze seal. Velocity head loss coefficients were specified at appropriate points in the model to account for the resistances of the various elbows, tees, and reducers throughout the system. Sonic velocities for each pipe were computed as a function of sodium temperature, pipe dimensions and pipe properties assuming clean, gas-free sodium. The rupture disc in the model and the test rig has a static burst pressure of 325 psid.

The Series II SWR-A2 test contains two working rupture discs in series near the bottom of the standpipe, as shown in Figure 1. However, TRANSWRAP does not have the capability to calculate the effects of multiple rupture disc assemblies in series in a loop. In fact, the actual TRANSWRAP rupture disc model does not calculate details of the dynamics of even a single disc rupturing. The TRANSWRAP model treats a line as being either closed when the line pressure is below an input value, or open, when the line pressure is higher. A second option, based on the results of the Analysis Support Tests Rupture Disc tests (Reference 17) allows the pressure derivative at the disc to delay the opening of the disc. That is, the static burst pressure of the disc is made a function of the pressure derivative, delaying the opening of the disc for high derivative values. Note that this second option does not treat the dynamics of the disc; it only approximates one characteristic of the disc behavior. This second option was used in the present Series II SWR-A2 analysis, although this quasi dynamic model produced little change in system pressures over those calculated with the simplified model.

The relief system model in TRANSWRAP assumes a well defined slug of fluid in the relief system. Series I results indicate that the leading interface of the relief system slug is not well defined but rather is composed of a liquid-spray mixture. As such, the actual velocities to be measured in SWR-A2 are expected to be higher than predicted here, due to lower fluid densities at the same mass flowrate (provided the system pressures are about the same).

Finally, it should be noted that the single rupture disc model in TRANSWRAP should overpredict the experimental velocities for a double disc relief system (system energy is needed to break the second disc), as suggested by the SRI test results (Reference 19). Thus, measured velocities would tend to be lower than velocities predicted by TRANSWRAP, partially off-setting the expected higher velocities in SWR-A2, due to anticipated spray flow, described above. Overall, however, the measured fluid velocities are expected to be higher than predicted by TRANSWRAP and presented in this report, due to the expected predominance of the spray flow phenomenon effect.

Other initial conditions, input assumptions and boundary conditions used during the TRANSWRAP analysis include:

1. Initial sodium pressure and temperature of 115 psia and 590°F.

2. Zero sodium initial mass flowrate.

3. Water injection mass flowrate as calculated by the RELAP code.

4. Adiabatic conditions in the reaction bubble.

5. Quasi-static rupture disc model (as discussed in a later section of this report).

6. Standard flow discharge coefficients as obtained from standard sources (Reference 13).

7. 65% hydrogen conversion efficiency.

8. Bubble temperatures of 1700°F.

VI. RELAP CODE RESULTS

The RELAP Code results for the Tank T1 side of the tube rupture are given on Figures 8 to 10 (break mass flowrate, fluid quality just upstream of the break, and mass flowrate at flow meter F501). The corresponding time histories on the Tank T2 side of the break are shown on Figures 11 to 13 (flowmeter F503 in the water loop). A composite flow history (the sum of Figures 8 and 11) is shown on Figure 14 and used as input to the TRANSWRAP analysis of the event. A discussion of several aspects of the RELAP analysis is in order.

A) Tank T1 Side of the Tube

Figure 8 shows that, following the rupture of the tube, the mass flowrate out through the break rises rapidly (within about 1.5 msec) to a peak value of about 3.4 #/sec, then drops to a relatively constant value of about 2.7 #/sec. RELAP output indicates that this flow became choked before 1.25 msec. The flow choking model used in RELAP was the Henry-Fauske/Homogeneous Equilibrium Model, described in Reference 11, as recommended in Reference 18. The flow remained choked during the RELAP run and calculations determined that the flow should remain choked well past 1 sec. of the transient.

Figure 10 shows the flow at the flowmeter F501. The flow is seen to oscillate with a frequency of about 50 Hz and a maximum amplitude of about 1.9 #/sec. around a mean of about 1.0 #/sec. The total system length excluding the prototypic tube is about 50 ft. At a sonic velocity of 5000 ft/sec, the calculated wavelength of the flowrate oscillations is about 100 ft. or twice the system length, as expected.

The flowrate entering the tube averages about 1 #/sec; the flowrate leaving the tube average about 2.7 #/sec. This imbalance is accounted for by the fact that, initially, the tube was filled with sub-cooled water at a temperature of 580°F and a pressure of 1700 psi. Shortly following the tube break, the pressure within the tube falls to about 1200 psi. At this pressure, saturation conditions are met and the water in the tube begins to flash to steam. The resultant fluid quality time history is shown on Figure 9.

At a tube pressure of about 1200 psi, the choked flow model assumed in the RELAP analysis yields a mass flowrate of approximately 2.7 #/sec (Figure 8). The flow out of the break was the only choked flow predicted by RELAP. The flow through the .141 inch orifice was sub-sonic. The fluid pressure upstream of this orifice was essentially constant near the initial pressure of 1700 psi. The pressure drop across the orifice was thus (1700 psi - 1200 psi) or 500 psi. Use of the standard pressure drop formula of Darcy yields a flow of about 1 #/sec for these conditions. The flow imbalance of (2.7 #/sec - 1.0 #/sec) or 1.7 #/sec will continue, provided the thermodynamic conditions described above continue.

The above described conditions will hold until either the Tank T1 depressurizes, thereby reducing the pressure of 1700 psi in Volumes 1 to 24, or the fluid in the tube completely vaporizes (that is, the fluid quality reaches 100% and the tube fluid becomes superheated). The Series II test request indicates that Tank T1 contains approximately 1000 # of water prior to the initiation of the event. At a mass flowrate out of Tank T1 of 1 #/sec, the pressure in the pipe should not be reduced appreciably in a time of 1 sec. It will be shown in a discussion of the TRANSWRAP results that 1 sec is needed for a complete analysis of the SWR-A2 tests.

For the thermodynamic conditions described above, the fluid quality should reach 100% well after 1 second of the transient. As the fluid quality increases, the flow from the break should decrease, thereby reducing the mass flowrate imbalance described above and also lengthening the time necessary to de-pressurize the tube. A lower exit mass flowrate in the test will also lead to lower reaction zone pressures in the latter stages of the test than those calculated by TRANSWRAP.

It is concluded that the RELAP analysis is stable from about 10 msec to well beyond one second and the flowrate calculated by RELAP at 0.1 seconds can be used through 1 second of the transient.

B) Tank T2 Side of the Tube

In contrast to the two distinct thermodynamic regions found on the Tank T1 side of the break (separated by the 0.141 inch orifice), the Tank T2 side of

the break is a more distributed system. That is, the Tank T2 side does not contain a major orifice restricting the flow. The total pressure drop of this side, however, is just slightly less than the Tank T1 side (the system length is roughly three times that of the tank T1 side and contained more fittings, thereby providing additional pressure drop terms that approach that of the .141 orifice). Consequently, the flow from the T2 side of the break is only slightly higher (about 3 #/sec from Figure 11) than the flow from the Tank T1 side of the break (2.7 #/sec from Figure 8).

The flow at sensor location F503 (Figure 13) shows the characteristics of all upstream-of-tube locations. It rises, with characteristic acoustical oscillations, to a value near the break flow. Thus, the flow into the tube balances the flow out of the tube. This is contrasted to the Tank T1 side flow where a 1.7 #/sec flow imbalance existed. The result is that the pressure distribution from Tank T2 to just upstream of the break is approximately linear with distance but with small local perturbations at junction area changes. The tank T2 side of the break will remain in this relatively stable condition as Tank T2 depressurizes. In time, however, Tank T2 will be depressurized to the point where flow into the tube becomes less than the choked flow out of the tube. From this time, the quality of the fluid in the tube should start to increase, maintaining choked flow at the tube exit. At this point in time the conditions in the T2 system will be phenomenologically similar to the Tank T1 system described above, although at a lower system pressure. Thus, the relatively constant flowrate shown on Figure 11 should hold for several seconds, even longer than the expected static condition time frame discussed above for the Tank T1 system, and well beyond the required 1 sec of transient time required for the TRANSWRAP analysis.

Note that the oscillations present on Figure 11 from 90 msec to 100 msec are believed to represent a mathematical instability as seen on previous RELAP analyses (Reference 7) and discussed in Reference 18.

VII. TRANSWRAP CODE RESULTS

The mass flowrates calculated on both sides of the tube break (Tank T1 side and Tank T2 side) are shown on Figures 8 and 11. The sum of these two curves is shown on Figure 14. This water flowrate is used as the basis for the input to the TRANSWRAP Code. TRANSWRAP calculated the resultant LLTR sodium and relief systems pressures and velocities. Curves of these parameters are shown on Figures 15-L through 46-L. Each parameter is shown on two figures, labeled for example, as Figures 15-L and 15-S. The -L designated curves show a total transient time of 1000 msec. The -S figures show the first 100 msec of each -L designated curve. A discussion of several aspects of these figures in in order.

A) Input Mass Flowrate

A comparison of Series I test results with analytical predictions (Reference 7) indicates that agreement between the two could be obtained by assuming a 65% hydrogen conversion efficiency and a reaction zone temperature of 1700°F. The analysis presented in this report was performed assuming these same conditions. Code use methodology developed from the Series I results was used to implement these assumptions by reducing the RELAP calculated mass flowrate (Figure 14) prior to the use of the flowrate as input into TRANSWRAP.

Consistent with the Series I analysis (Reference 7), the mass flowrate input into TRANSWRAP is held constant at the value obtained from RELAP at 100 msec. This is indicated by the dashed portion on the flowrate curve (Figure 14) at a value of 6.1 #/sec. In actuality, examination of Figures 8 to 13 indicate that the flowrate will probably increase slightly, then peak and start decreasing well before the 1000 msec time frame of the analysis. The flowrate will peak when the flow on the Tank T2 side of the break peaks. This will occur when the fluid quality at the break reaches a minimum, which appears to be occurring at the end of the RELAP analysis (Figures 9 and 12).

RELAP analysis indicated that the flow became choked within the first 1.25 msec of the event and remained choked at the end of the RELAP cases (100 msec). It has been shown previously that this constant flow/choked flow condition will hold at least for the first second of the transient (and

probably significantly longer). Slightly more than one second is needed, as will be shown later, for the trailing edge/bubble interface of the fluid slug entering the relief system to enter the Reaction Product Separation Tank (RPST) in the LLTR. At that time a significant depressurization occurs in the system. This system depressurization during test SWR-A2 is a positive indication that the relief system has cleared.

Since the break flow is still choked at this time, the flowrate upstream of the break will show no change since, for choked flow conditions, the mass flowrate at the leaksite is independent of the back pressure. No significant change in the upstream flowrate (flow meters F501 and F503 on Figure 2) will confirm that choked flow conditions were present in the tests.

B) Rupture Disc Behavior

As described previously, two rupture disc models are available in TRANSWRAP. The first instantaneously opens the disc when the pressure at the disc exceeds an input static burst pressure. The second model again instantaneously opens the disc when the pressure reaches a value that is higher than the input value. The excess burst pressure is determined by the rupture disc diameter, thickness, and composition, and the time derivative of pressure at the disc. The model increases (delays) the time at which the TRANSWRAP disc bursts for the SWR-A2 tests. The pre-test predictions given in this report are based on this quasi-static rupture disc model which generally predicts higher system pressures (especially near the rupture disc) than predicted by the input static burst pressure model.

The pressure at the disc (Figure 30-S) exhibits a double peak around the time that the disc breaks. Both peaks exceed the rated static burst pressure of the disc (which, for the LLTR back pressure of 15 psia, is 340 psia). However, the time history of the first peak of the disc pressure was such that the calculated disc pressure was not sufficient to burst the disc using the quasi-static disc in TRANSWRAP. The second pressure spike did cause the disc to burst at a time of 10.8 msec. This curve shows the major difference between the TRANSWRAP quasi-static rupture disc and the static rupture disc models, in that the static model would have burst the disc the first time that the pressure exceeded 340 psia (that is, at a time of about 6 msec).

Previous Series I test results (Reference 7) indicate that the actual dynamics of the bursting of the disc are significantly more complicated than assumed by the TRANSWRAP analysis. In particular, apparent disc opening times in the range of 40 to 50 msec were observed in the Series I tests, compared with a 7 msec delay calculated by the quasi-static TRANSWRAP disc model and the instantaneous disc opening assumed in the TRANSWRAP static disc simulation. Relief afforded by the bursting of the disc is thus transmitted into the system at 10.8 msec by TRANSWRAP, compared with a possible time near 50 msec, as observed in the Series I tests. Consequently, the actual pressures in the Series II, SWR-A2, test may be higher than predicted by TRANSWRAP, especially near the disc, in the 10 to 50 msec time range. However, the time at initiation of first disc buckling (as measured by the disc knife contact sensor) is expected to be fairly close to the disc burst time of 10.8 msec predicted by TRANSWRAP, with the possibility that a contact signal might occur as early as 6 msec.

C) System Pressures

The TRANSWRAP calculated system pressures are shown on Figures 15-L to 33-S. As explained previously, a figure designation of -S indicates the "short" time scale portion (100 msec) of the previous -L ("long") figure, which presented the 1000 msec transient. In those cases where the parameter did not change significantly in the first 100 msec, no -S curve is given.

The ETEC designations for the various pressure sensors (as well as the flow sensors) are shown for reference on the figures. Reference to Figures 1 and 7 will show the physical location of the sensors.

Figures 15-L and 15-S give the calculated source pressure at the break. Examination of Figure 15-S shows an initial acoustic spike of about 360 psi, a drop in pressure to about 130 psi, a rise to about 425 psi, then an exponential type decay to a value of about 80 psi. The initial 360 psi spike is not expected in the tests; it is due solely to the method of initializing the reaction zone model in TRANSWRAP. The method results in an effective step input of the water mass flowrate into the reaction zone, instead of a linear increase in the flowrate, during the first 0.9 msec of the transient. This initial spike is seen at other loop locations (Figures 16-S, 24-S, 25-S, 26-S,

and 27-S) and should be ignored. Additional analysis that artificially removed this initialization problem resulted in no significant changes to the TRANSWRAP calculated pressures and velocities, other than the removal of the initial pressure spike shown on the above figures.

The source pressure rises from its minimum of 125 psi at about 1 msec until 15 msec, when the pressure peaks at 430 psi. Prior to 15 msec, the source pressure rises since the relief afforded by the bursting of the disc at 10.8 msec cannot be transmitted back to the reaction zone, thereby offsetting the rise in pressure due to the sodium-water reaction. After 15 msec, the system relief due to bursting of the disc has been transmitted back to the reaction zone, hence the decrease in the reaction zone pressure. The acoustical transport time between the reaction zone and the disc is about 3 msec.

Figures 16-L through 22-S show the typical behavior of the pressure sensors on the expansion tank side of the break (including the upper part of the LLTV and the upper sodium line). Pressure pulses (both compression and rarefaction pulse) are "ringing" throughout this part of the system. It is known that TRANSWRAP generally underpredicts the damping mechanisms found in a system. It is therefore probable that the actual measured pressure traces will follow the given figures until the actual system damping forces dissipate the energy of the fluid. The measured pressures should then exhibit typical damped behavior, contrasting with the slightly damped traces shown on these figures.

Figure 23-L shows that the expansion (Surge) tank pressure rises about 1/2 psi during the first quarter second of the transient, then falls about 10 psi during the remainder of the event.

Figures 24-L through 27-S and 30-L through 31-L again show the typical "ringing" behavior of the system pressures caused by the relatively undamped reflections of the acoustical spike throughout the system, in this case, from the bubble interface to the leading edge of the relief slug. However, at different times, these curves show an abrupt transition to a smooth curve. This transition occurs when the bubble interface reaches the sensor location, at which time, TRANSWRAP sets the sensor pressure equal to the bubble pressure. This occurs at about 100 msec for location P-618, 180 msec for locations P-619 and PT-A-11, 500 msec for location P519, 550 msec for location P525, and 600 msec

for location P526. Locations P-522 and the RPST inlet do not show this effect since the fluid slug did not clear these locations until about 1200 ms which is slightly beyond the time frame of this analysis. Locations P520 and P521 (located within the system standpipe), also do not show the transition to the bubble pressure since sodium remained in the standpipe for the duration of the transient.

Figures 31-L to 33-L also give an indication of the time required for the relief slug to reach different parts of the relief system. The pressures at these locations remain constant at 15 psi until the relief slug reaches the sensor locations, at which time TRANSWRAP begins to calculate the pressures. From these curves, the analysis indicates that the slug reaches locations P526, P522, and the RPST inlet at about 50 msec, 450 msec and 550 msec.

Finally note (from Figures 15-L and 23-L) that, until about 60 msec, the pressure differential from the break to the surge tank tends to promote positively defined velocity (that is, fluid flow into the tank). After 60 msec, the flow should reverse and flow toward the break. Examination of the velocity, Figures 34-L through 36-S, shows that this change from positive to negative velocity actually occurs near 200 msec. This time difference reflects the time constant needed to establish bulk flow in the system.

D) System Velocities

Figures 34-L through 46-L present the system fluid velocities calculated by TRANSWRAP. The velocities on the surge tank side of the break typically show a value of less than 6 ft/sec (maximum), with the flow oscillating with high frequency cycles in response to the acoustical pressure pulses "ringing" in the system as described above. These surge tank side flows (Figures 34-L to 36-S) are slightly attenuated, positive on average for the first 200 msec of the transient, then on the whole negative for the duration of the event. The negative velocity is in response to the reversing of the source pressure to surge tank pressure differential described previously. The actual expected flow traces in the LLTR should fall within the envelope defined by the extremes of the velocity curves shown.

The fluid velocities are significantly different on the relief system side of the break. Here, peak velocities typically reach 50 ft/sec to 100 ft/sec (depending on the diameter of the pipe). As with the previously discussed system pressures, the behavior of the velocity curves indicate the timing sequence of the relief system slug. Until the slug reaches the sensor location, the fluid velocity is zero. The velocity then becomes positive until the slug clears the sensor location, at which time, TRANSWRAP stops calculating the velocity at that location and sets the velocity equal to the last calculated value from that time onward. For example, in the relief system at location F508A (Figure 39-L), the fluid slug reaches the sensor at about 30 msec and clears the location at about 600 msec. The fluid slug in this pipe travels at about 80 ft/sec, is about 46 ft long and contains, at a pipe diameter of 1.31 ft, about 62 ft^3 of sodium. Arrows along the time axis on each Figure from 37-L to 46-L shows the time at which the slug reaches, then leaves the sensor location.

Figure 33-L indicates that the relief slug reaches the RPST at about 550 msec. From this time until the trailing edge of the relief system slug enters the RPST, the amount of fluid remaining in the slug continually decreases. For a given driving pressure, this means that the slug should be accelerating. Close examinations of Figures 44-L through 46-L shows this fluid acceleration.

Although TRANSWRAP has the capability to calculate the system blowdown when the relief slug completely enters the RPST, the current analysis was unable to proceed to that point. Examination of the TRANSWRAP output at the end of the analysis indicates that the bubble interface above the reaction zone (in TRANSWRAP pipe #1, Figure 7) was within 1-1/4 inches of the reaction zone. TRANSWRAP cannot calculate the movement of the bubble interface past the reaction zone, hence the computer run terminated at about 950 msec. However, analysis of Figures 33-L and 45-L, can indicate the approximate time of the expected LLTR blowdown.

Figure 33-L again indicates that the front interface of the relief system slug enters the RPST at about 550 msec. The trailing edge of the relief system slug was located at flow sensor location F508G at about .94 seconds (Figure 45-L). Flow sensor F508G is located about 20 ft. from the RPST. At an assumed constant velocity of 85 ft/sec (from Figure 45-L), the trailing edge

of the relief system slug should reach the RPST at about .94 sec + (20 ft/85 ft/sec) = 1.18 seconds. In actuality, the fluid slug is expected to be accelerating during this time period (as described previously), the fluid velocity is expected to be higher than 85 ft/sec and the blowdown time is expected to be less than 1.18 sec.

E) Relief System Behavior

It should be pointed out that TRANSWRAP calculates a well defined fluid slug in the relief system. The Series I tests (Reference 7) as well as the Stanford Research Institute Tests (Reference 19) indicate that at least the leading edge of the slug is probably a spray flow front traveling at a higher velocity than would be indicated if the front were all liquid.

It is therefore expected that spray flow will be present in the actual SWR-A2 tests. In anticipation of this spray flow phenomenon, the spark plug sensors and associated electronics were significantly modified in an attempt to differentiate between spray and all liquid flow. In addition, drag discs are also installed in the relief line to help resolve the composition of the relief system flow.

In conclusion, minimal system attenuation in TRANSWRAP, a single, simple rupture disc model in TRANSWRAP, and spray flow in the relief lines of the test will produce different pressures and velocities in the test than those predicted by this TRANSWRAP. However, use of the relief line drag disc flow measuring devices and the improved spark plug detector electronics may compensate for the spray flow effect. On average, however, the velocities and pressures presented in this report are expected to be slightly higher than will be found in the tests, except at locations near the rupture disc, where measured pressures should be somewhat higher.

REFERENCES

1. Memorandum, C. F. Wolfe to John O. Bradfute, "Preliminary Pre-Test Predictions of LLTR, Series II SWR A1a and A1b Test Results," YL-611-80077, September 28, 1978.

2. Memorandum, C. F. Wolfe to John O. Bradfute, "Revision of the Preliminary Pre-Test Predictions of LLTR Series II, SWR A1a and A1b Test Results," YL-611-80090, dated November 28, 1978.

3. 598SDM-76-70, S. D. McClelland, "TRANSWRAP II Parametric Study."

4. 598BSY/LSL-76-78, B. Yang, L. Lee, "Parametric Study on Water Injection Subprogram of the Interim Code, TRANSWRAP II."

5. J. C. Amos, S. D. McClelland and J. J. Regimbal, "Interim Evaluation of Sodium-Water Reaction Test No. 1 Data and Comparison with TRANWRAP Analyses - Series 1 Large Leak Test Program," GEFR-00027 (1).

6. J. J. Regimbal, J. O. Bradfute, L. S. Lee, S. D. McClelland, J. C. Amos, "Interim Evaluation of Sodium-Water Reaction Test No. 2 Data and Comparison with TRANSWRAP Analyses - Series I Large Leak Test Program," GEFR-00309, April 1978.

7. J. O. Sane, J. J. Regimbal and P. C. Brown, "Evaluation of the Sodium-Water Reaction Tests No. 1 through 6 Data and Comparison with TRANSWRAP Analyses, Series I Large Leak Test Program," GEFR-00420.

8. C. R. Davidson, "LLID Development Final Report," AI Document No. N037TR330-002, January 13, 1976.

9. J. A. Bray, et. al., "Sodium-Water Reaction Experiments on Model P.F.R. Heat Exchanger - The Noah Rig Tests," TRG-Report 1519, UKEA, 1967.

10. K. Dumm, et. al., "Experimental and Theoretical Investigations on Safety of the SWR-Straight Tube Design Steam Generator with Sodium-Water Reactions," ERDA-TR-27, Vol. 1, April 24, 1972.

11. "RELAP4/MOD5 A Computer Program for Transient Thermal-Hydraulic Analysis of Nuclear Reactors and Related Systems," prepared by Aerojet Nuclear Company for the U.S. Nuclear Regulatory Commission and Energy Research and Development Administration under Contract E (10-1)-1375, ANCR-NEREG-1335, September, 1976.

12. Test Specification, "LLTR Series II Test Request," Spec. No. 23A2062.

13. I. E. Idelchik, "Handbook of Hydraulic Resistance - Coefficients of Local Resistance and of Friction," Translated from Russian by the Israel Program for Scientific Translations for the U.S. Atomic Energy Commission, AEC-TR-6630, 1966.

14. Streeter, V. L. and Wylie, E. B., Hydraulic Transients, Mc-Graw Hill, 1967.

15. Atomics International Supporting Document Number TI-001-130-025, "TRANSWRAP - A Compressible Hydrodynamic Code for Large-Leak Sodium/Water Reaction Analysis," February 5, 1973.

16. R. C. Yang, "Safeguard BMD System Theoretical Formulation of the Hydraulic Transient Problem and Comparison of Hytran Computer Results with Experimental Data," Ralph M. Parsons Company, No.SAF-77, January 26, 1977.

17. YL-598-50080, TRANSWRAP Rupture Disc Dynamic Buckling Model, derived from AST Data, D. Knight, August 16, 1976.

18. Report, K. R. Katsma and G. E. Koester, "LLTR Simulation Review," Energy Incorporated, Idaho Falls, Idaho, No. EI-78-29,.September 1978.

19. Report, D. W. Ploeger, "Simulation Experiments for a Large Leak Sodium Water Reaction Analysis, Vol. 4: IHTS/Relief System Simulation Tests," SRI Report for the General Electric Company, Sunnyvale, California, Project 6272, 1978.

20. K. Bathe, E. L. Wilson and R. H. Iding, "NONSAP, A Structural Analysis Program for Static and Dynamic Response of Nonlinear Systems," Structural Engineering Laboratory, University of California, Report No. UC SESM 74-3, February 1974.

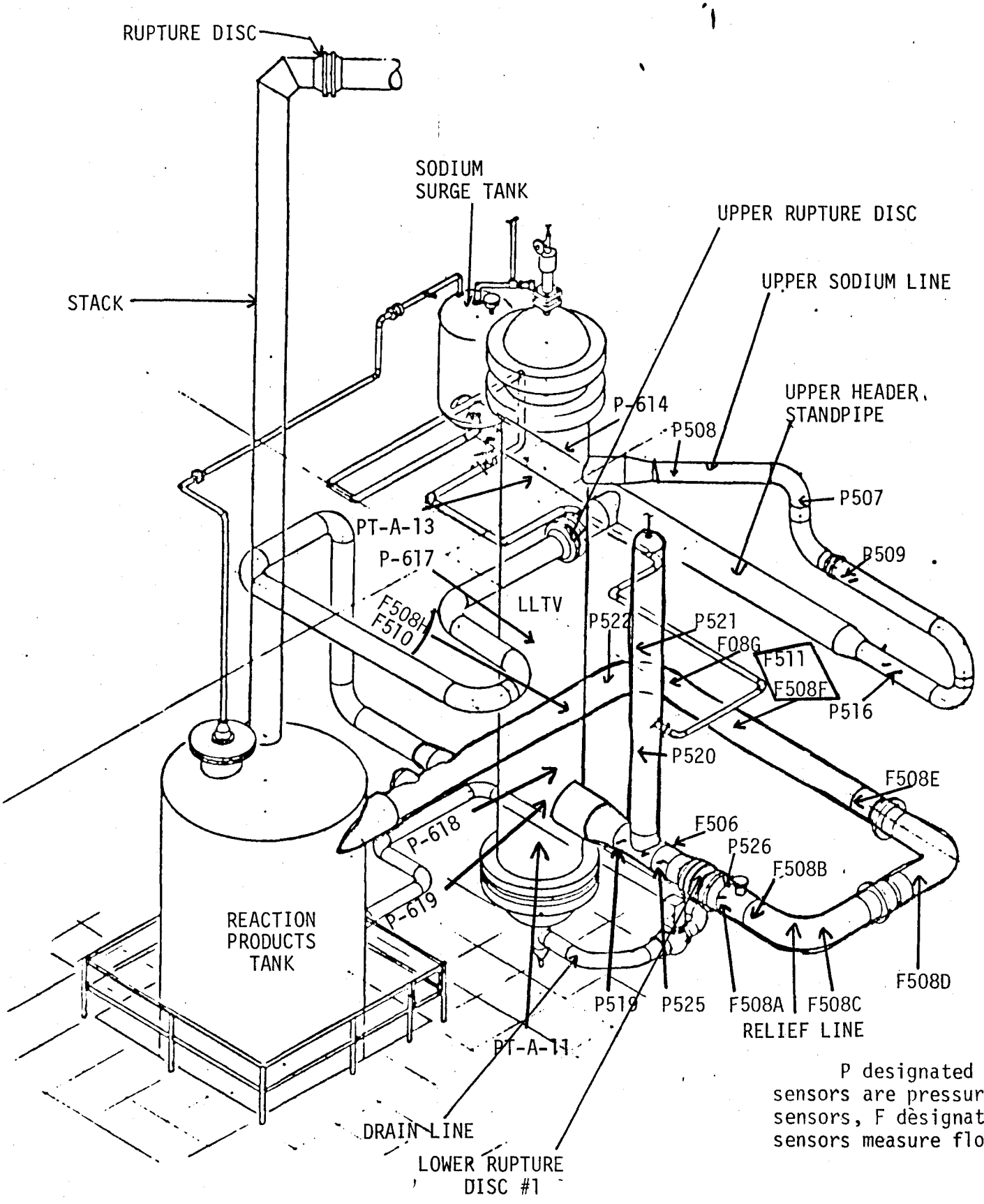

FIGURE 1

LLTR Sodium and Relief Systems

Flow and Pressure Sensor Locations

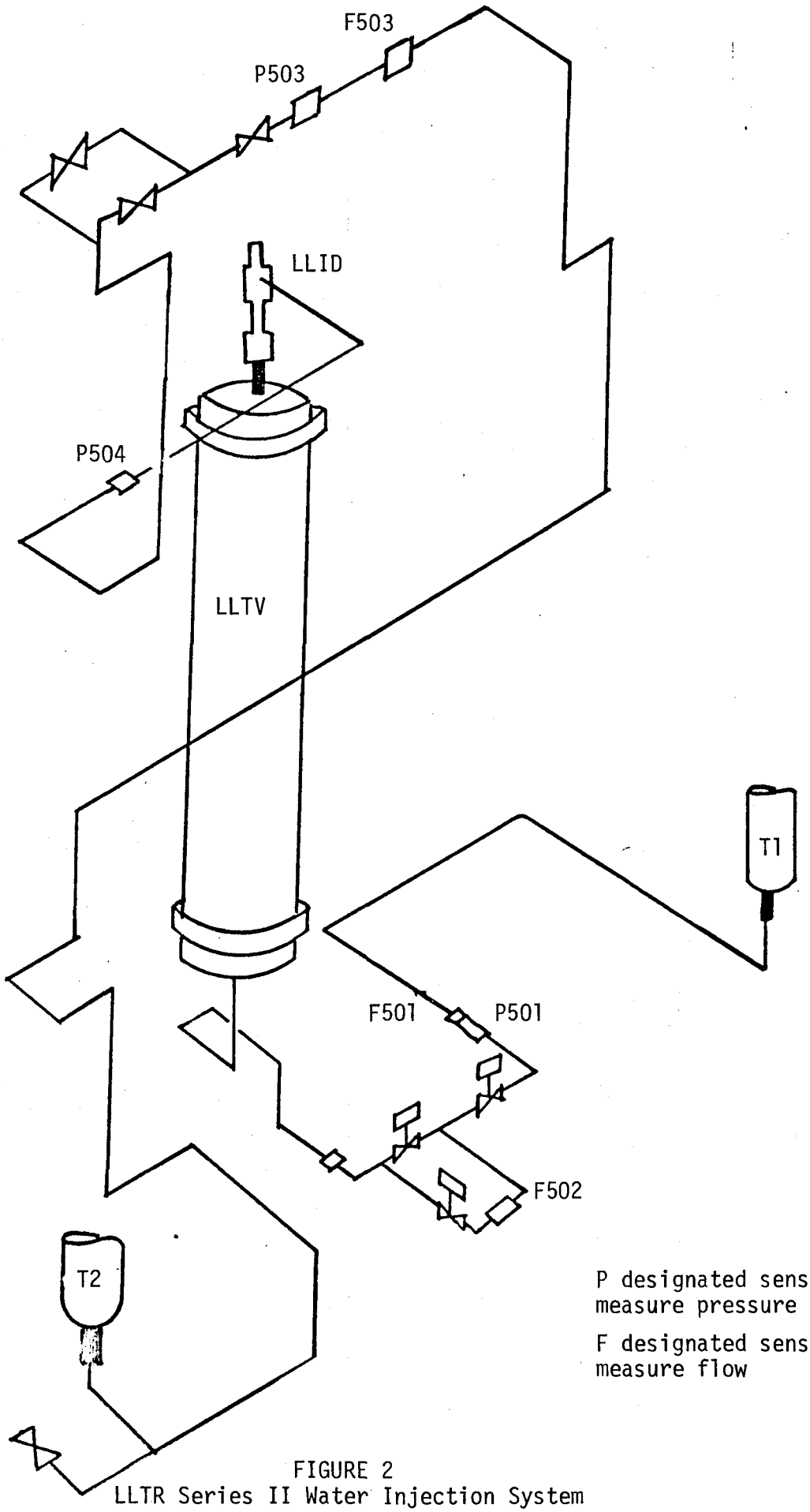

FIGURE 2
LLTR Series II Water Injection System

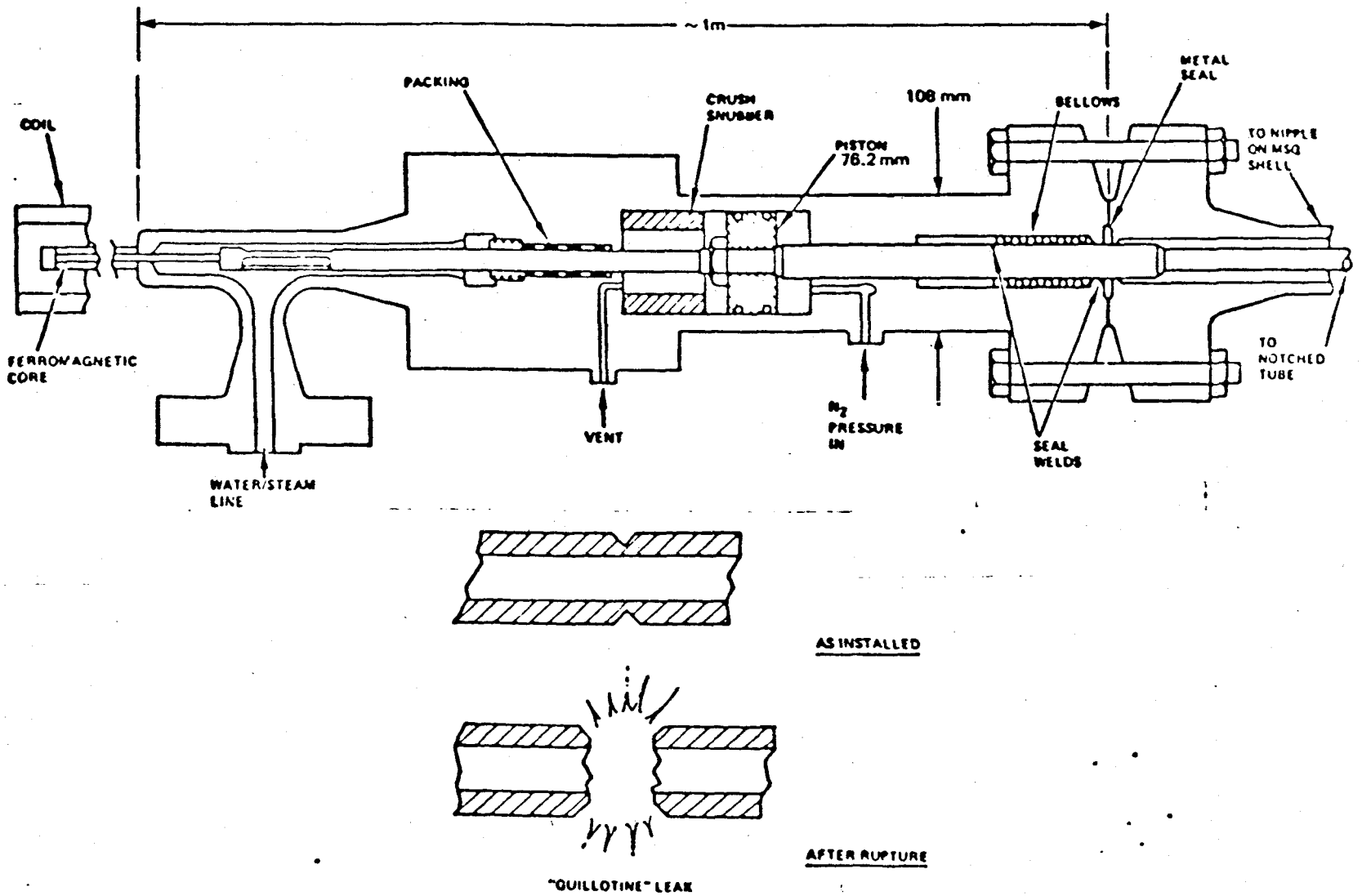

FIGURE 3

Large Leak Injection Device (LLID)

COMPUTATION/RECORD SHEET

Prepared By: JAF	GENERAL ELECTRIC COMPANY	Page No:
Checked By:	Advanced Reactor Systems Department	
Date: 2-14-79	TITLE RELAP MODEL SCHEMATIC	

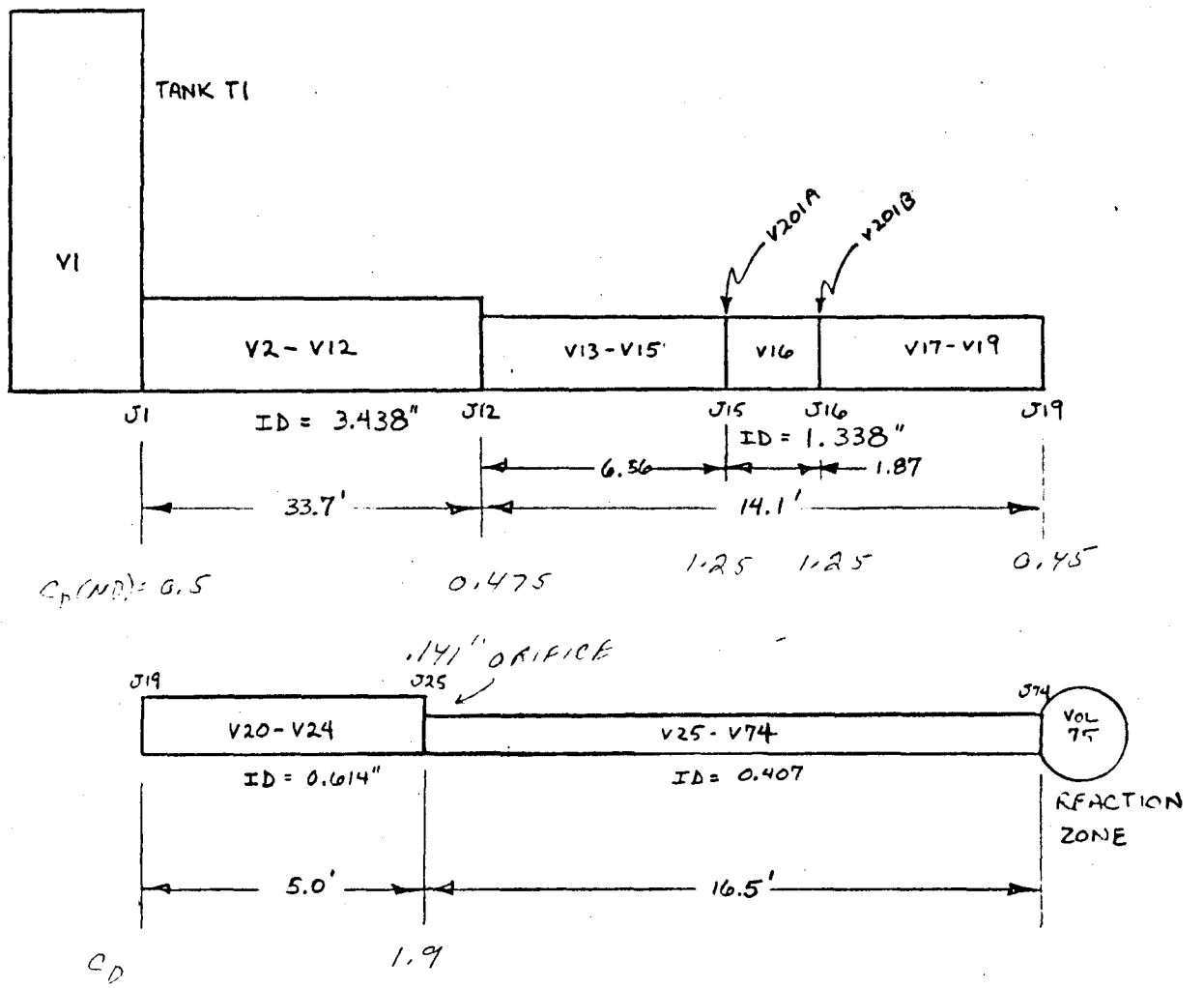

FIGURE 4
RELAP MODEL SCHEMATIC
LLTR Series II - Test A2
Tank T1 Side

COMPUTATION/RECORD SHEET

Prepared By: CFW	GENERAL ELECTRIC COMPANY	Page No:
Checked By:	Advanced Reactor Systems Department	
Date: 5/10/79	TITLE RELAP MODEL SCHEMATIC	

Relap Model Schematic
LLTR Series II, Test A2, Tank T2 Side

FIGURE 5

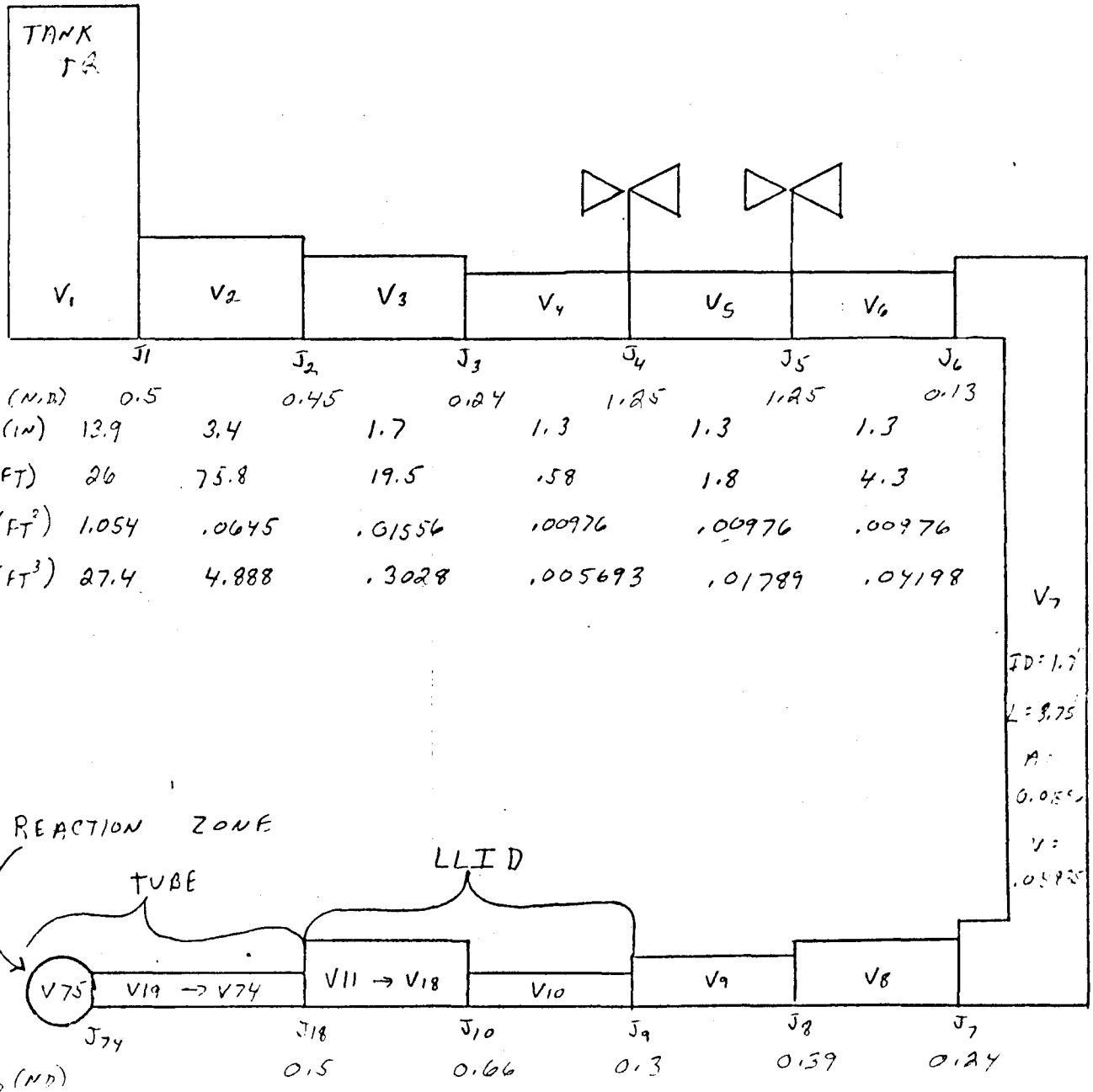

C_D (N,D)	0.5	0.45	0.24	1.25	1.25	0.13
ID(IN)	13.9	3.4	1.7	1.3	1.3	1.3
L(FT)	26	75.8	19.5	.58	1.8	4.3
A(FT^2)	1.054	.0645	.01556	.00976	.00976	.00976
V(FT^3)	27.4	4.888	.3028	.005693	.01789	.04198

C_D (ND)		0.5	0.66	0.3	0.39	0.24
ID(IN)	.41	1.4	0.6	0.8	1.3
L(F-)	.36 EA.	.08 EA	.46	7.2	6.1
A(FT^2)	.000903	.0101	.00196	.00362	.00976
V(FT^3)	.000271 EA	.0009 EA	.0009	.02612	.05954

FIGURE 7

TRANSWRAP COMPUTATIONAL MODEL

LLTR - SERIES II

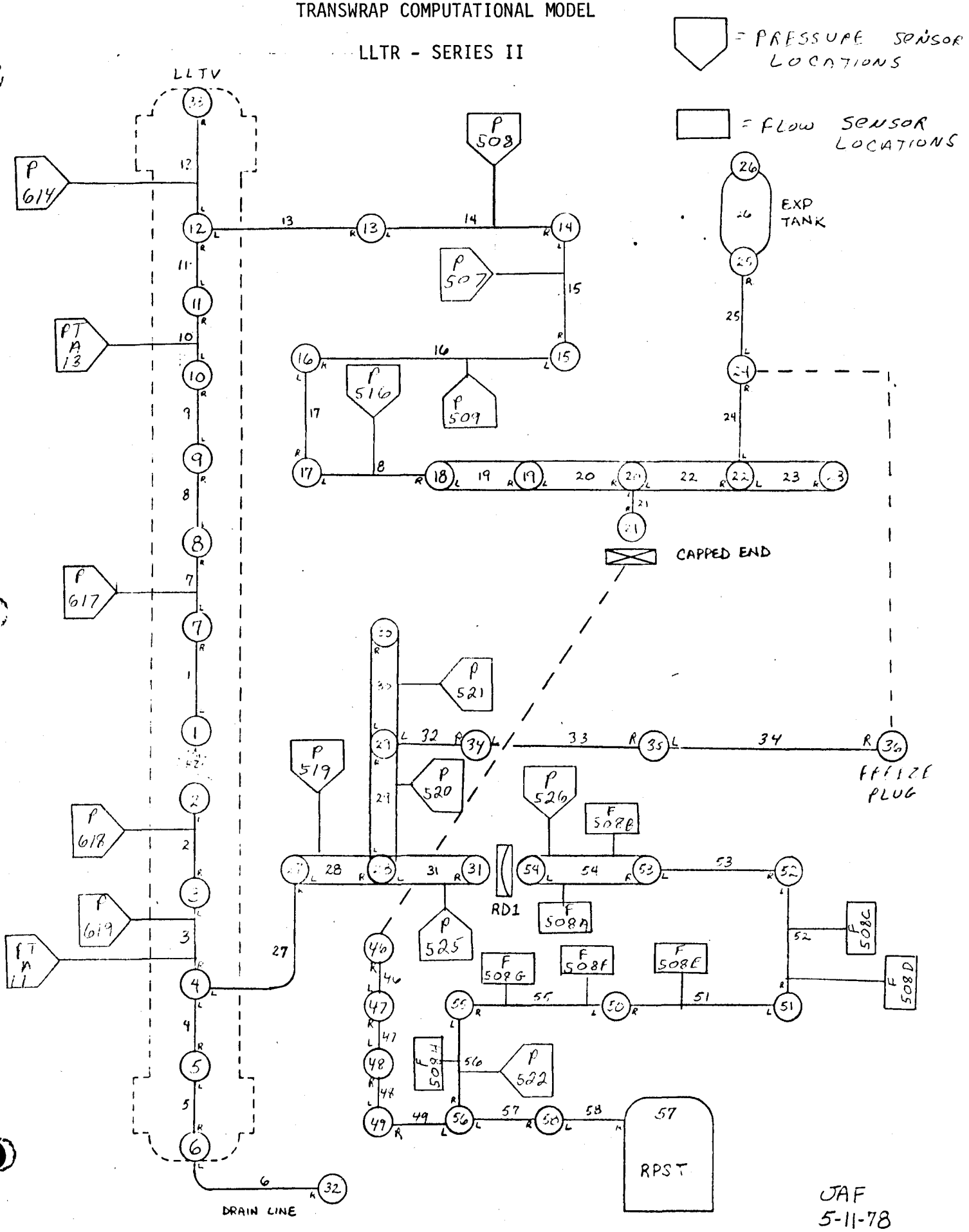

FIGURE 8

BREAK LOCATION FLOW

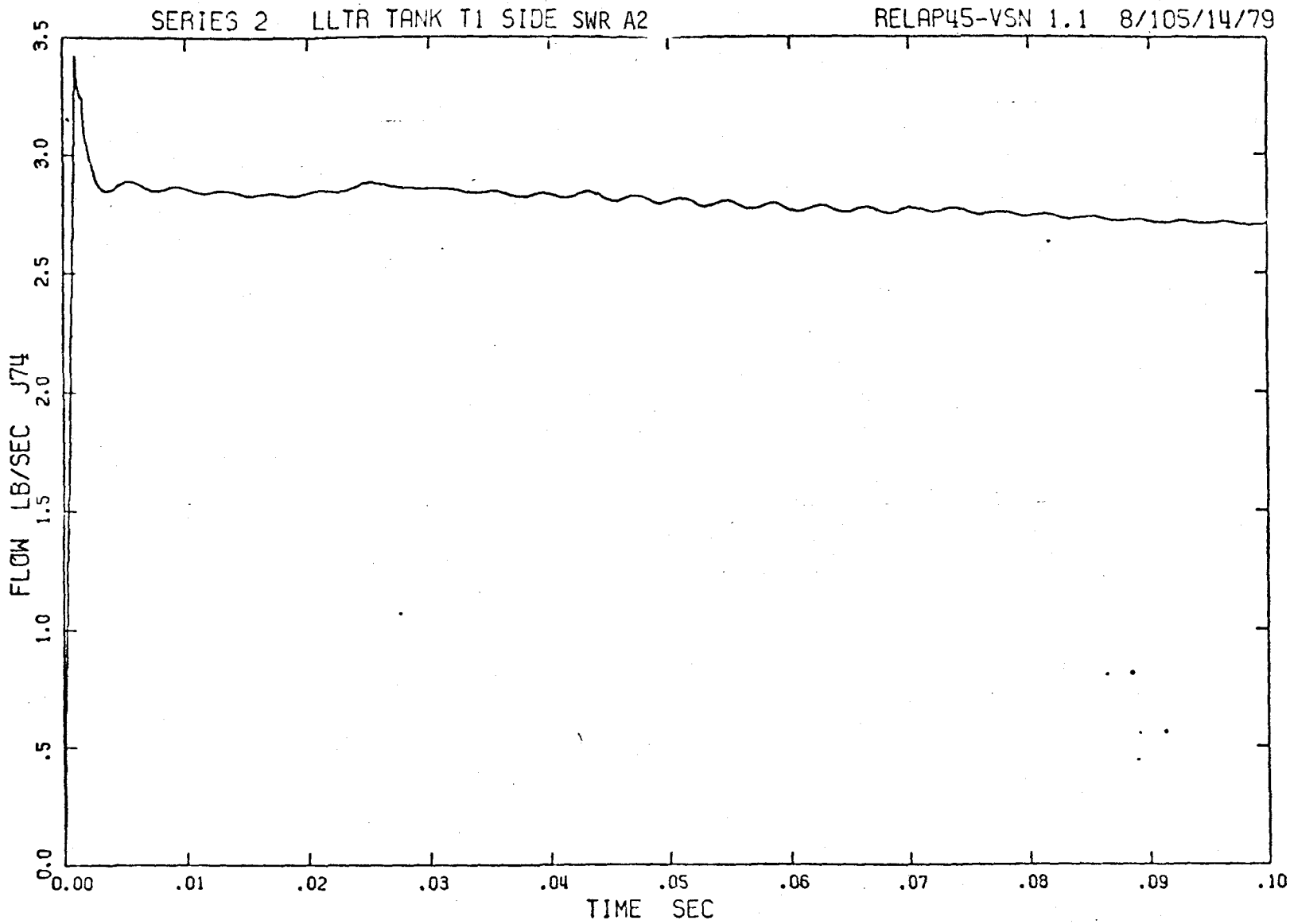

FIGURE 9

BREAK LOCATION QUALITY

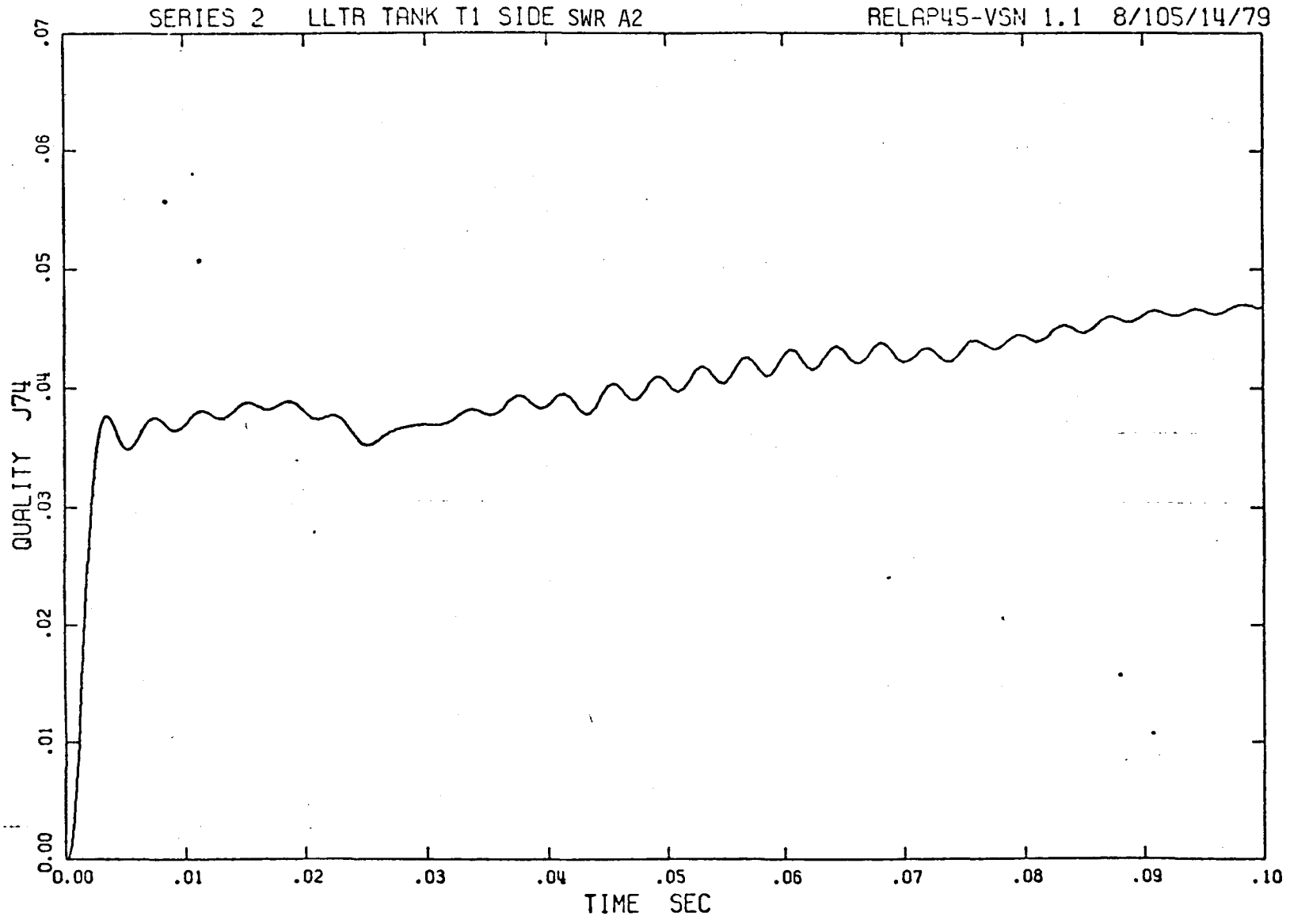

FIGURE 10

FLOW METER F501 FLOW

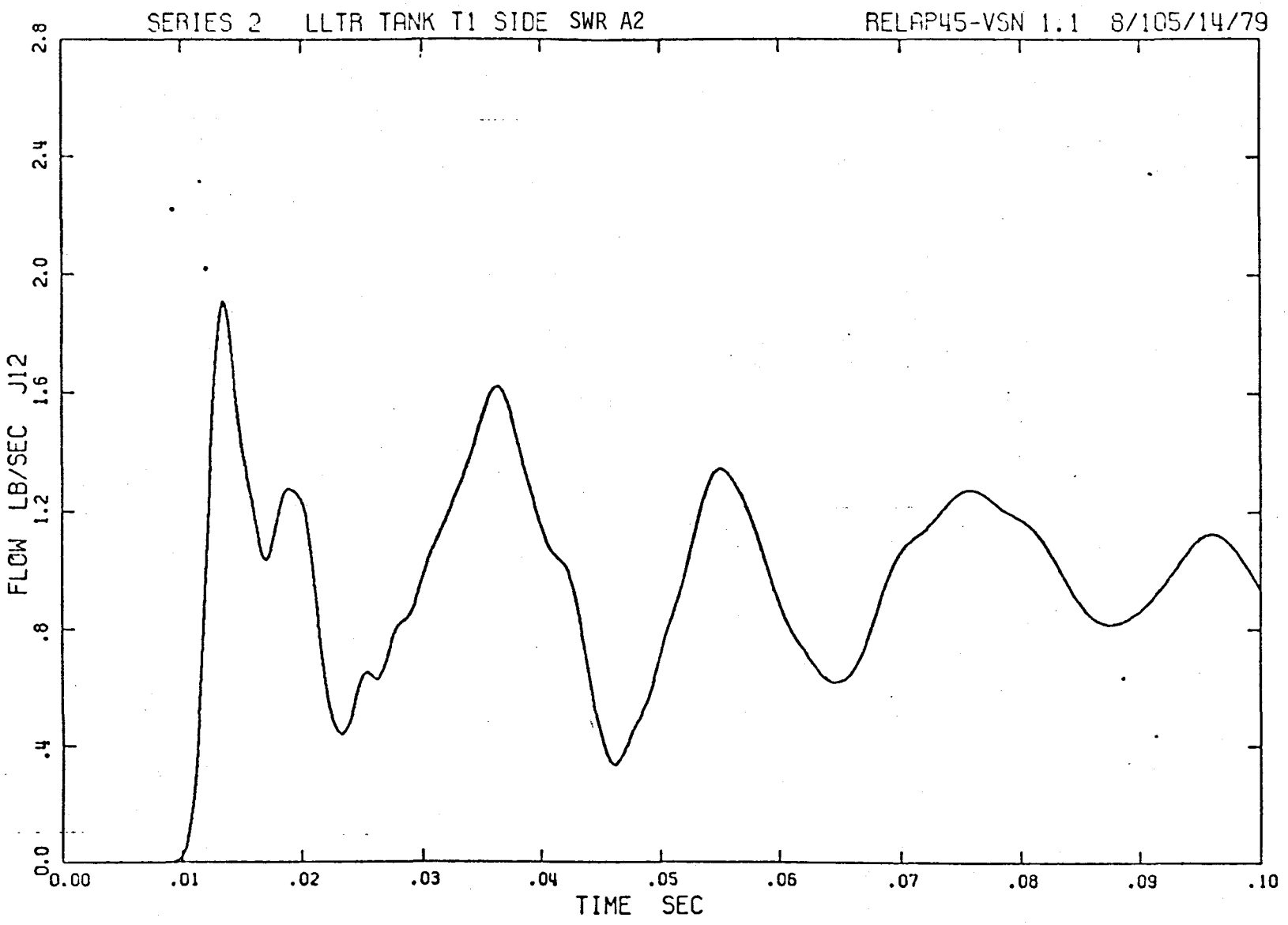

FIGURE 11

BREAK LOCATION FLOW

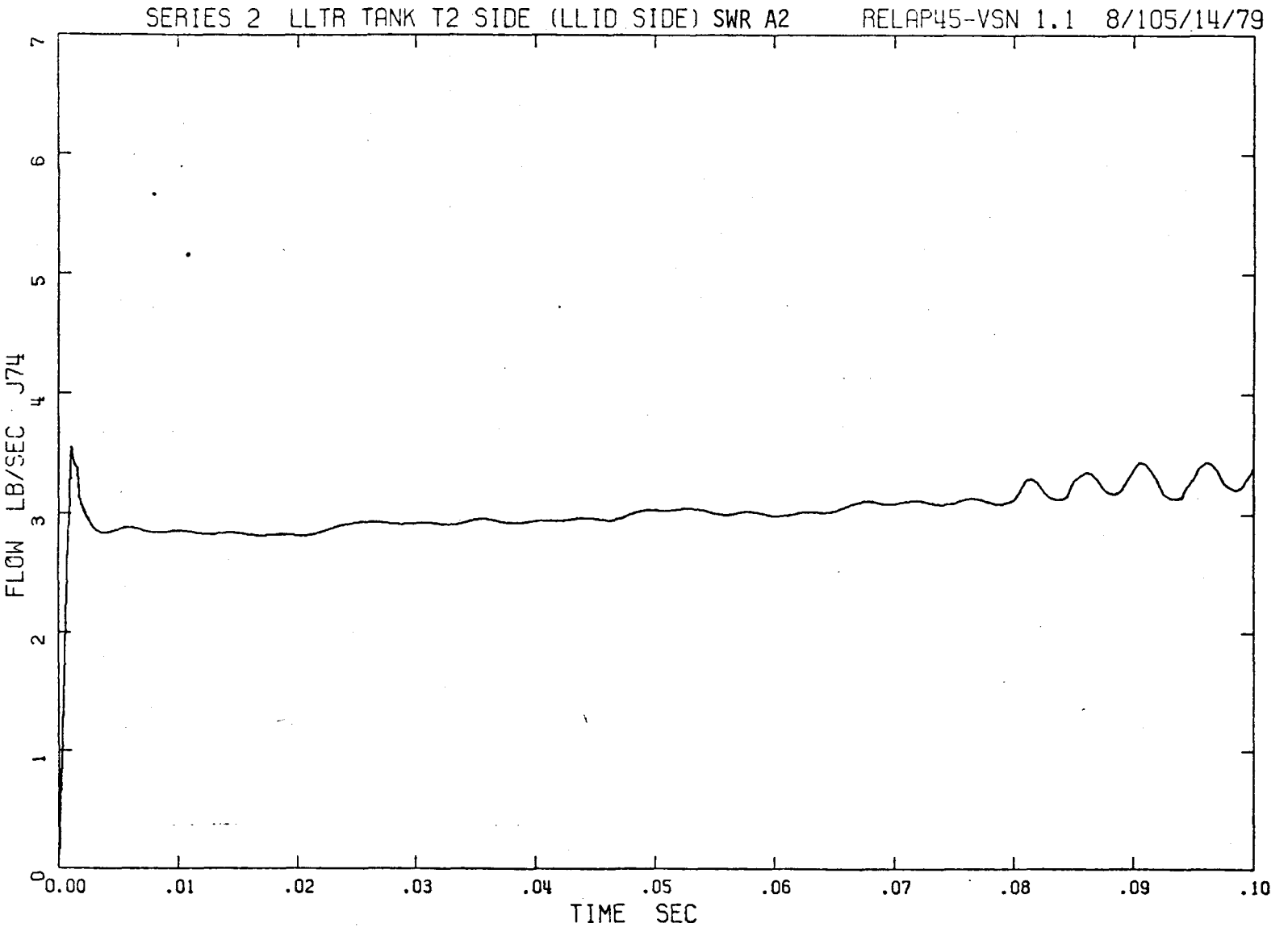

FIGURE 12

BREAK LOCATION QUALITY

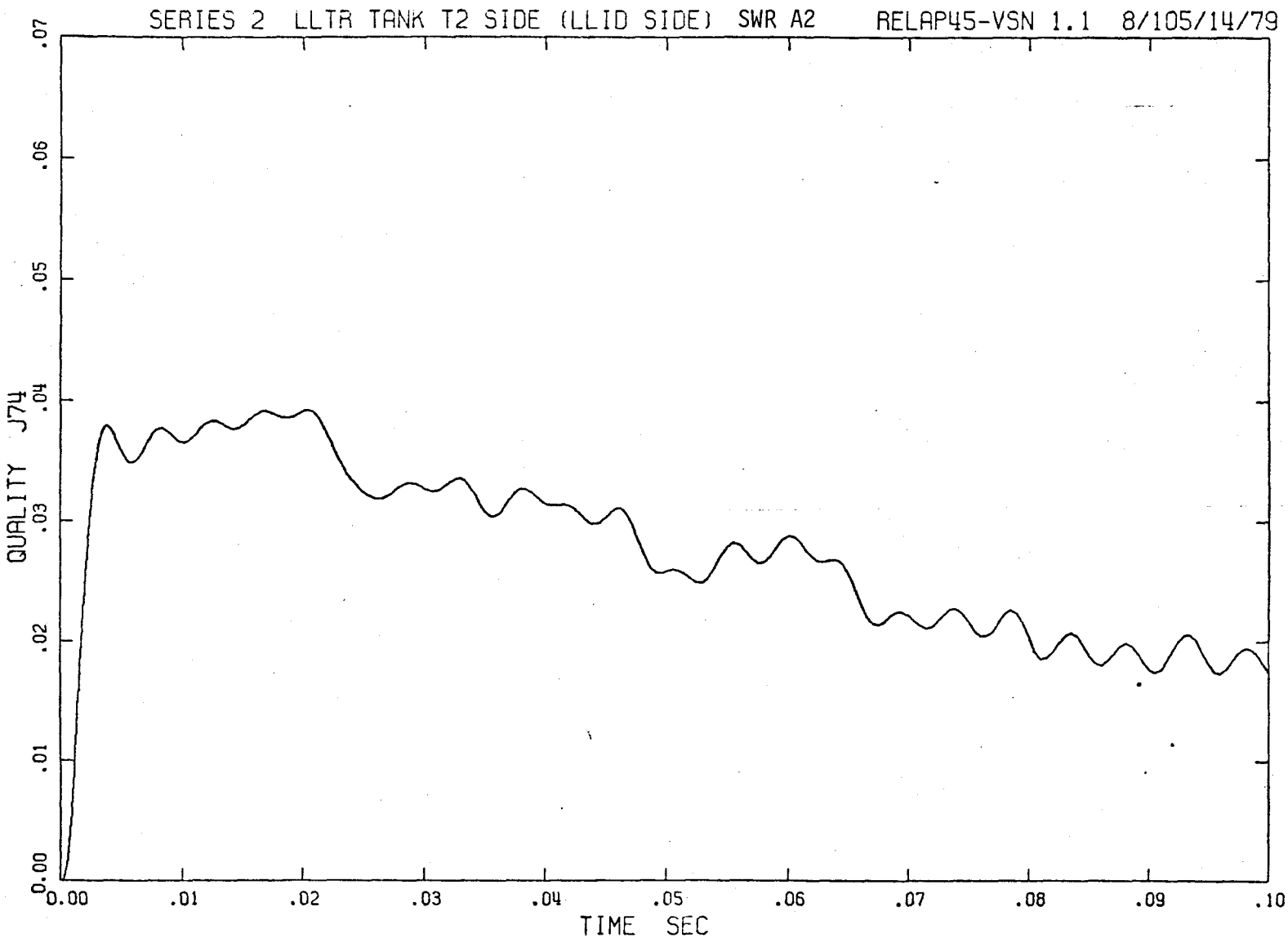

FIGURE 13

FLOW METER F503 FLOW

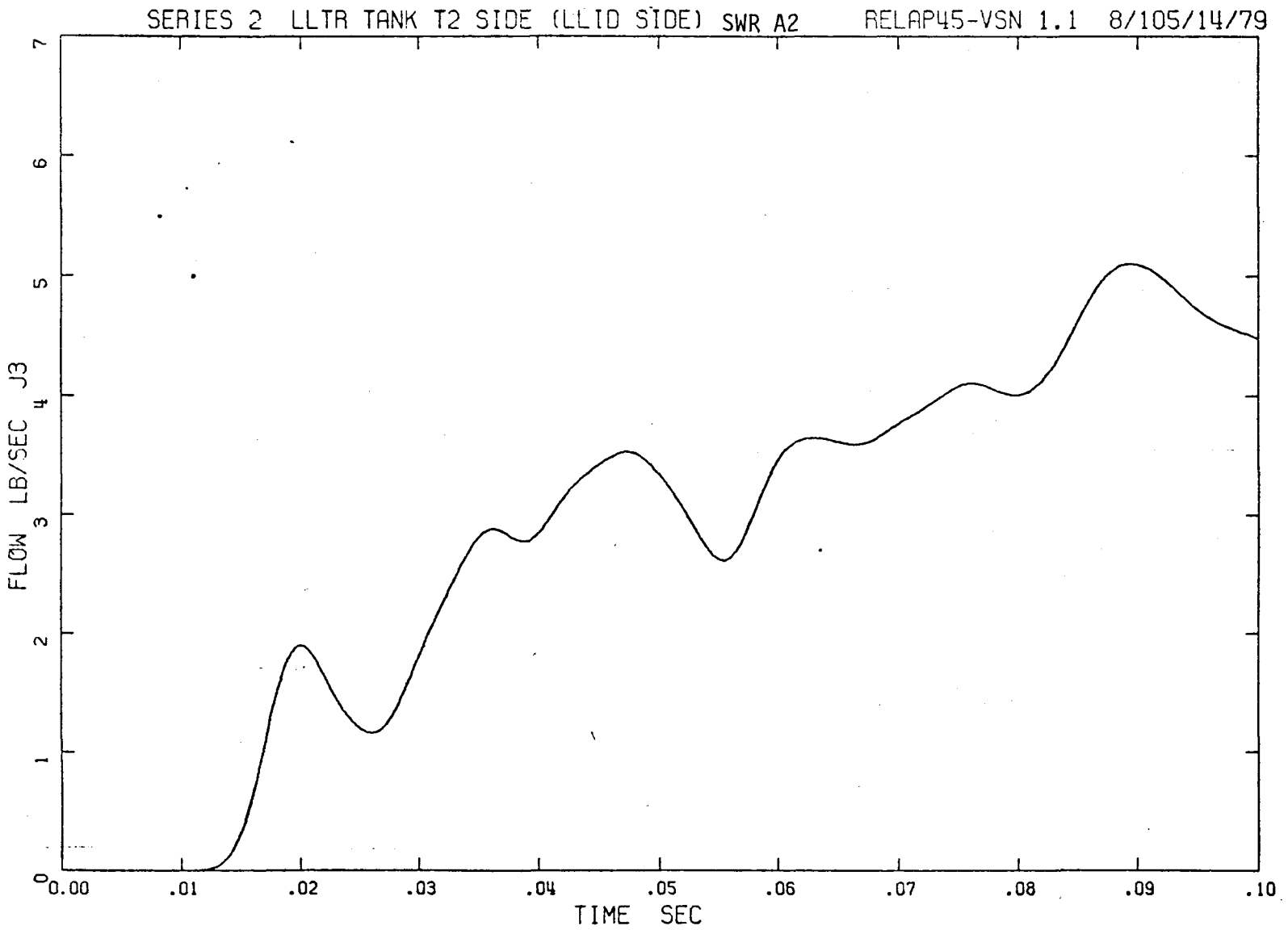

FIGURE 14

LLTR SERIES II - SWR A2 65 PCNT 1700 °F

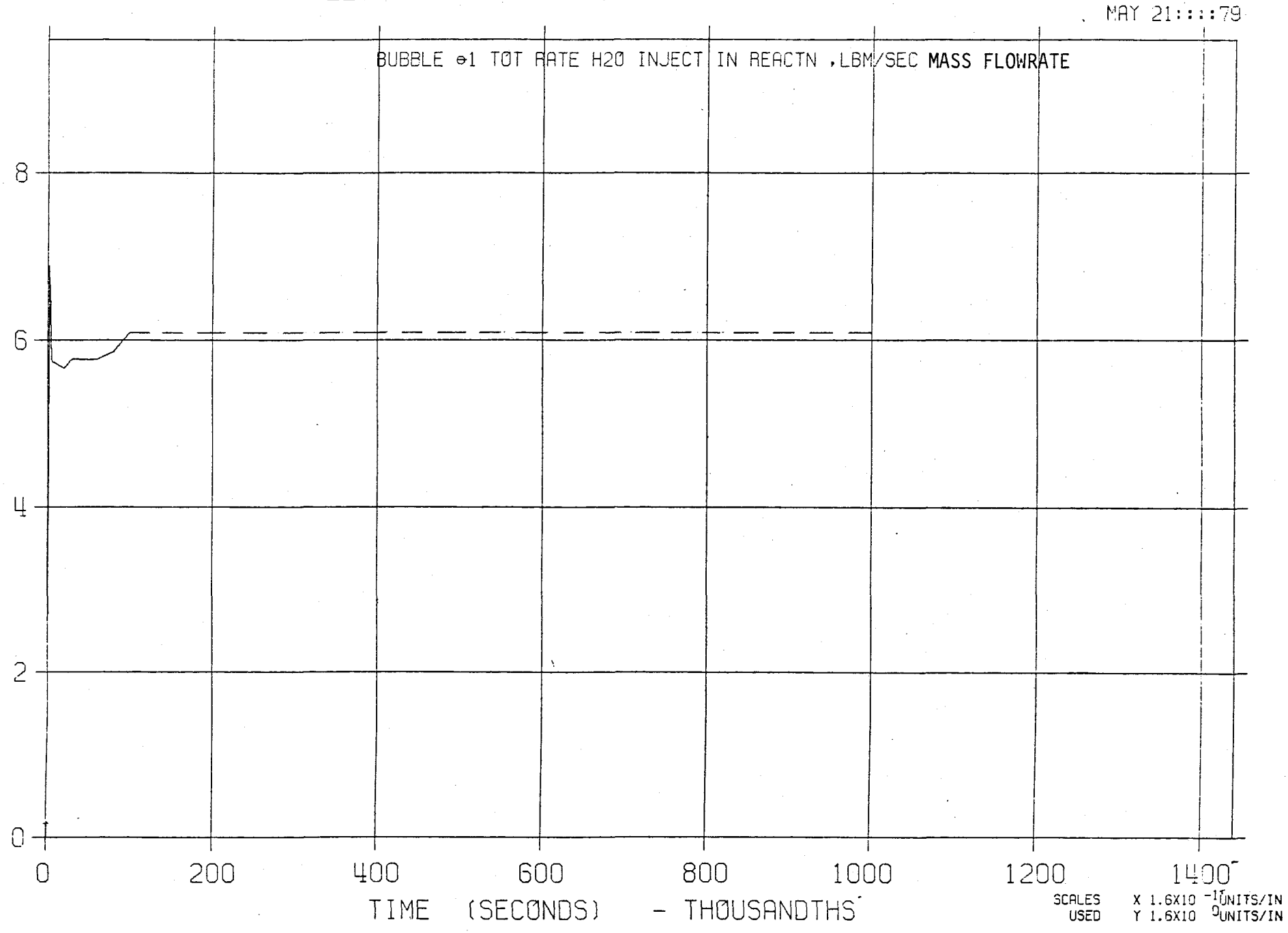

15-L

FIGURE 15-L

LLTR SERIES II - SWR A2 65 PCNT 1700 °F

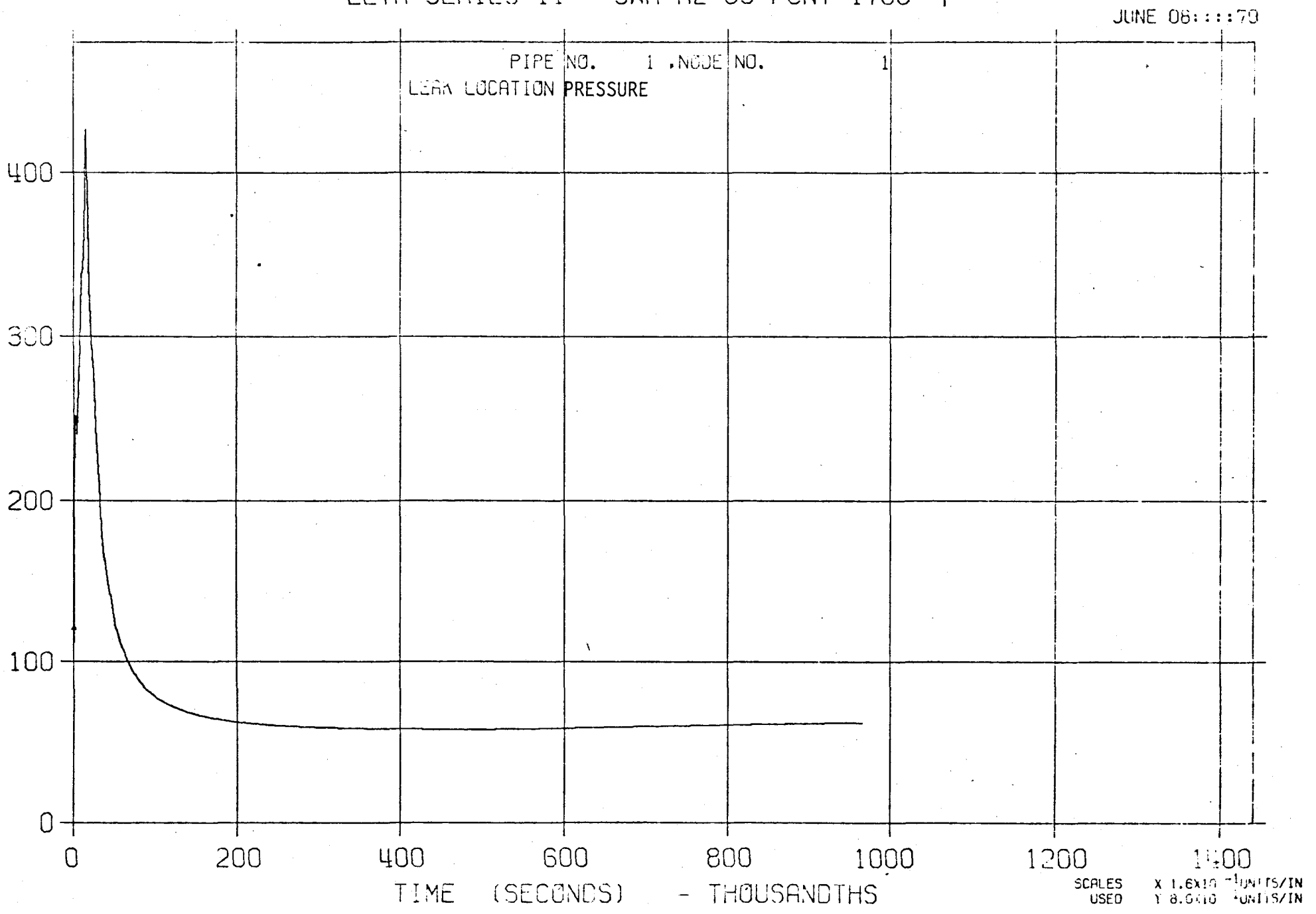

FIGURE 15-S

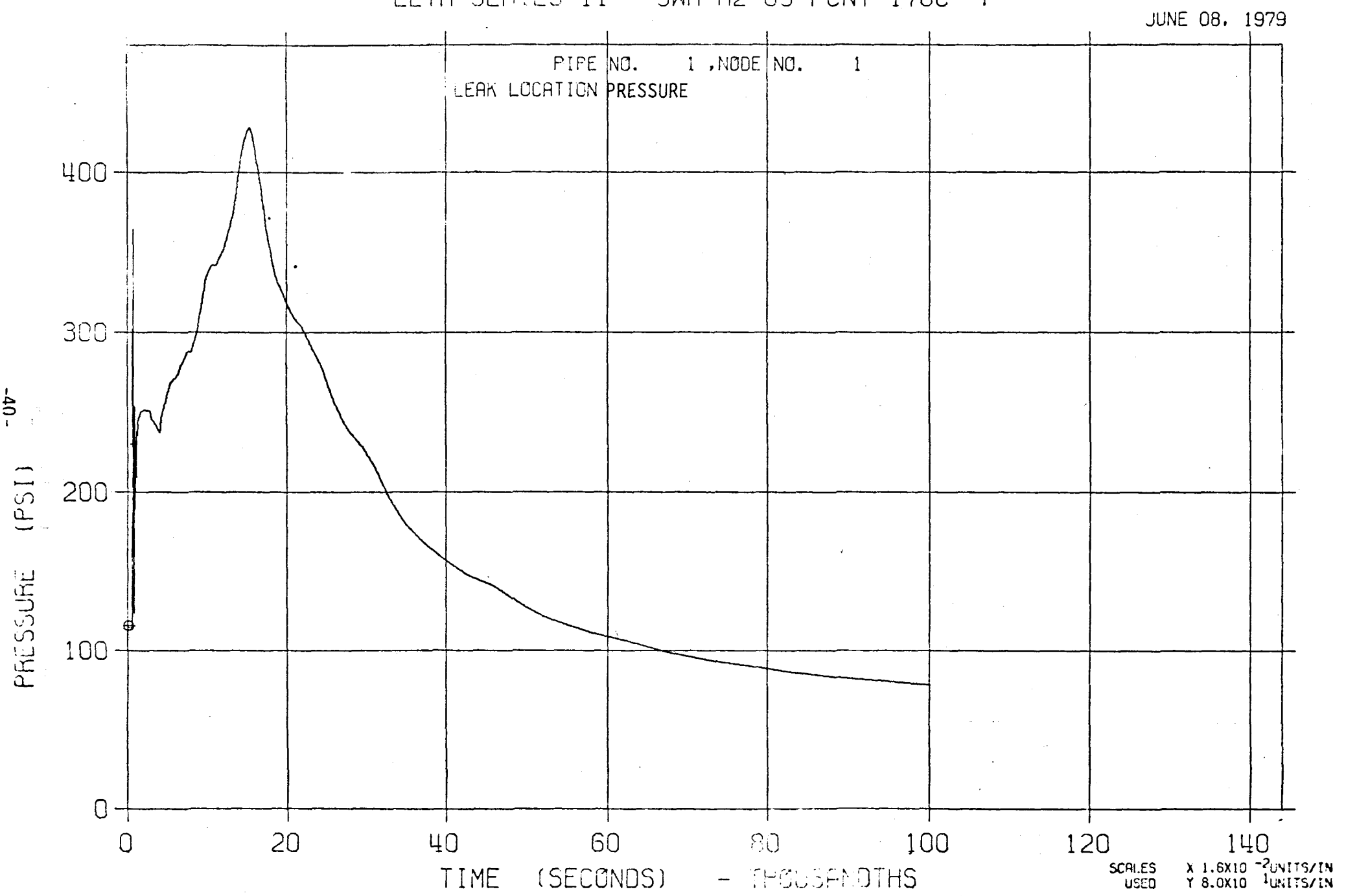
LLTR SERIES II - SWR A2 65 PCNT 1700 °F
JUNE 08, 1979
PIPE NO. 1 ,NODE NO. 1
LEAK LOCATION PRESSURE
PRESSURE (PSI)
400
300
200
100
0
0
20
40
60
80
100
120
140
TIME (SECONDS) - THOUSANDTHS
SCALES USED
X 1.6X10 -2 UNITS/IN
Y 8.0X10 1 UNITS/IN

FIGURE 16-L

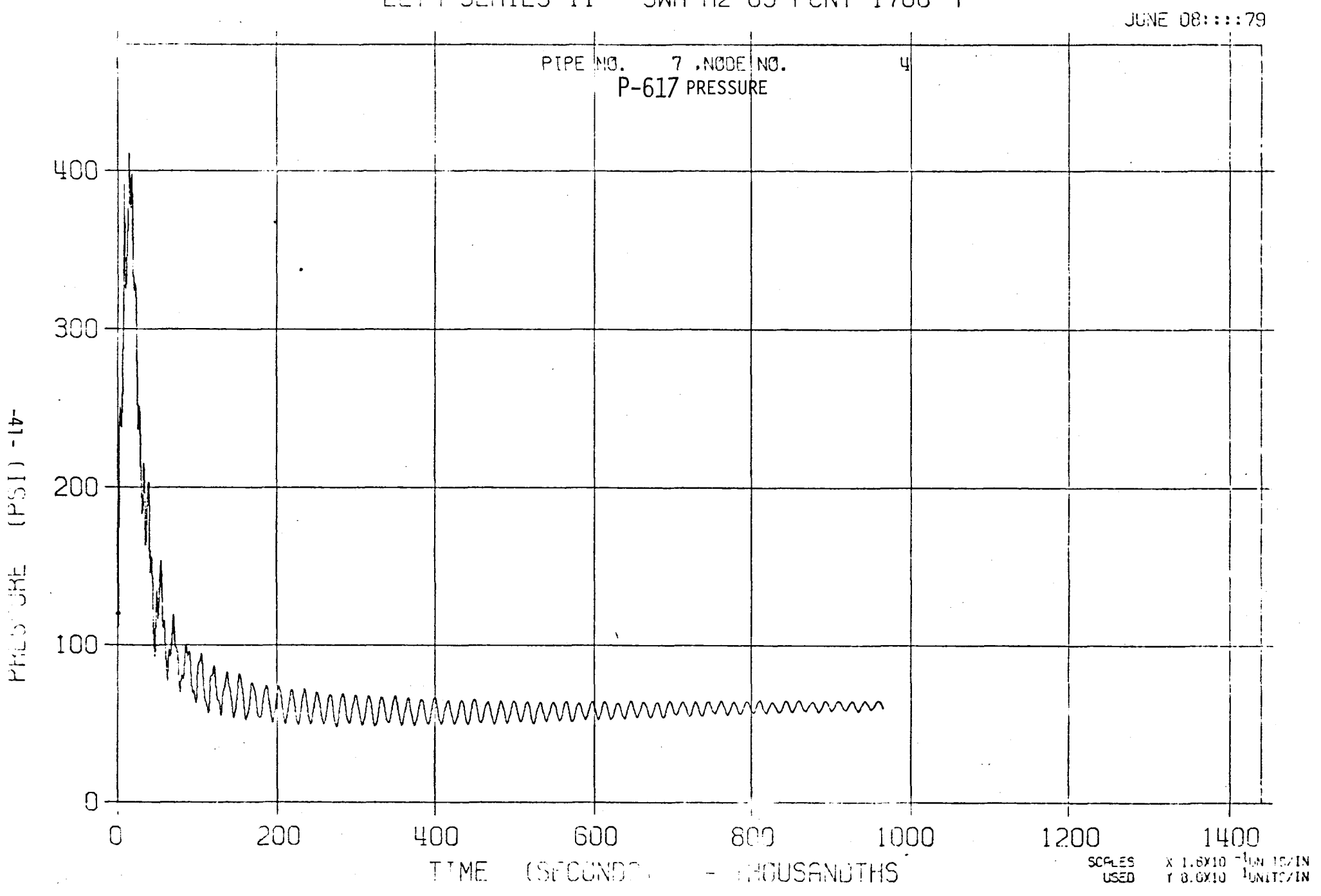
LLTA SERIES II - SWR A2 65 PCNT 1700 °F
JUNE 08::::79
PIPE NO. 7 ,NODE NO. 4
P-617 PRESSURE
400
300
200
100
0
0
200
400
600
800
1000
1200
1400
TIME (SECONDS - THOUSANDTHS
SCALES USED
X 1.6X10 -1 IN 1S/IN
Y 8.0X10 1 UNITS/IN

FIGURE 16-S

LLTR SERIES II - SWR A2 65 PCNT 1700 °F

JUNE 08, 1979

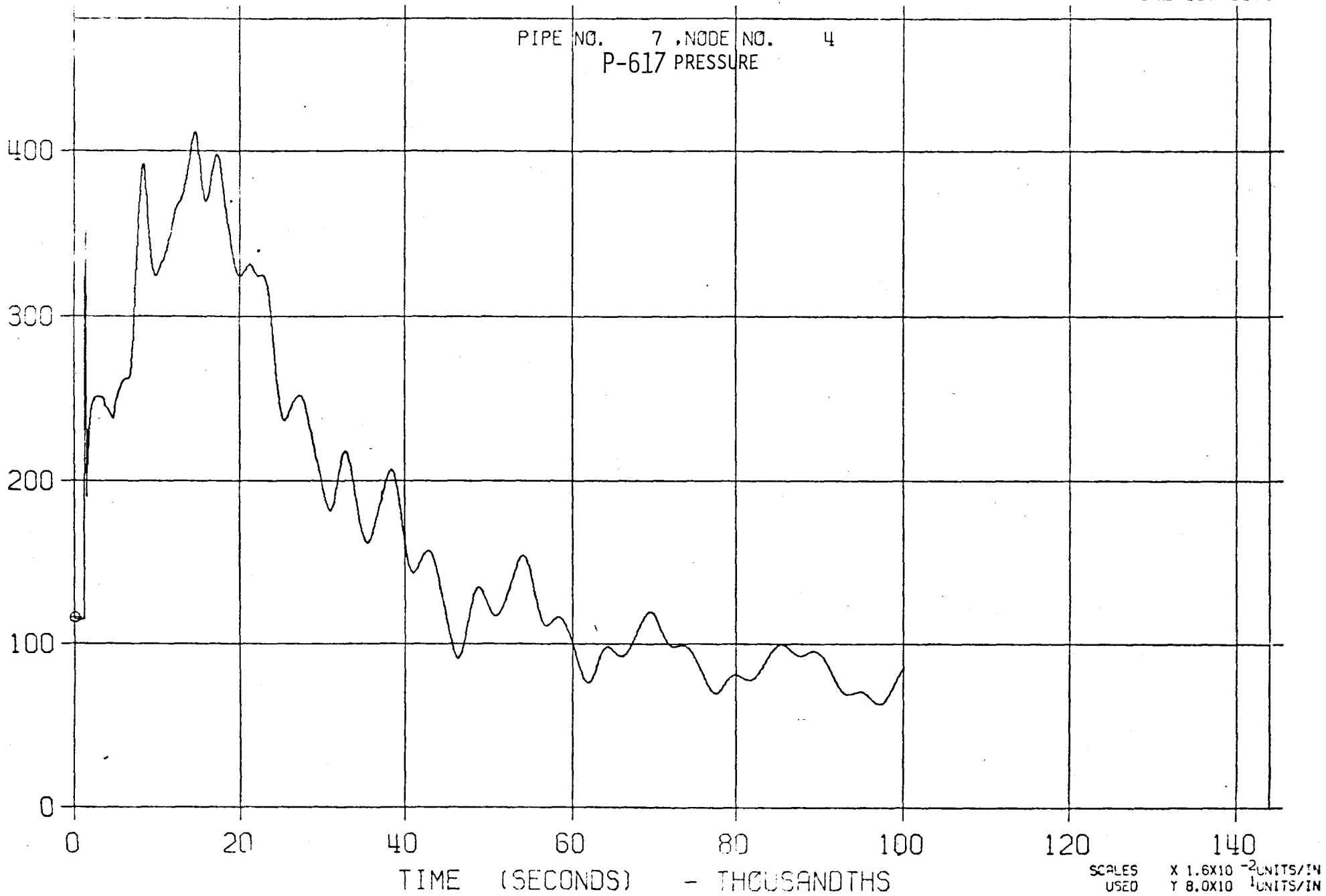

FIGURE 17-L

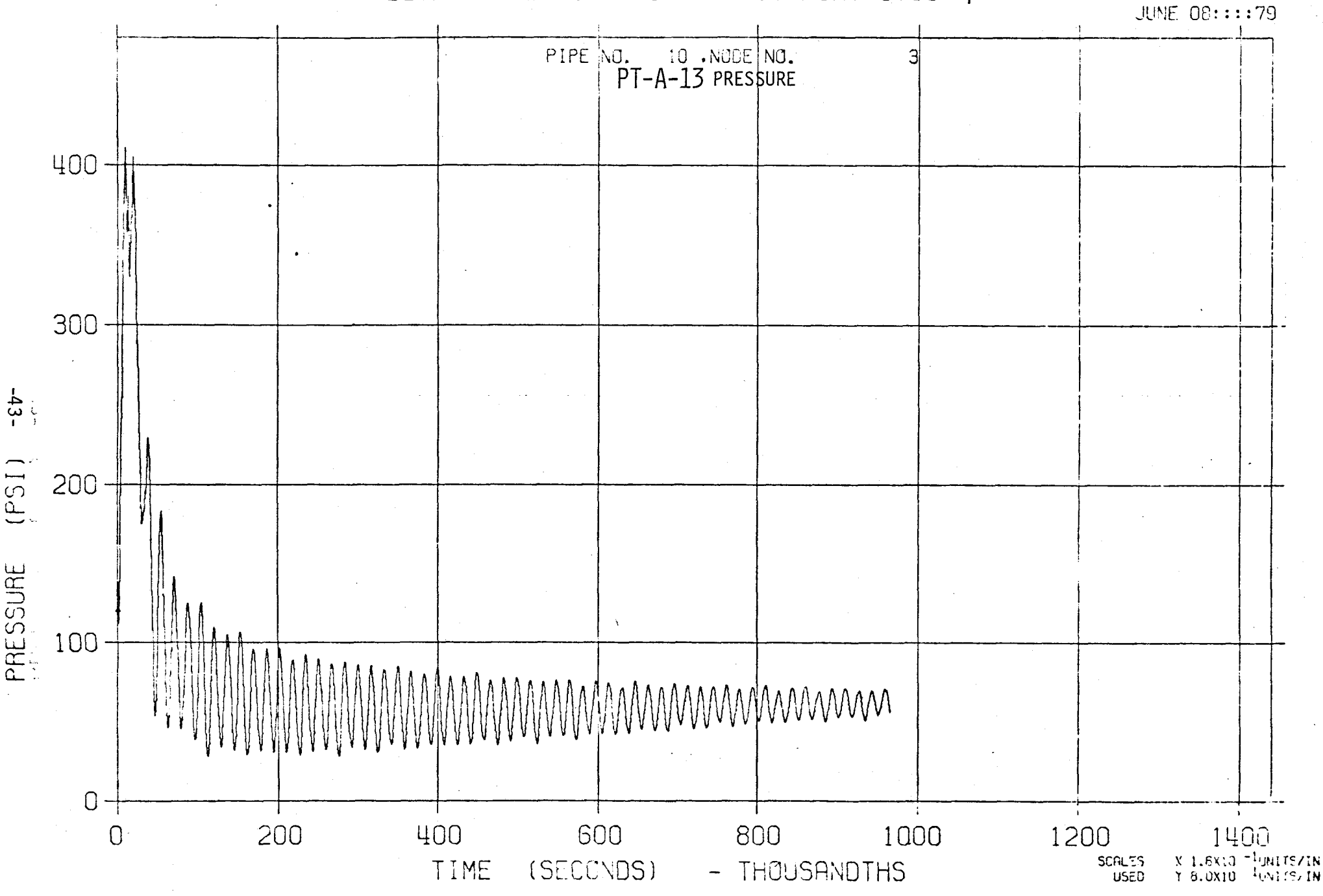
LLTR SERIES II - SWR A2 65 PCNT 1700 °F
JUNE 08::::79
PIPE NO. 10 .NODE NO. 3
PT-A-13 PRESSURE
400
300
200
100
0
PRESSURE (PSI)
0
200
400
600
800
1000
1200
1400
TIME (SECONDS) - THOUSANDTHS
SCALES USED
X 1.6X10 -1 UNITS/IN
Y 8.0X10 1 UNITS/IN

FIGURE 17-S

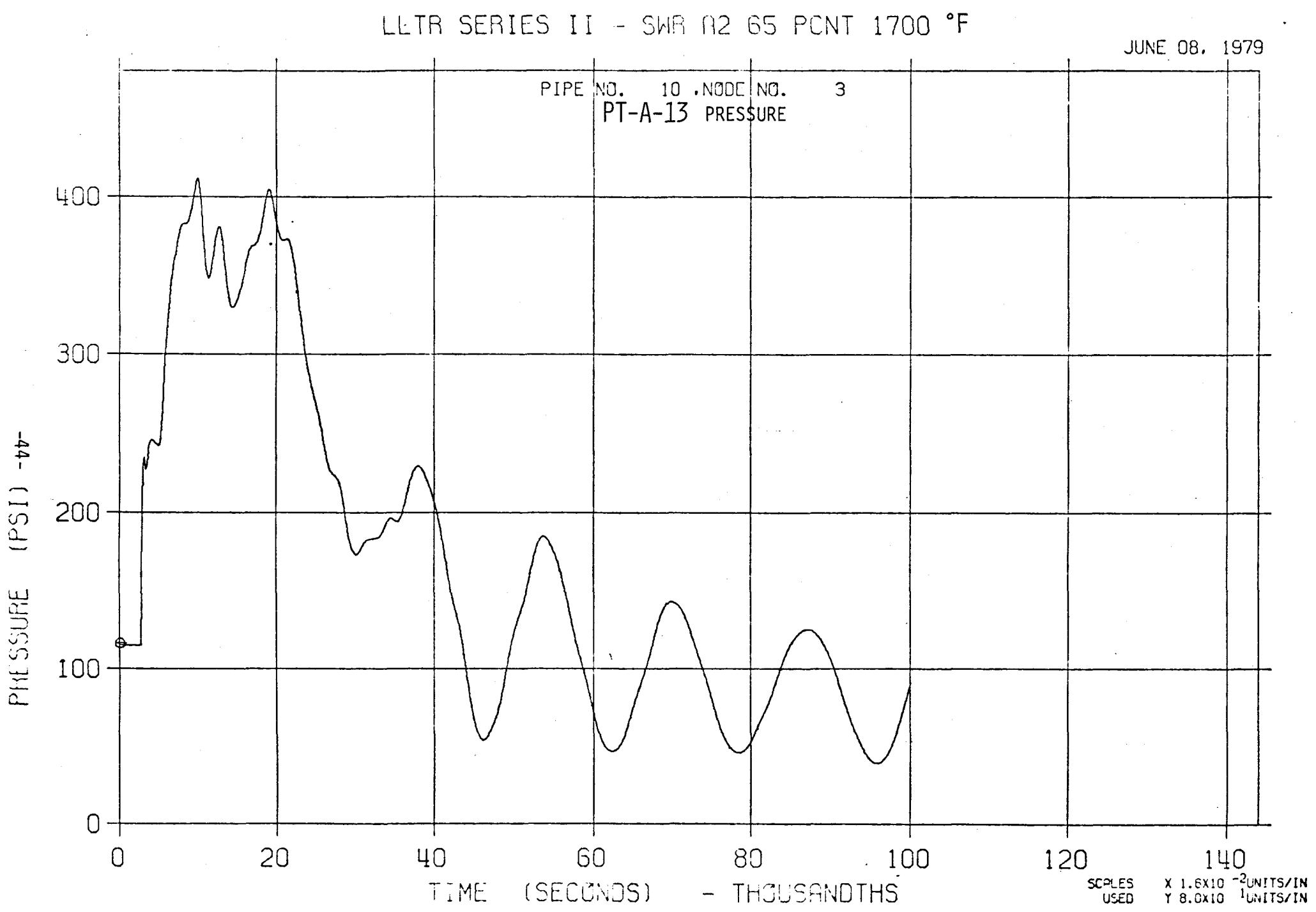
LLTR SERIES II - SWR A2 65 PCNT 1700 °F
JUNE 08, 1979
PIPE NO. 10 .NODE NO. 3
PT-A-13 PRESSURE
400
300
200
100
0
PRESSURE (PSI)
0
20
40
60
80
100
120
140
TIME (SECONDS) - THOUSANDTHS
SCALES USED
X 1.6X10 -2 UNITS/IN
Y 8.0X10 1 UNITS/IN

FIGURE 18-L

LLTR SERIES II - SWR A2 65 PCNT 1700 °F

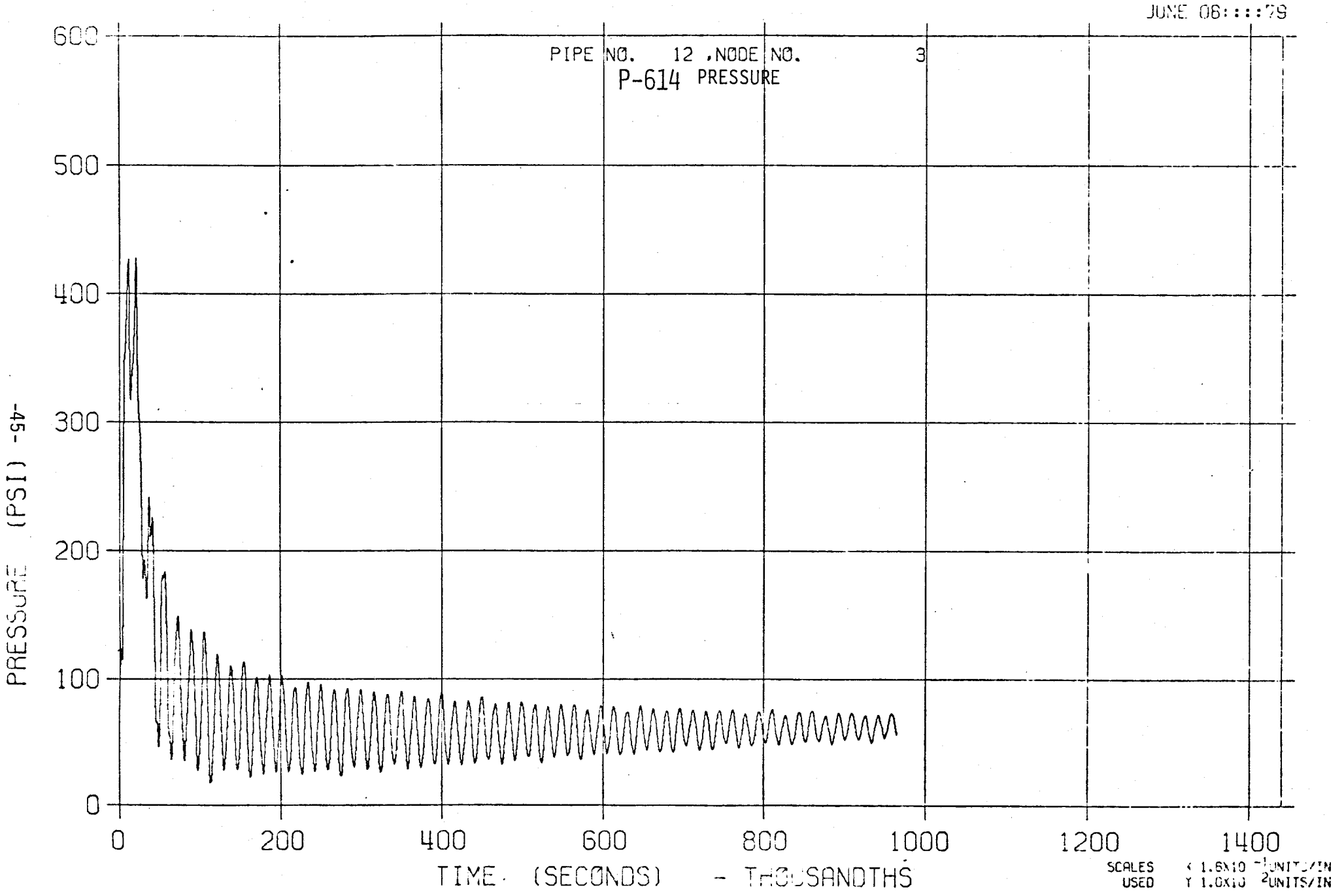

FIGURE 18-S

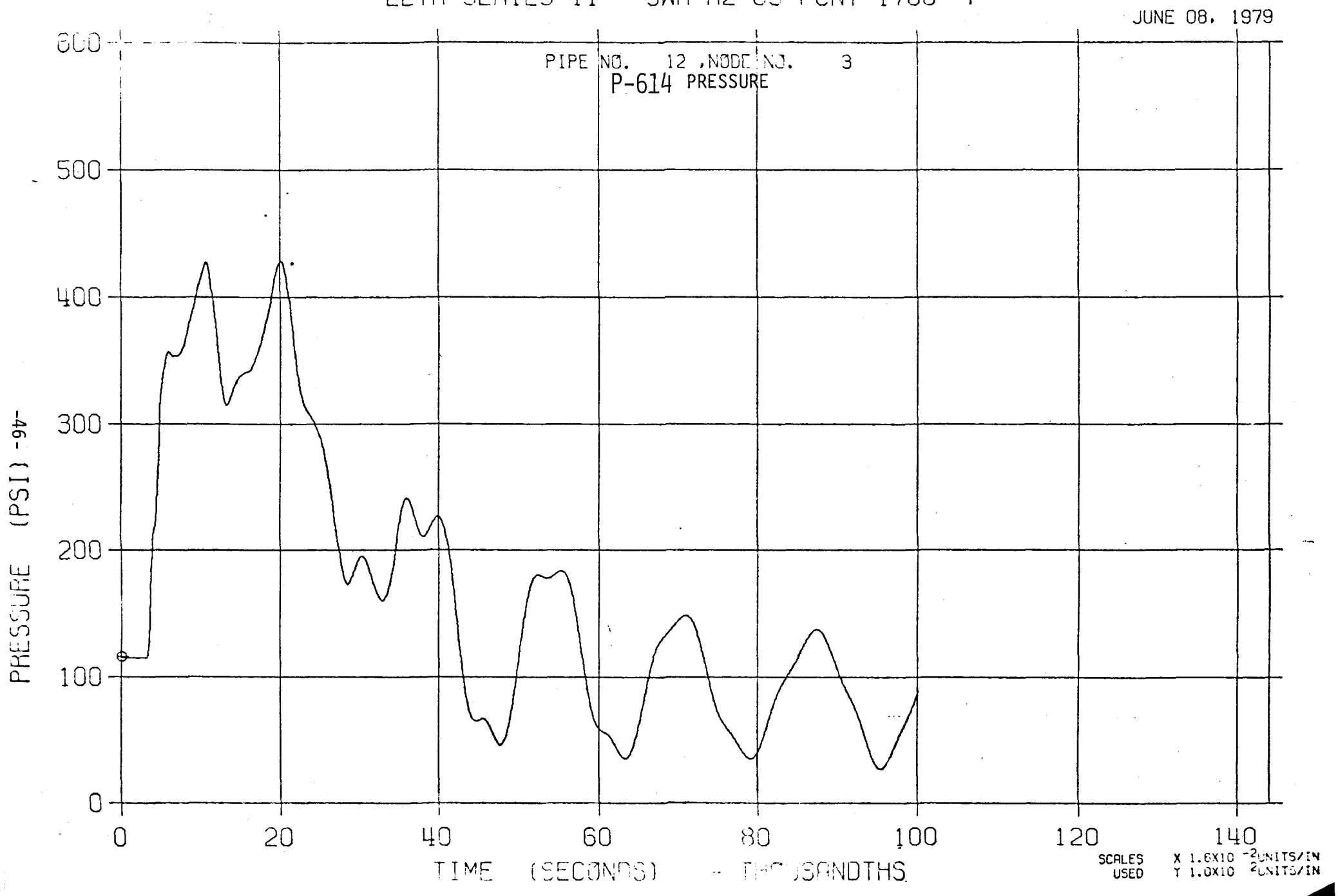
LLTR SERIES II - SWR A2 65 PCNT 1700 °F
JUNE 08, 1979
PIPE NO. 12 ,NODE NO. 3
P-614 PRESSURE
PRESSURE (PSI)
600
500
400
300
200
100
0
0
20
40
60
80
100
120
140
TIME (SECONDS) - THOUSANDTHS
SCALES USED
X 1.0X10 -2 UNITS/IN
Y 1.0X10 2 UNITS/IN

19-L

FIGURE 19-L

LLTR SERIES II - SWR A2 65 PCNT 1700 °F

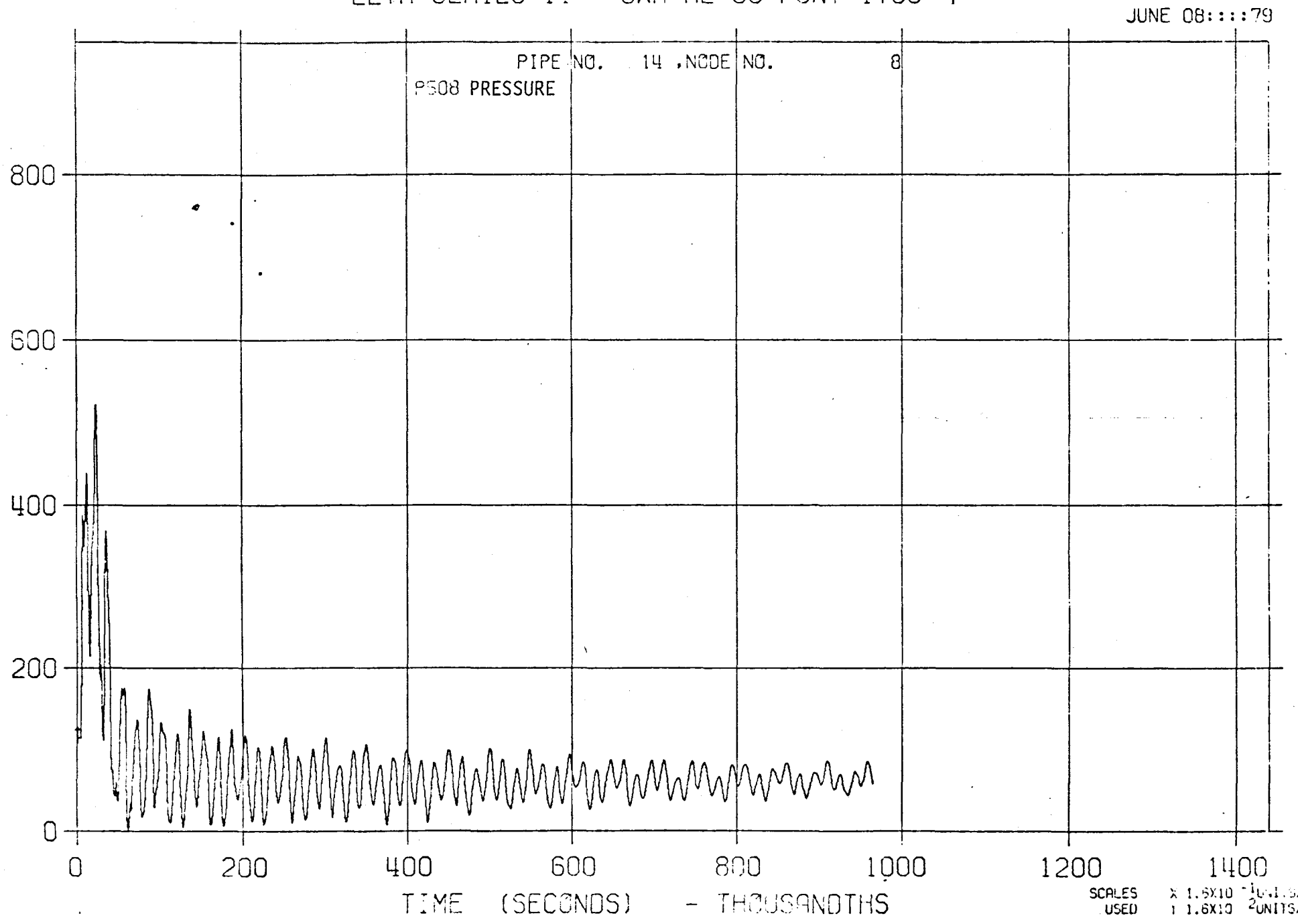

FIGURE 19-S

LLTR SERIES II - SWR A2 65 PCNT 1700 °F

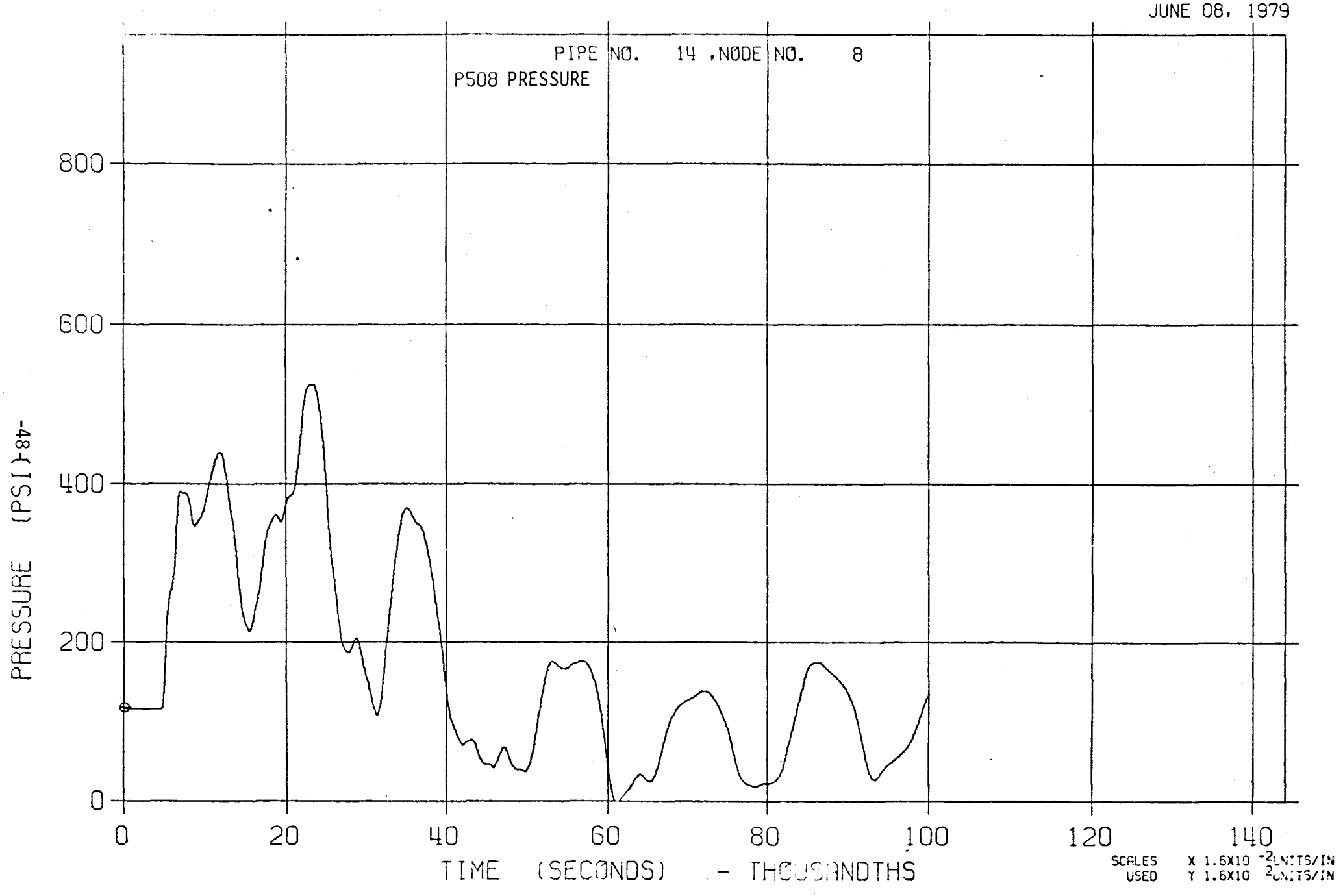

FIGURE 20-L

LLTR SERIES II - SWR A2 65 PCNT 1700 °F

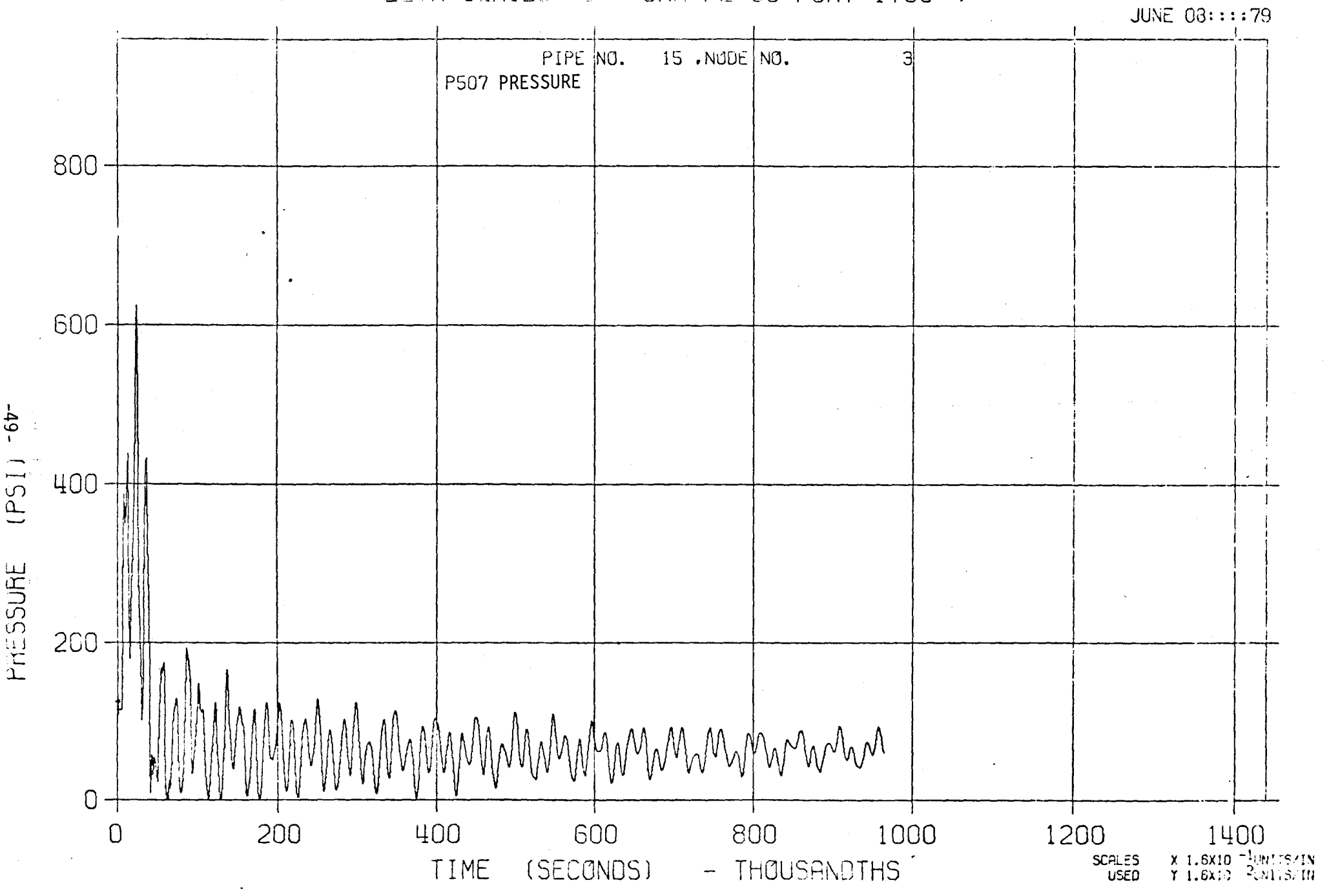

FIGURE 20-S

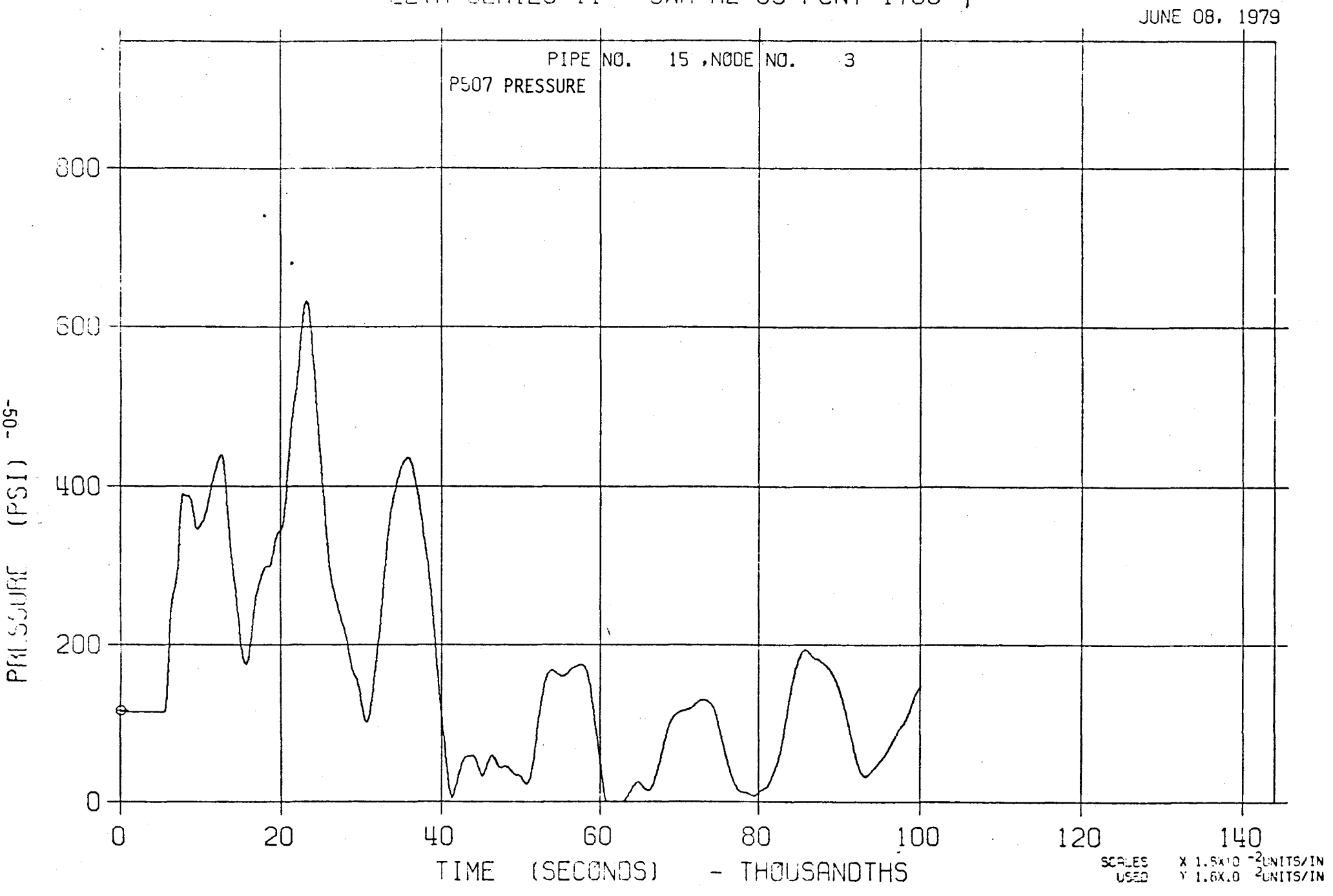
LLTR SERIES II - SWR A2 65 PCNT 1700 °F
JUNE 08, 1979
PIPE NO. 15 ,NODE NO. 3
P507 PRESSURE
800
600
400
200
0
PRESSURE (PSI)
0
20
40
60
80
100
120
140
TIME (SECONDS) - THOUSANDTHS
SCALES USED
X 1.6X10 -2UNITS/IN
Y 1.6X.0 2UNITS/IN

FIGURE 21-L

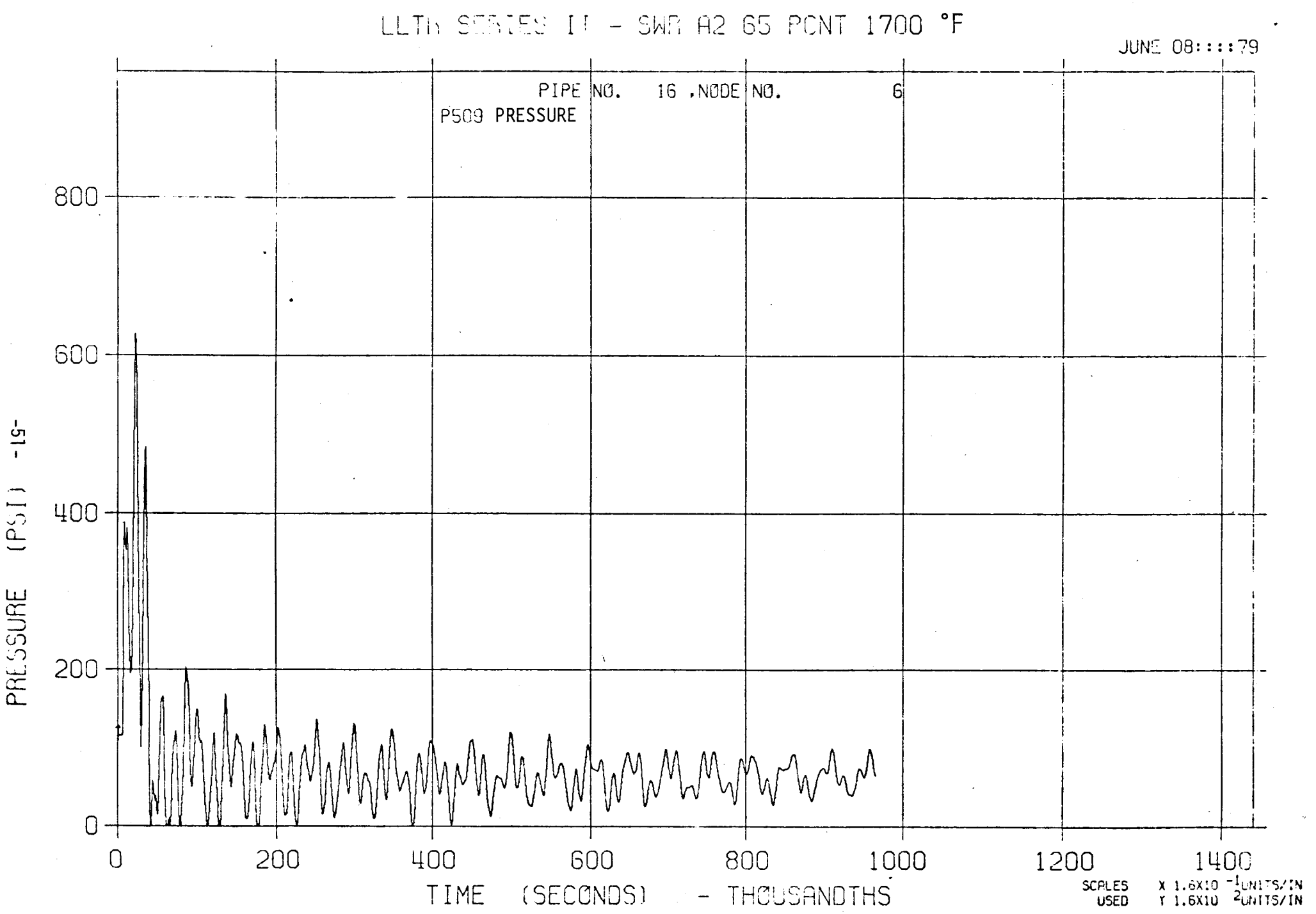
LLTH SERIES II - SWR A2 65 PCNT 1700 °F
JUNE 08::::79
PIPE NO. 16 ,NODE NO. 6
P509 PRESSURE
800
600
400
200
0
PRESSURE (PSI)
0
200
400
600
800
1000
1200
1400
TIME (SECONDS) - THOUSANDTHS
SCALES USED
X 1.6X10 -1 UNITS/IN
Y 1.6X10 2 UNITS/IN

FIGURE 21-S

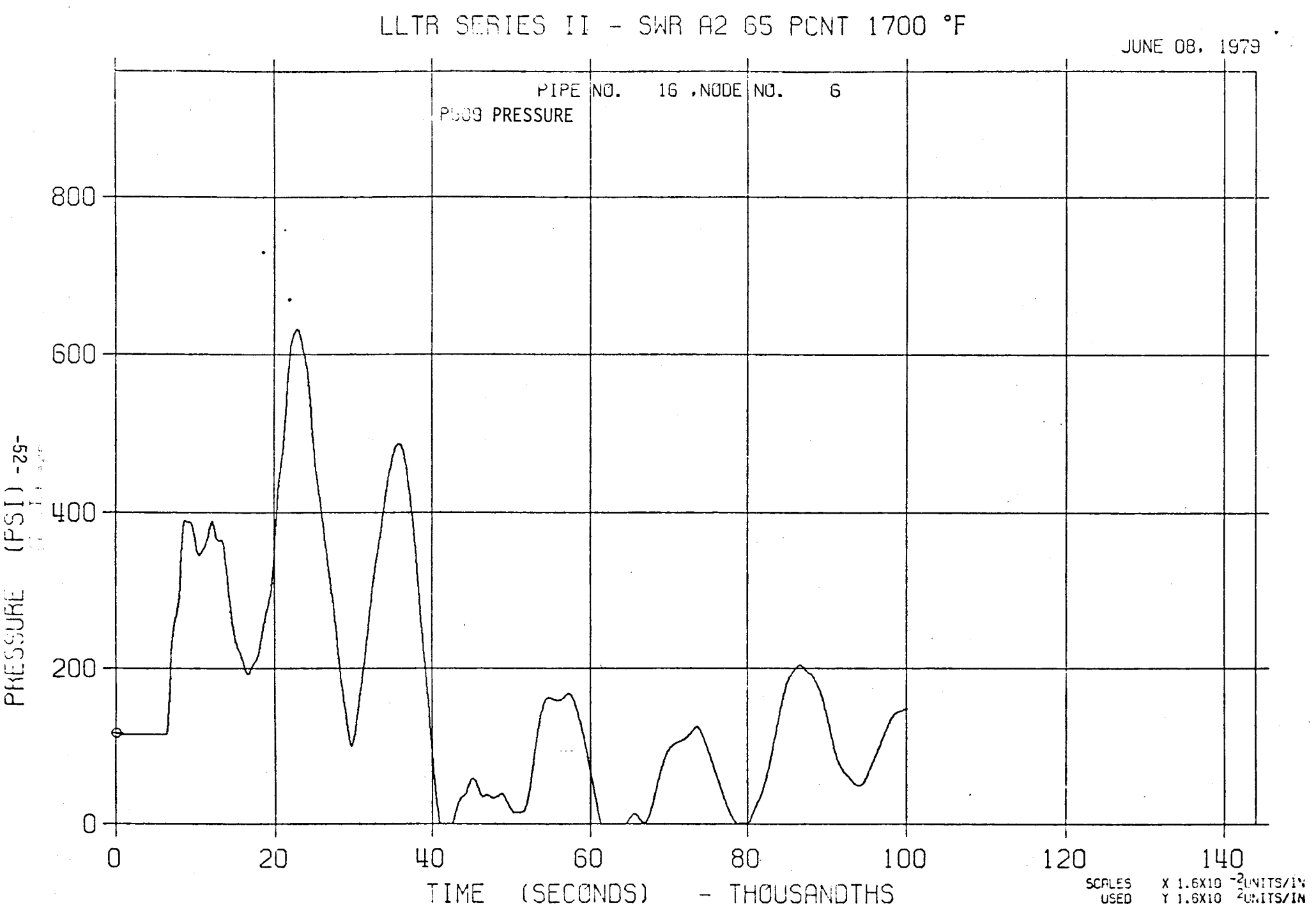
LLTR SERIES II - SWR A2 65 PCNT 1700 °F
JUNE 08, 1979
PIPE NO. 16 ,NODE NO. 6
P609 PRESSURE
800
600
400
200
0
PRESSURE (PSI) -52-
0
20
40
60
80
100
120
140
TIME (SECONDS) - THOUSANDTHS
SCALES USED
X 1.6X10 -2 UNITS/IN
Y 1.6X10 -2 UNITS/IN

FIGURE 22-L

LLTR SERIES II - SWR A2 65 PCNT 1700 °F

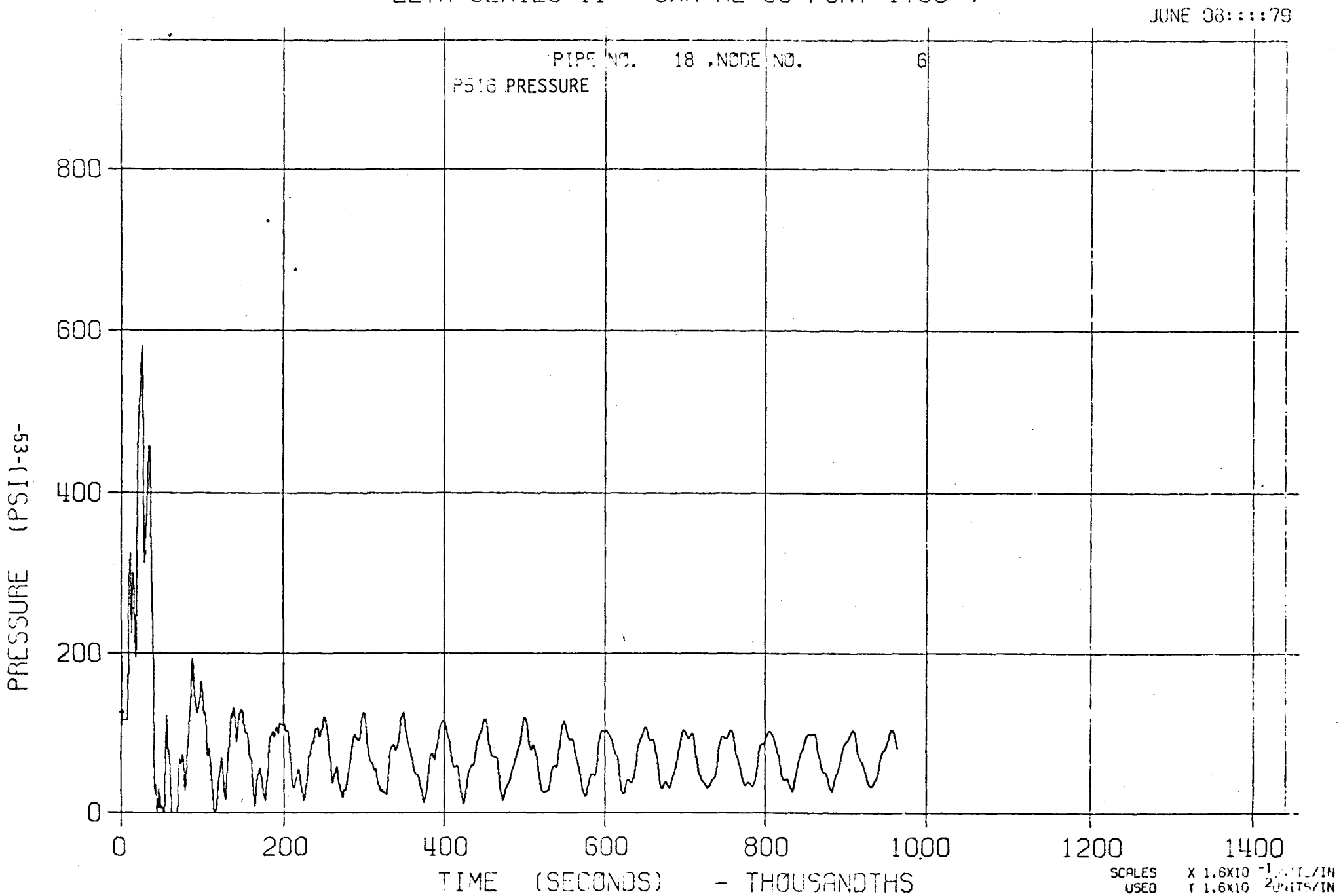

FIGURE 22-S

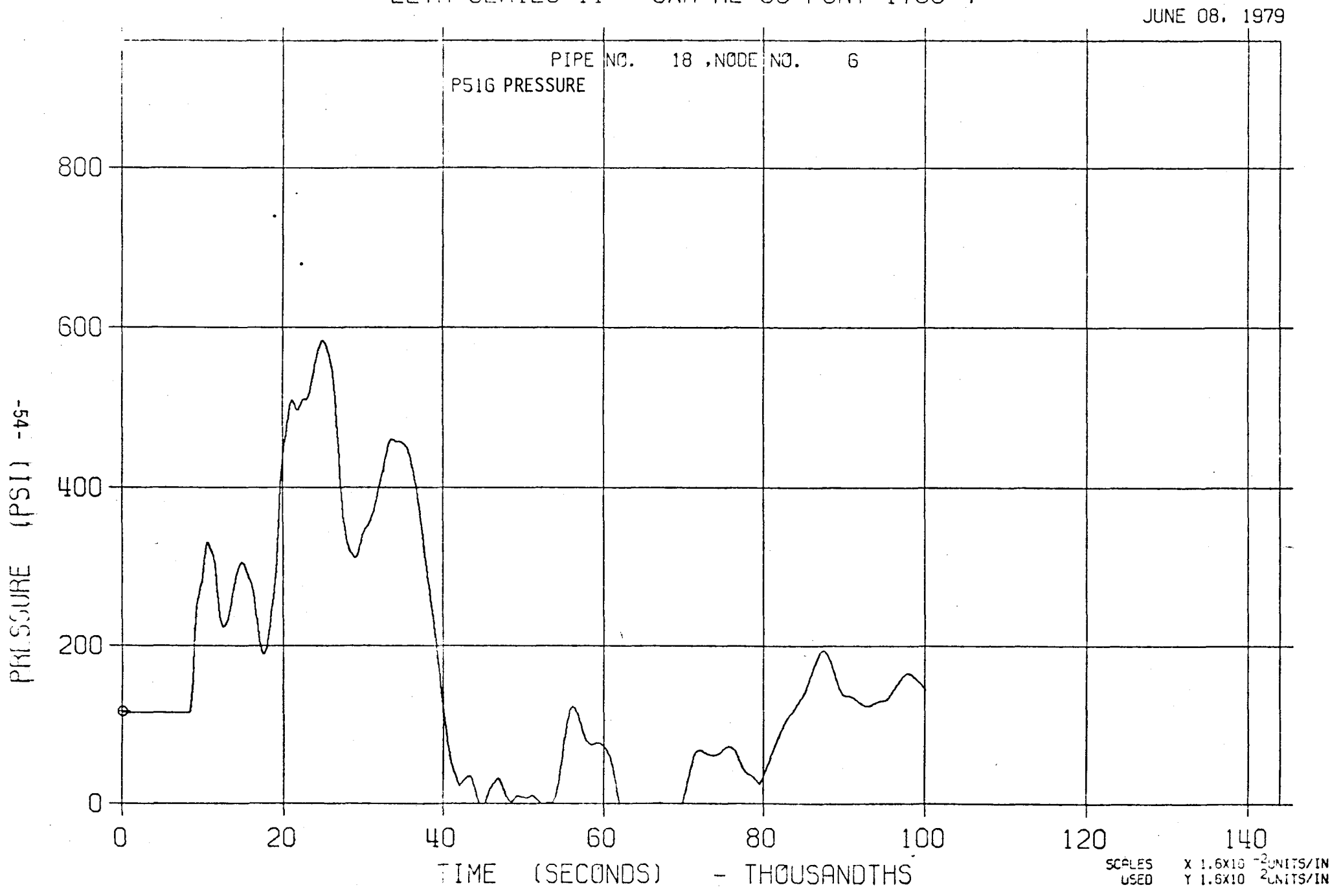
LLTR SERIES II - SWR A2 65 PCNT 1700 °F
JUNE 08, 1979
PIPE NO. 18 ,NODE NO. 6
P51G PRESSURE
800
600
400
200
0
0
20
40
60
80
100
120
140
PRESSURE (PSI)
TIME (SECONDS) - THOUSANDTHS
SCALES USED
X 1.6X10 -2 UNITS/IN
Y 1.6X10 2 UNITS/IN

FIGURE 23-L

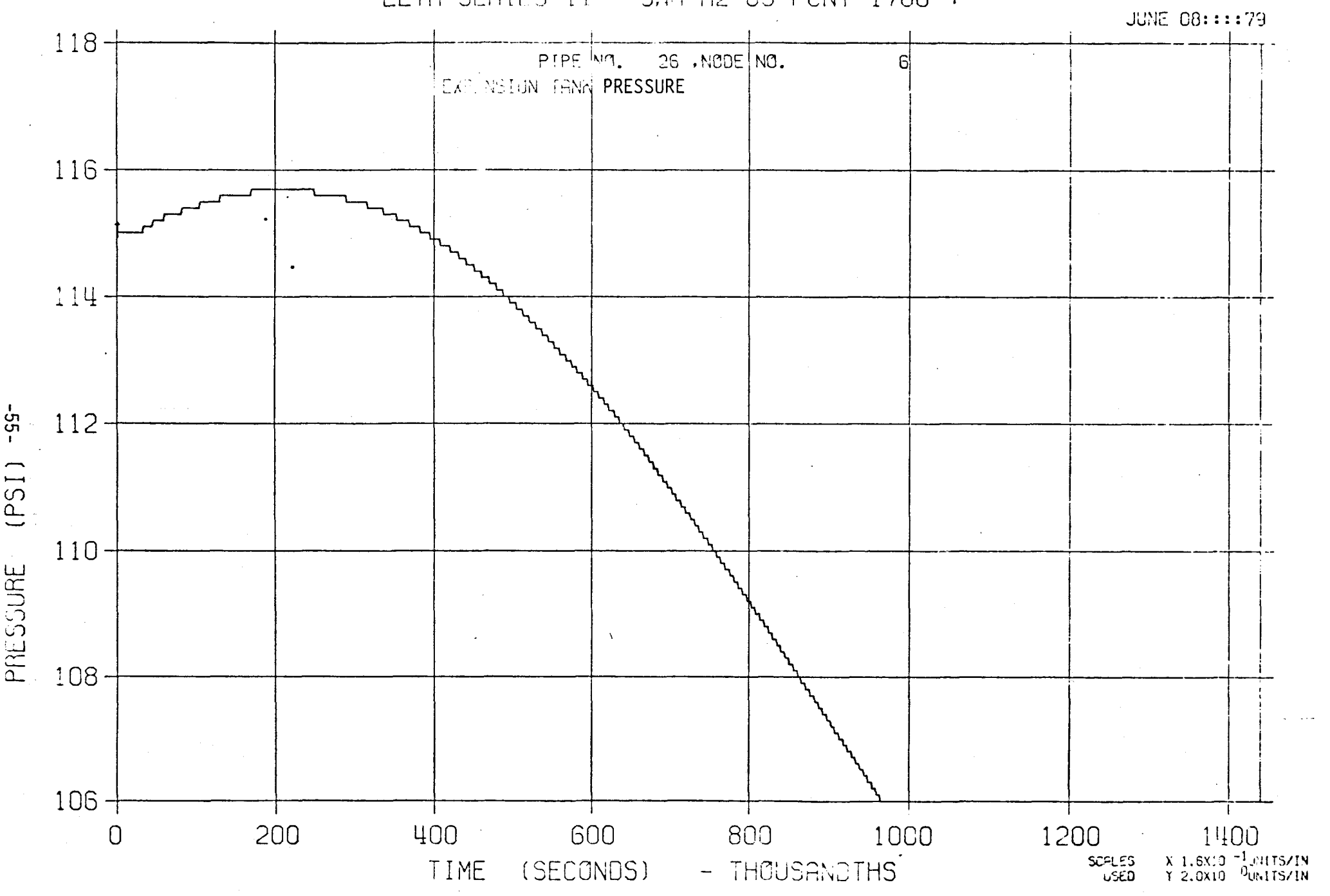
LLTR SERIES II - SWR A2 65 PCNT 1700 °F
JUNE 08::::79
PIPE NO. 26 ,NODE NO. 6
EXPANSION TANK PRESSURE
118
116
114
112
110
108
106
PRESSURE (PSI)
0
200
400
600
800
1000
1200
1400
TIME (SECONDS) - THOUSANDTHS
SCALES USED
X 1.6X10 -1 UNITS/IN
Y 2.0X10 0 UNITS/IN

FIGURE 24-L

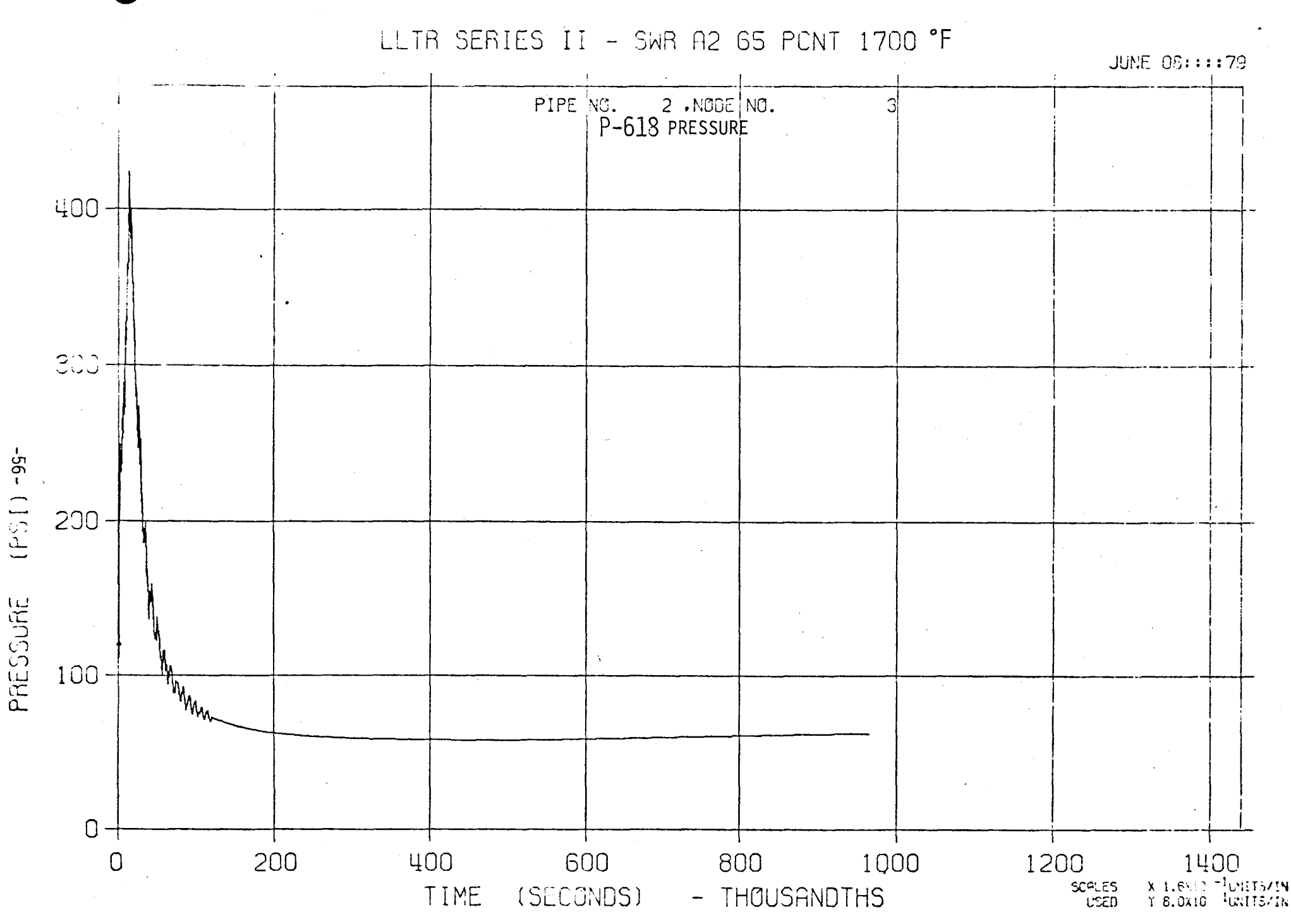
LLTR SERIES II - SWR A2 65 PCNT 1700 °F
JUNE 06::::79
PIPE NO. 2 ,NODE NO. 3
P-618 PRESSURE
400
300
200
100
0
PRESSURE (PSI)
0
200
400
600
800
1000
1200
1400
TIME (SECONDS) - THOUSANDTHS
SCALES USED
X 1.6X10 -1 UNITS/IN
Y 8.0X10 1 UNITS/IN

5

FIGURE 24-S

LLTR SERIES II - SWR A2 65 PCNT 1700 °F

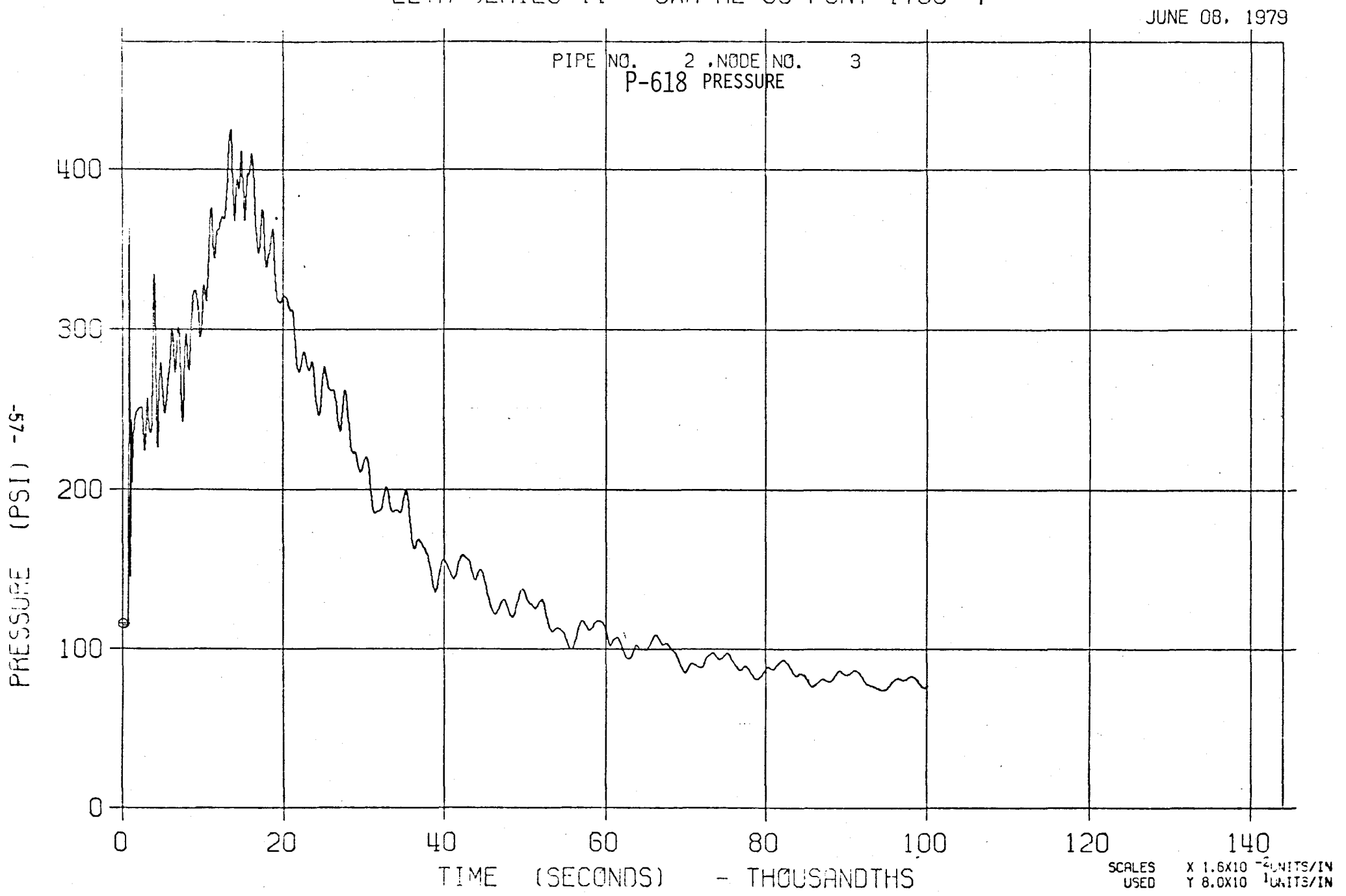

FIGURE 25-L

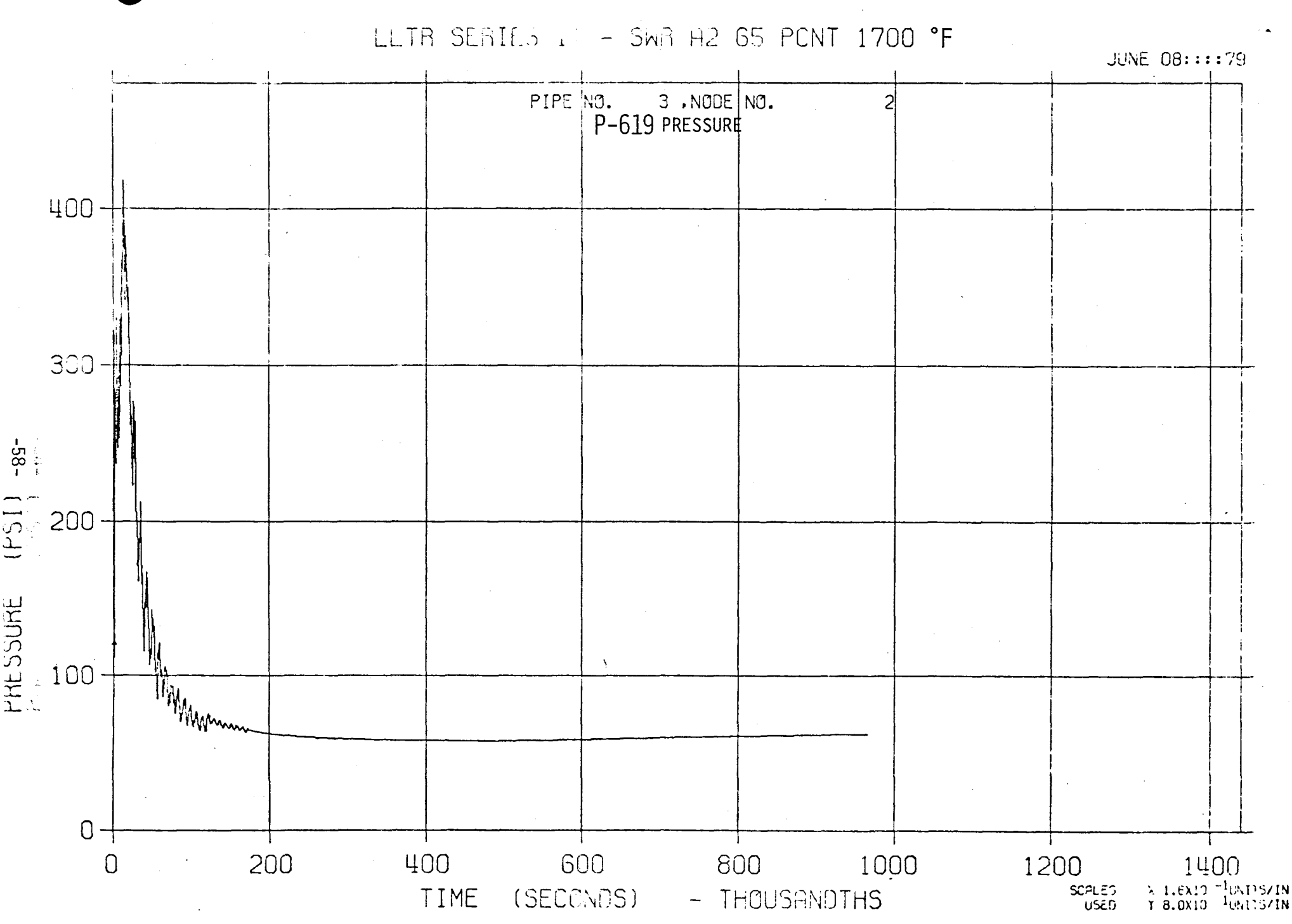
LLTR SERIES 1 - SWR H2 65 PCNT 1700 °F
JUNE 08::::79
PIPE NO. 3 ,NODE NO. 2
P-619 PRESSURE
400
300
200
100
0
PRESSURE (PSI)
0
200
400
600
800
1000
1200
1400
TIME (SECONDS) - THOUSANDTHS
SCALES USED
X 1.6X10 -1 UNITS/IN
Y 8.0X10 1 UNITS/IN

FIGURE 25-S

LLTR SERIES II - SWR A2 65 PCNT 1700 °F

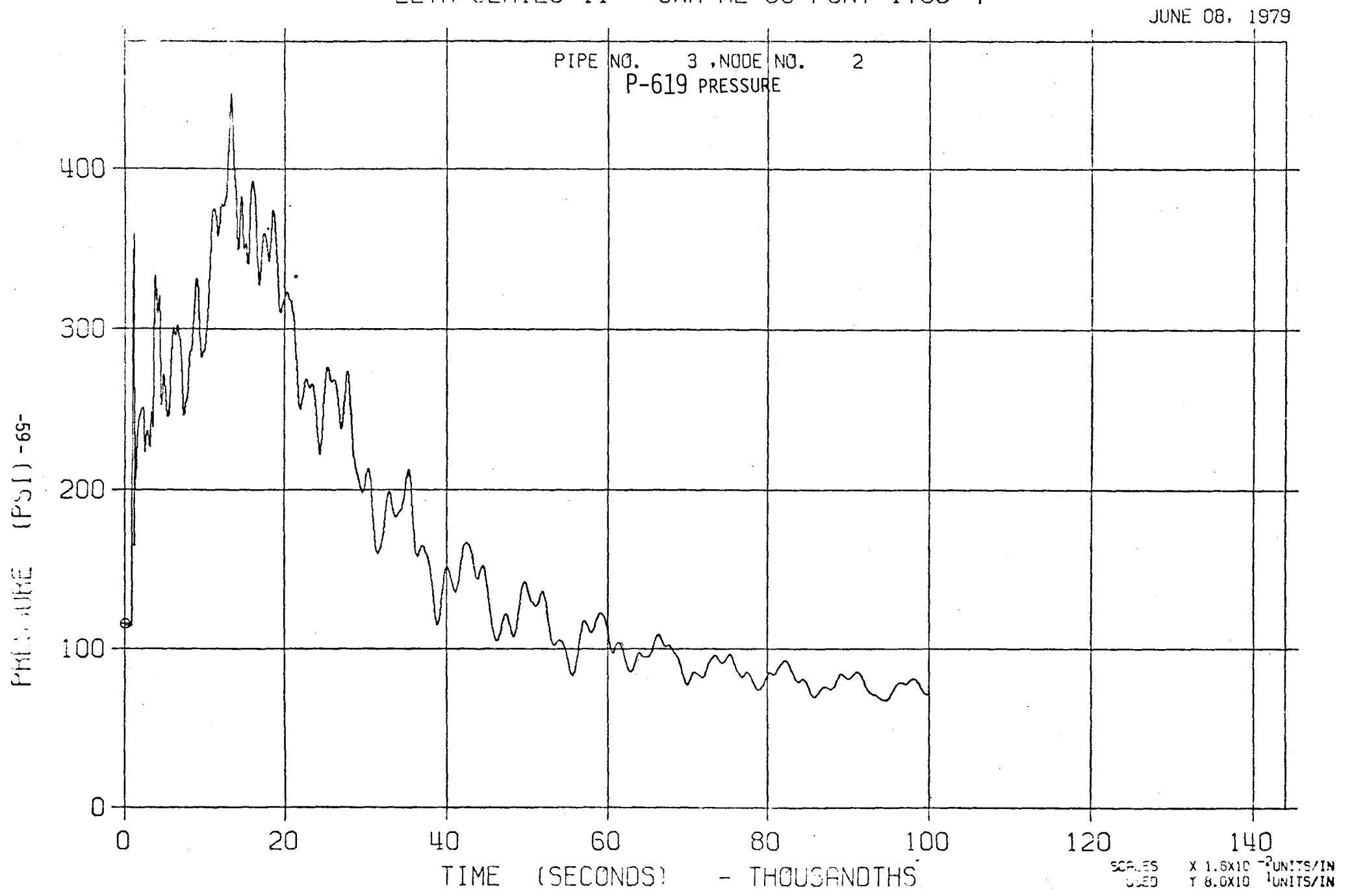

FIGURE 26-L

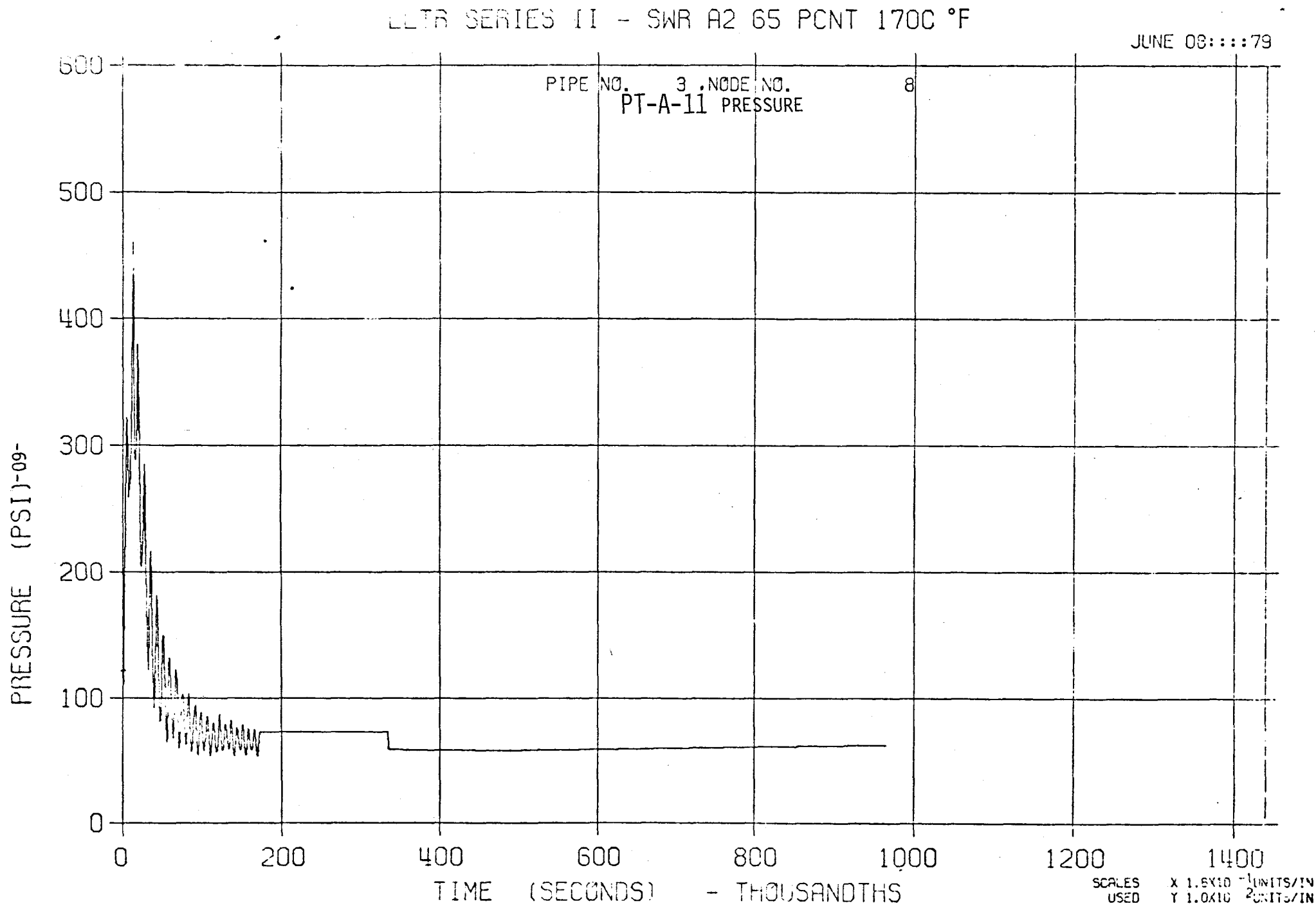
LLTR SERIES II - SWR A2 65 PCNT 170C °F
JUNE 08::::79
PIPE NO. 3 ,NODE NO. 8
PT-A-11 PRESSURE
PRESSURE (PSI)-09-
600
500
400
300
200
100
0
0
200
400
600
800
1000
1200
1400
TIME (SECONDS) - THOUSANDTHS
SCALES USED
X 1.6X10 -1 UNITS/IN
Y 1.0X10 2 UNITS/IN

FIGURE 26-S

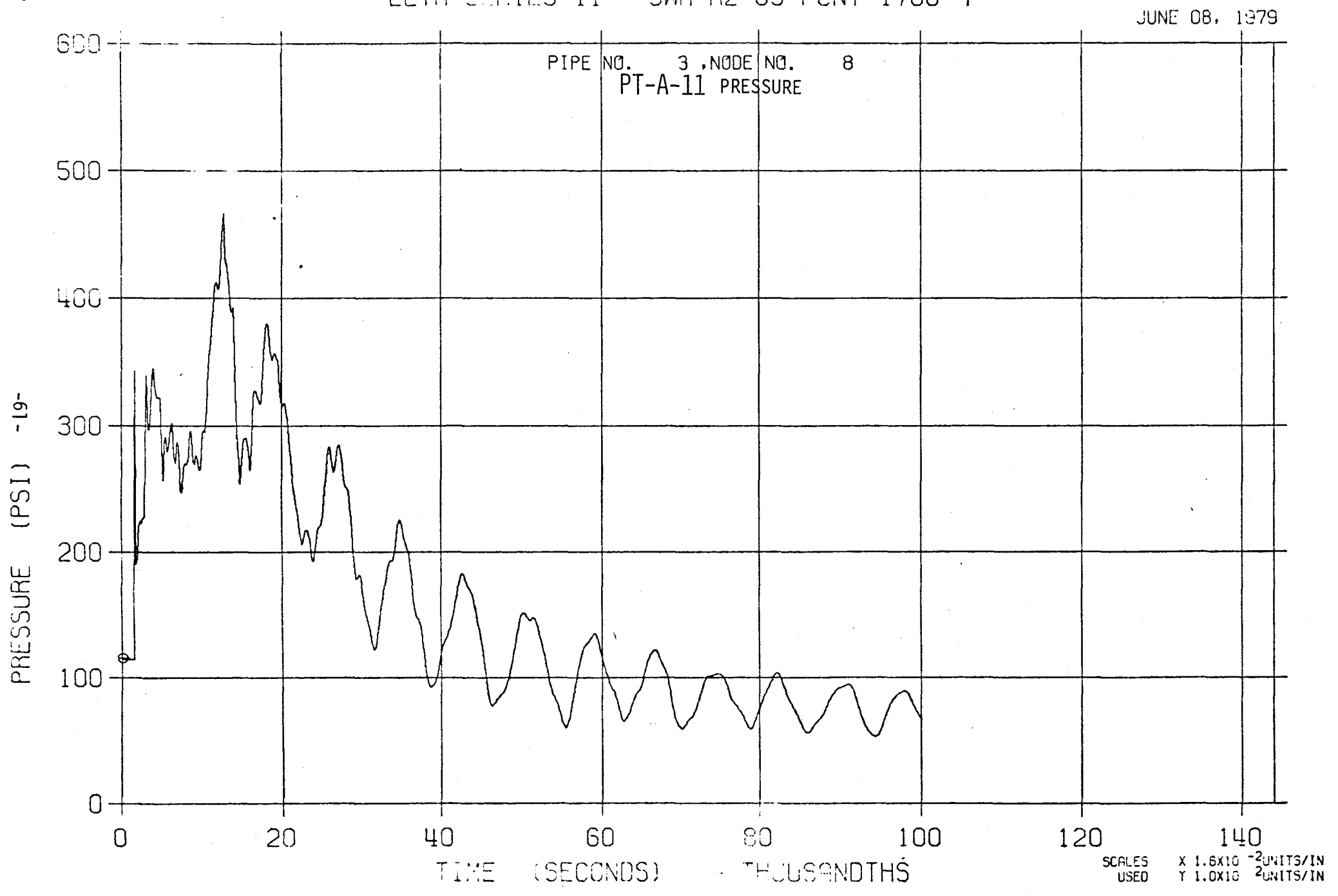
LLTA SERIES II - SWR A2 65 PCNT 1700 °F
JUNE 08, 1979
PIPE NO. 3 ,NODE NO. 8
PT-A-11 PRESSURE
PRESSURE (PSI)
600
500
400
300
200
100
0
0
20
40
60
80
100
120
140
TIME (SECONDS) - THOUSANDTHS
SCALES USED
X 1.6X10 -2 UNITS/IN
Y 1.0X10 2 UNITS/IN

27-L

FIGURE 27-L

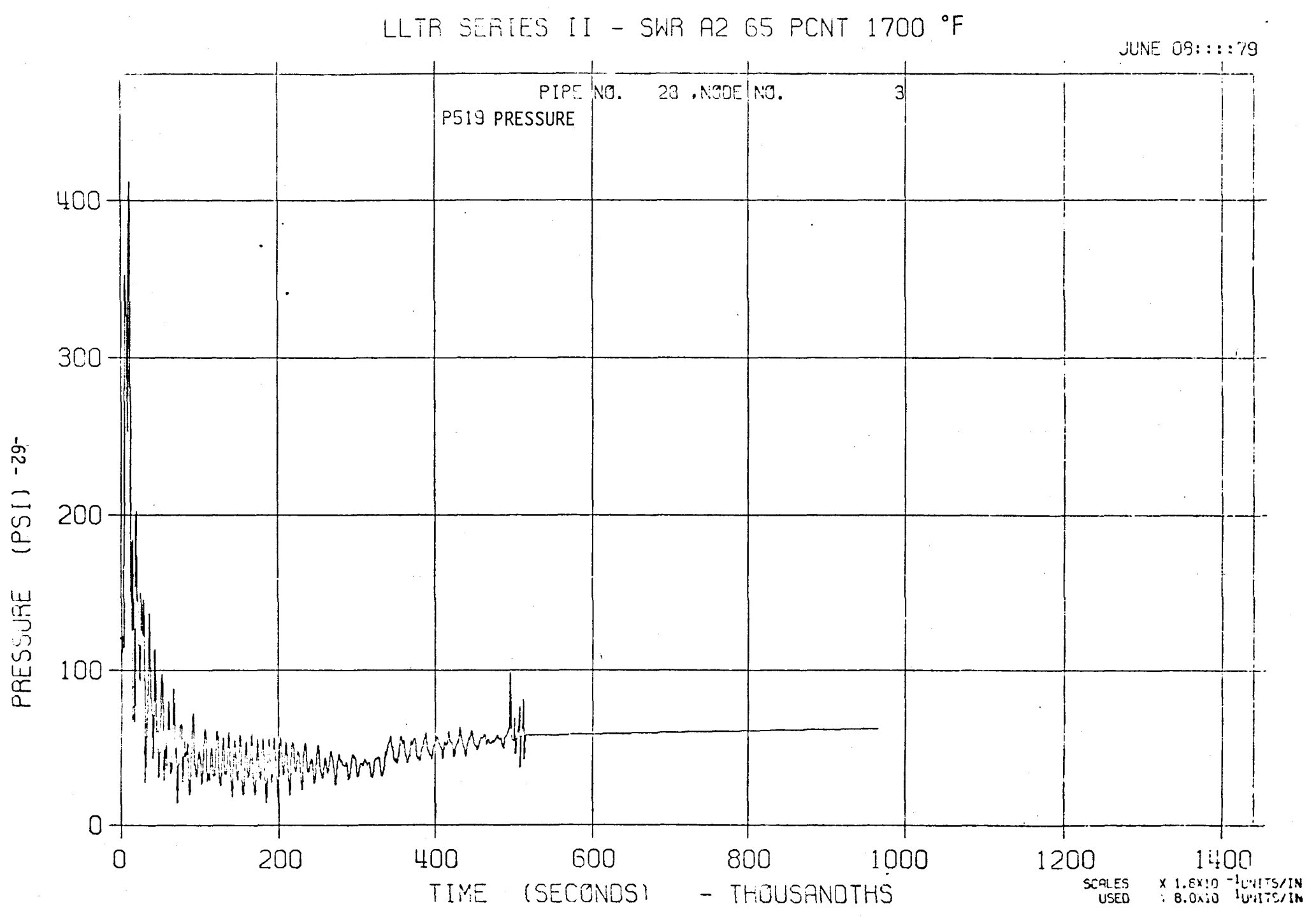

27-S

FIGURE 27-S

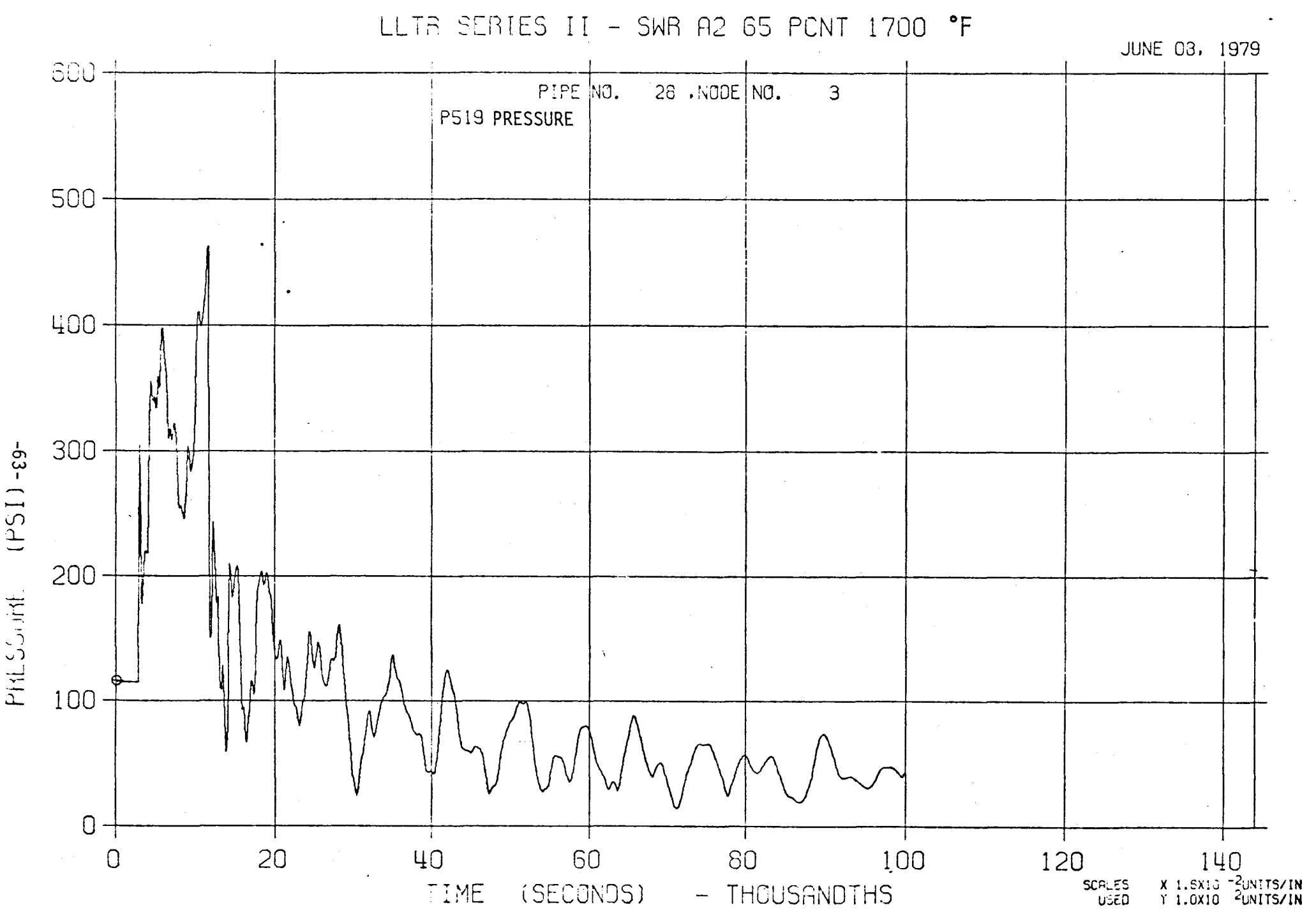

28-L

FIGURE 28-L

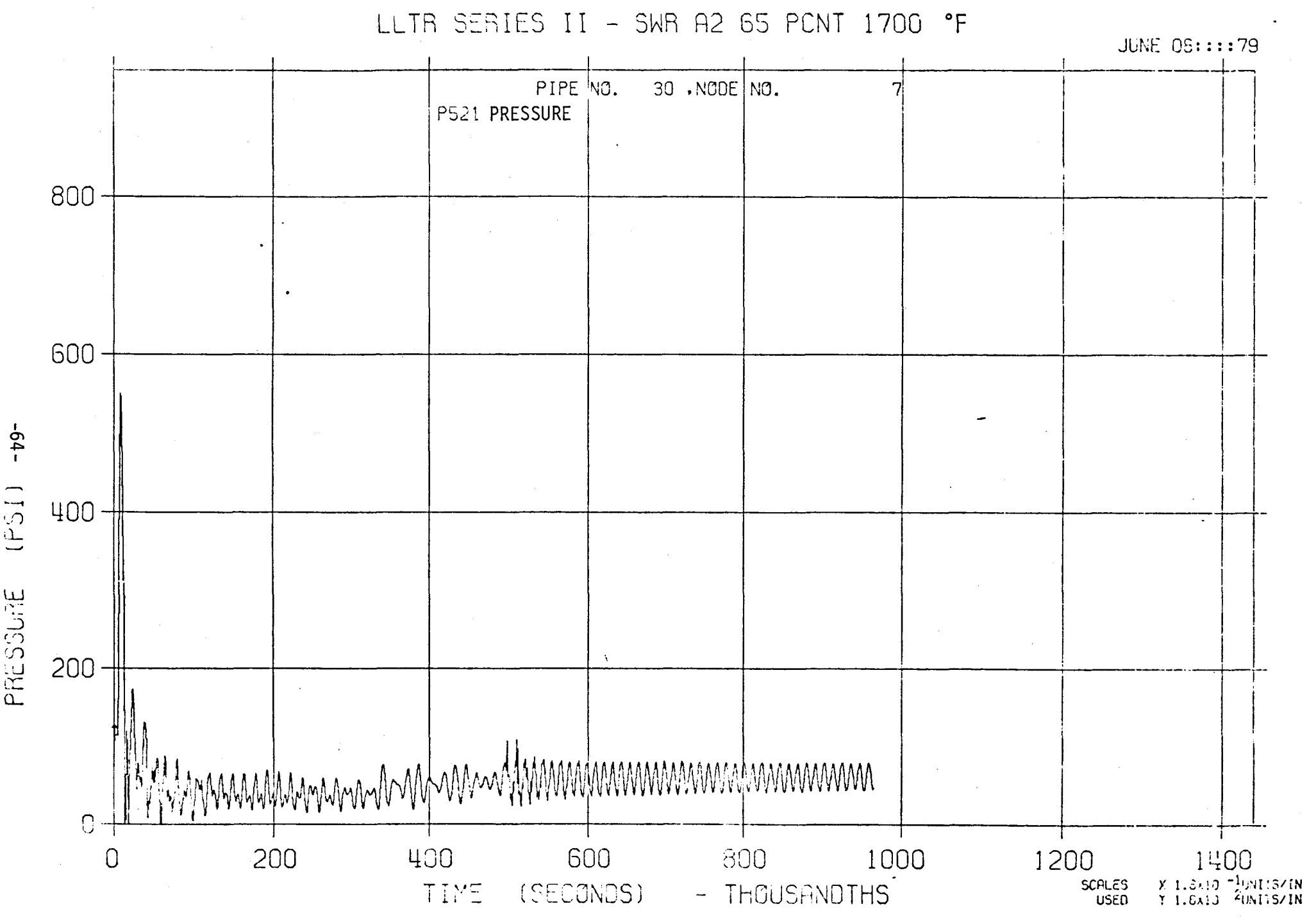

FIGURE 28-S

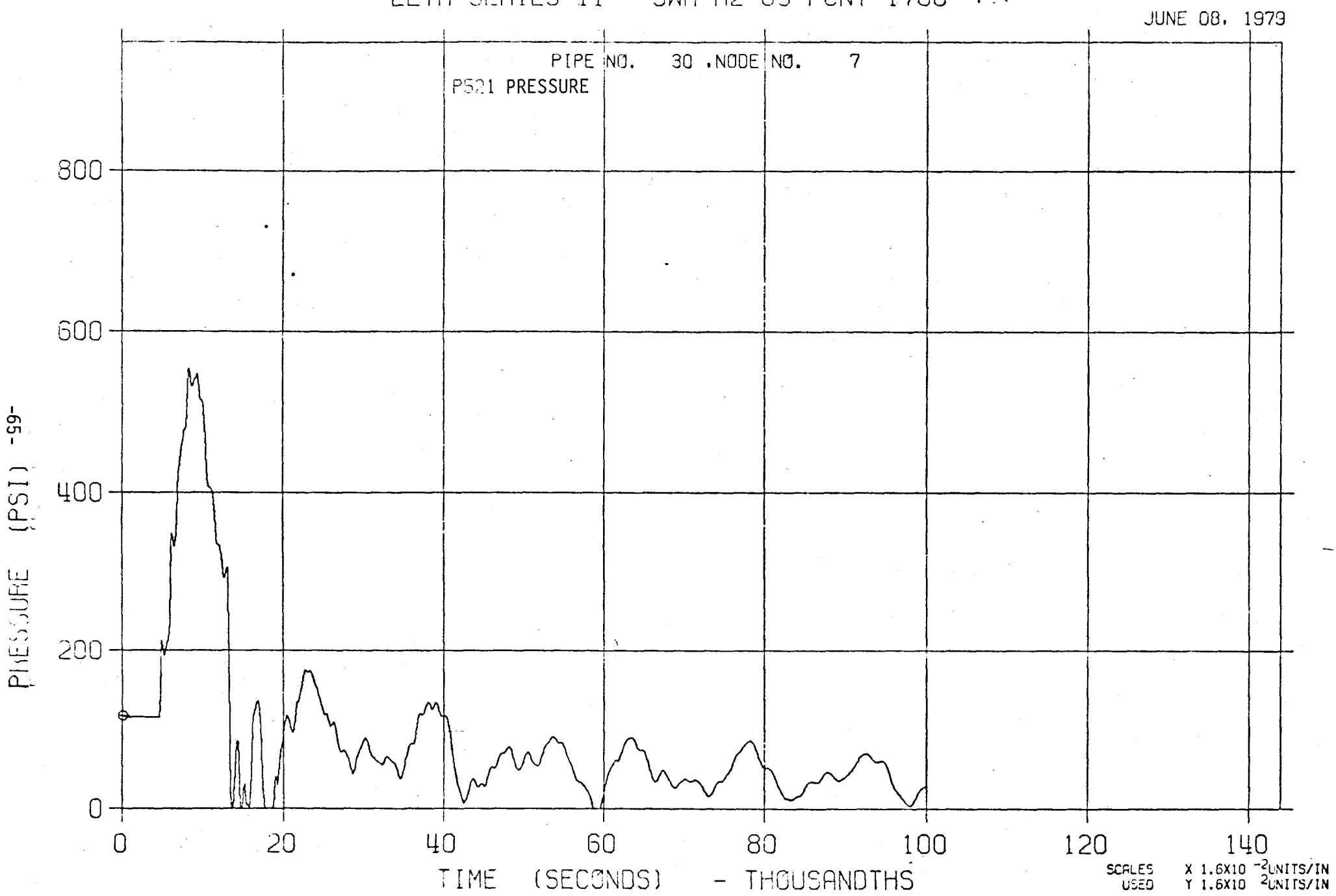
LLTR SERIES II - SWR A2 65 PCNT 1700 °F
JUNE 08, 1979
PIPE NO. 30 .NODE NO. 7
P521 PRESSURE
800
600
400
200
0
PRESSURE (PSI) -99-
0
20
40
60
80
100
120
140
TIME (SECONDS) - THOUSANDTHS
SCALES USED
X 1.6X10 -2UNITS/IN
Y 1.6X10 2UNITS/IN

29-L

FIGURE 29-L

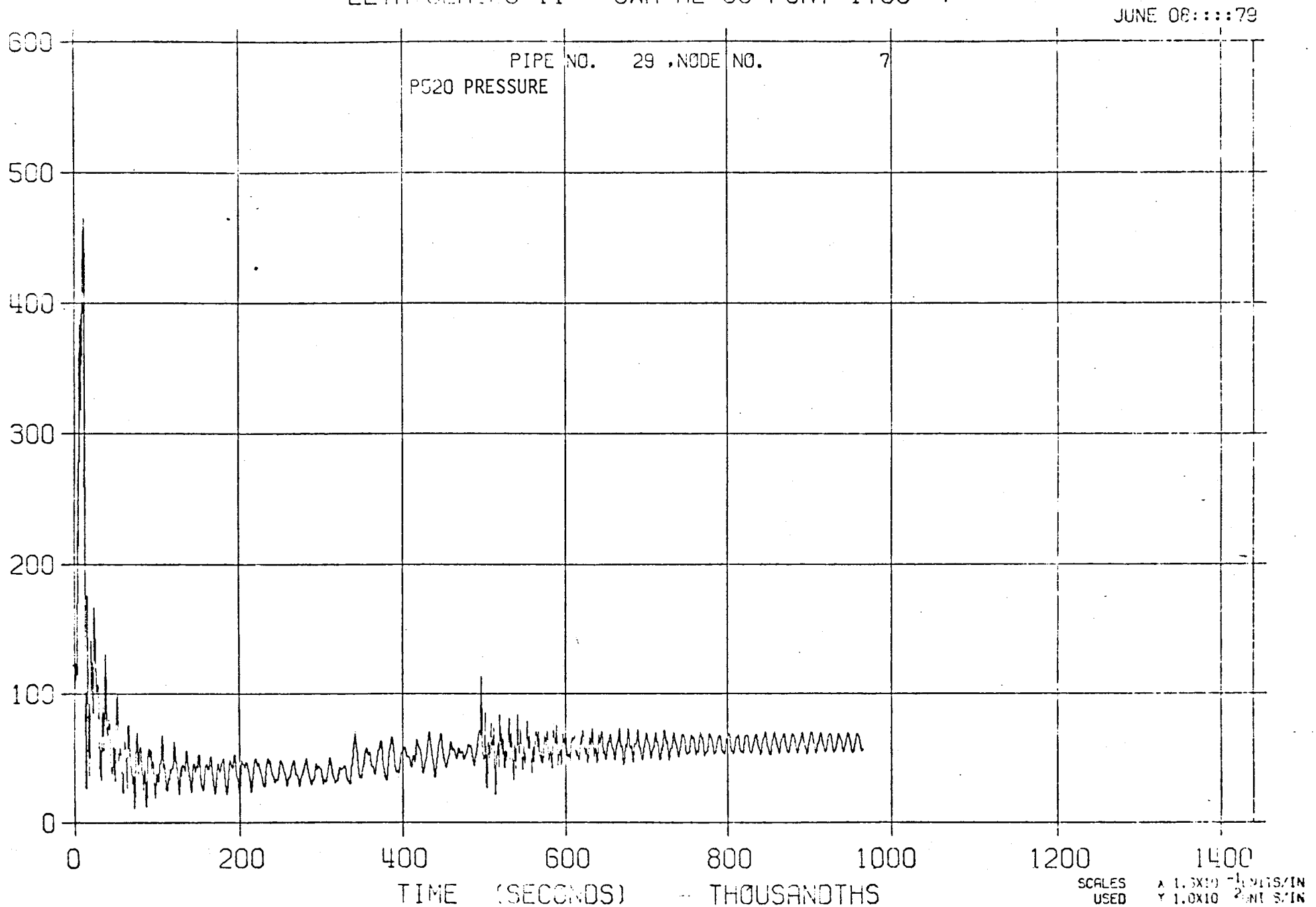

FIGURE 29-S

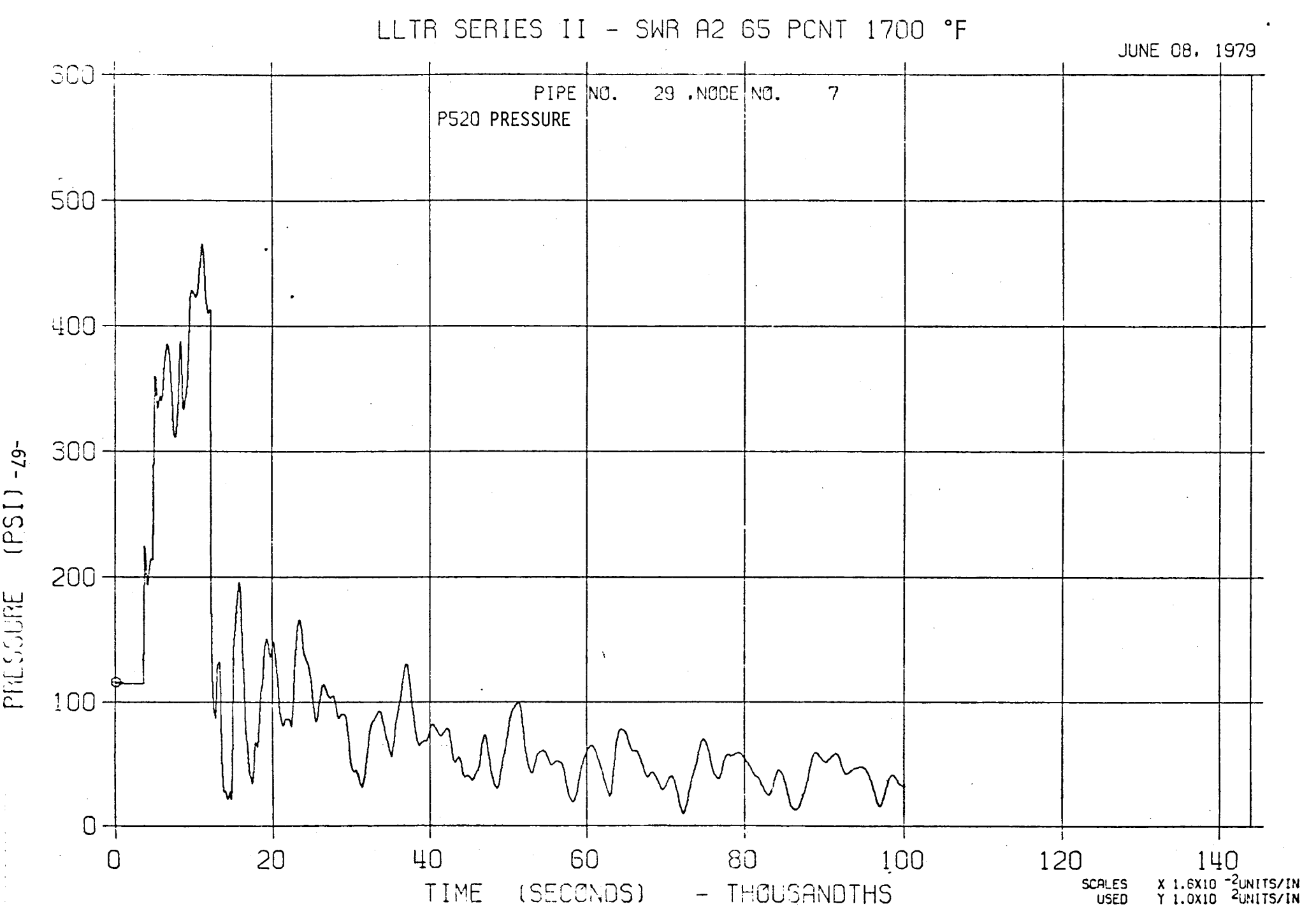
LLTR SERIES II - SWR A2 65 PCNT 1700 °F
JUNE 08, 1979
PIPE NO. 29 ,NODE NO. 7
P520 PRESSURE
PRESSURE (PSI) -29-
300
500
400
300
200
100
0
0
20
40
60
80
100
120
140
TIME (SECONDS) - THOUSANDTHS
SCALES USED
X 1.6X10 -2 UNITS/IN
Y 1.0X10 2 UNITS/IN

FIGURE 30-L

LLTR SERIES II - SWR A2 65 PCNT 1700 °F

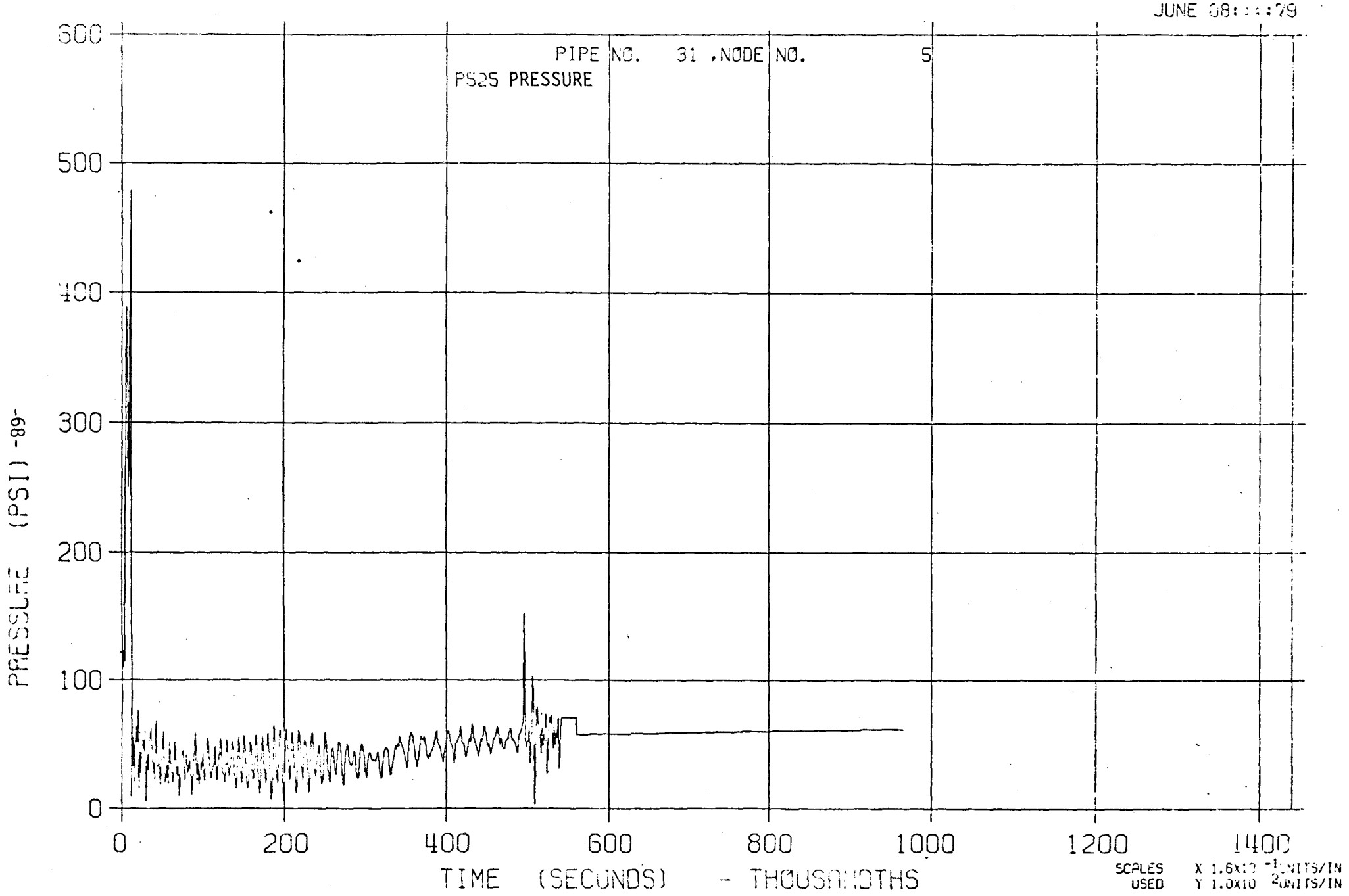

FIGURE 30-S

LLTR SERIES II - SWR A2 65 PCNT 1700 °F

JUNE 08, 1979

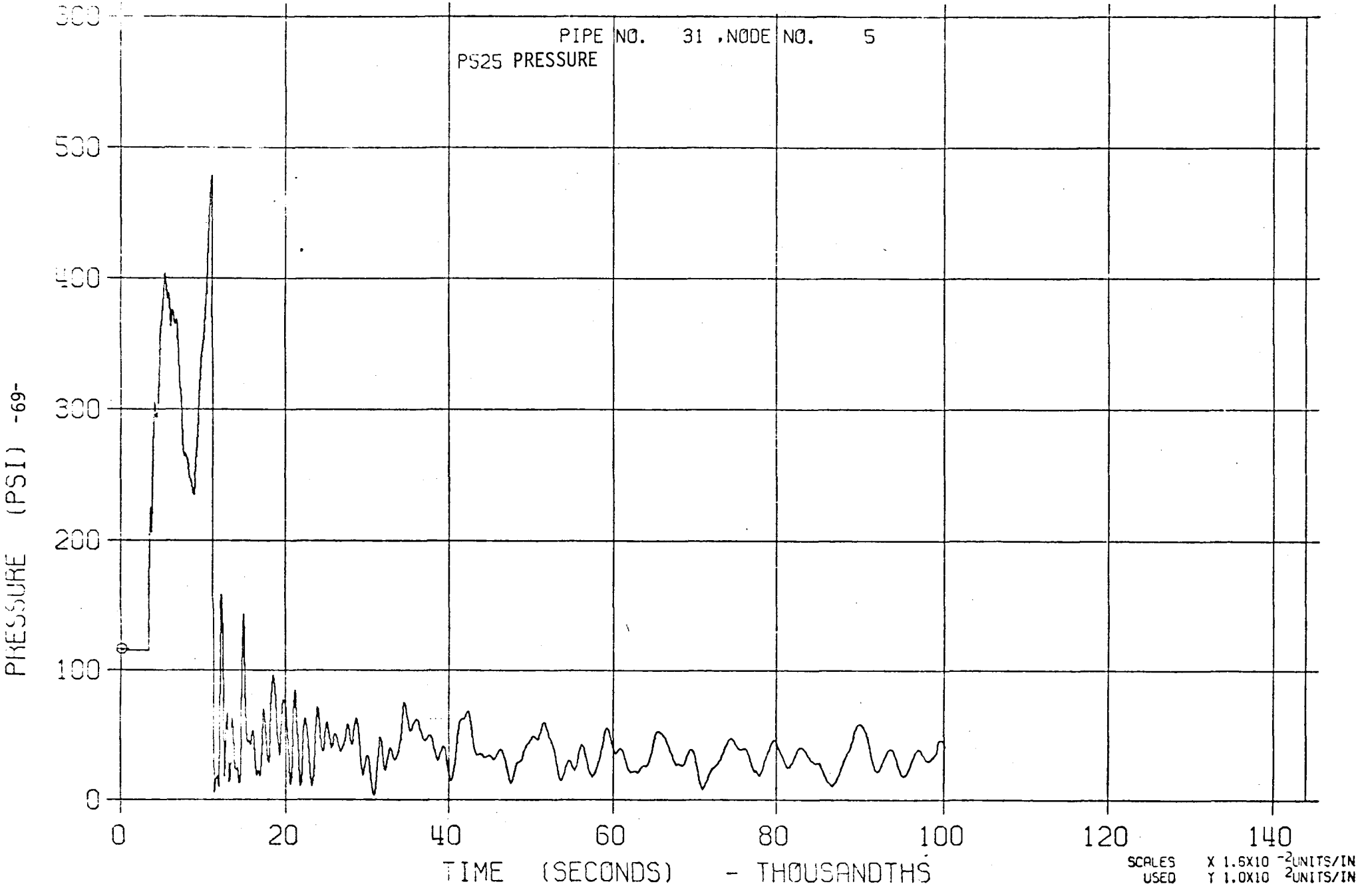

FIGURE 31-L

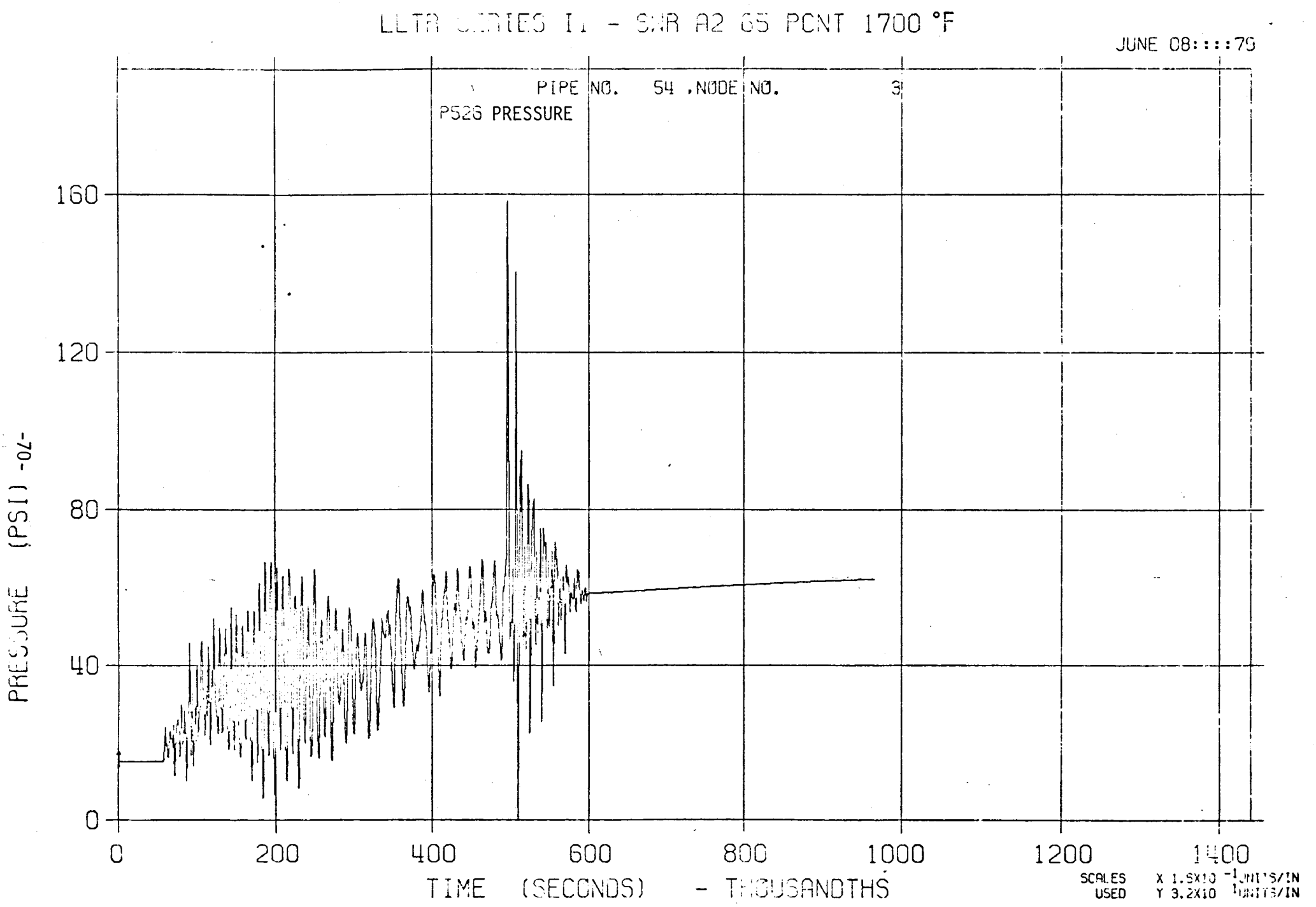
LLTR SERIES I - SNR A2 65 PCNT 1700 °F
JUNE 08::::79
PIPE NO. 54 ,NODE NO. 3
PS26 PRESSURE
160
120
80
40
0
PRESSURE (PSI) -07-
0
200
400
600
800
1000
1200
1400
TIME (SECONDS) - THOUSANDTHS
SCALES USED
X 1.5X10 -1 UNITS/IN
Y 3.2X10 1 UNITS/IN

31-S

FIGURE 31-S

LLTR SERIES II - SWR A2 65 PCNT 1700 °F

JUNE 08, 1979

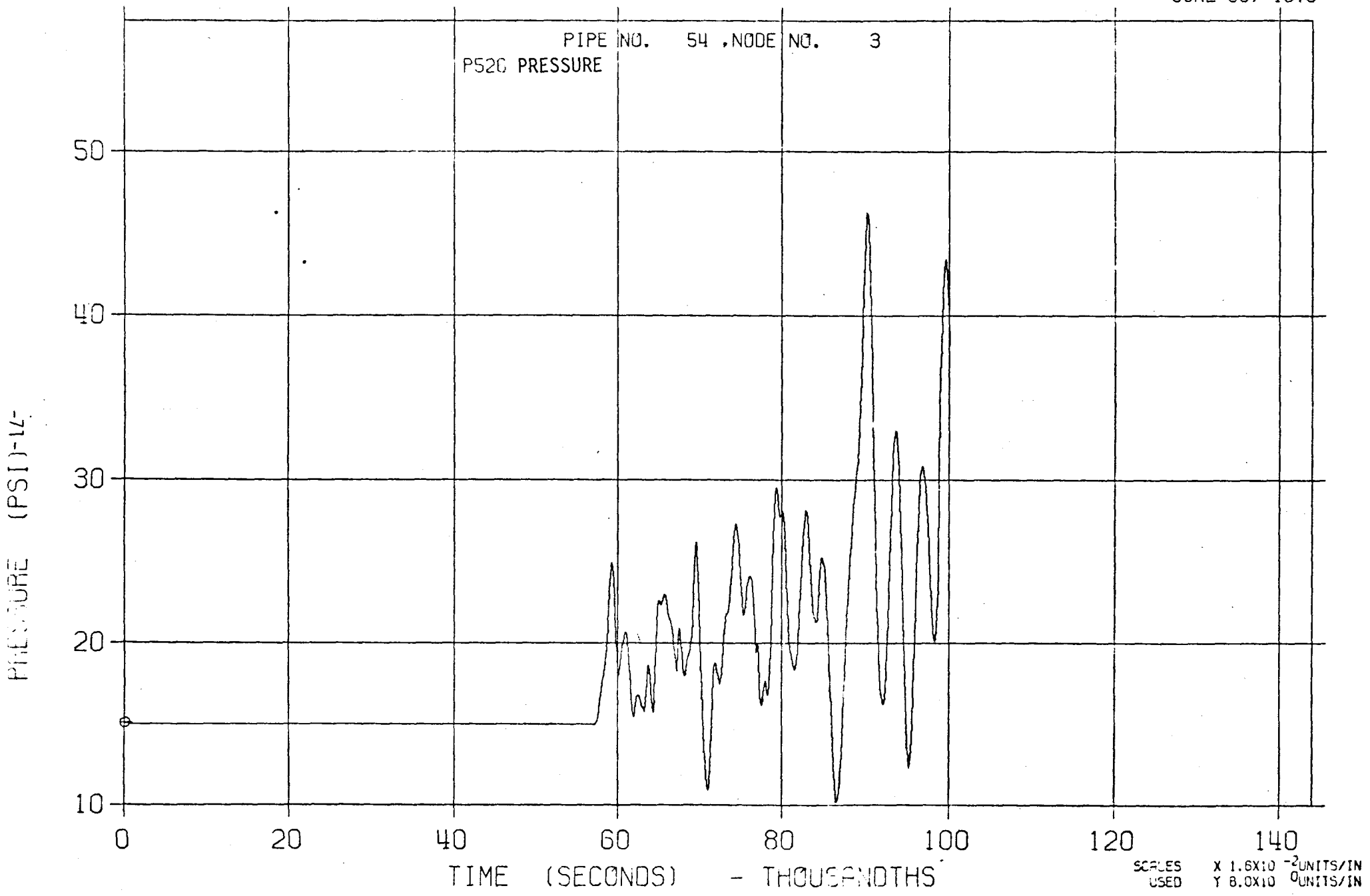

32-4

FIGURE 32-L

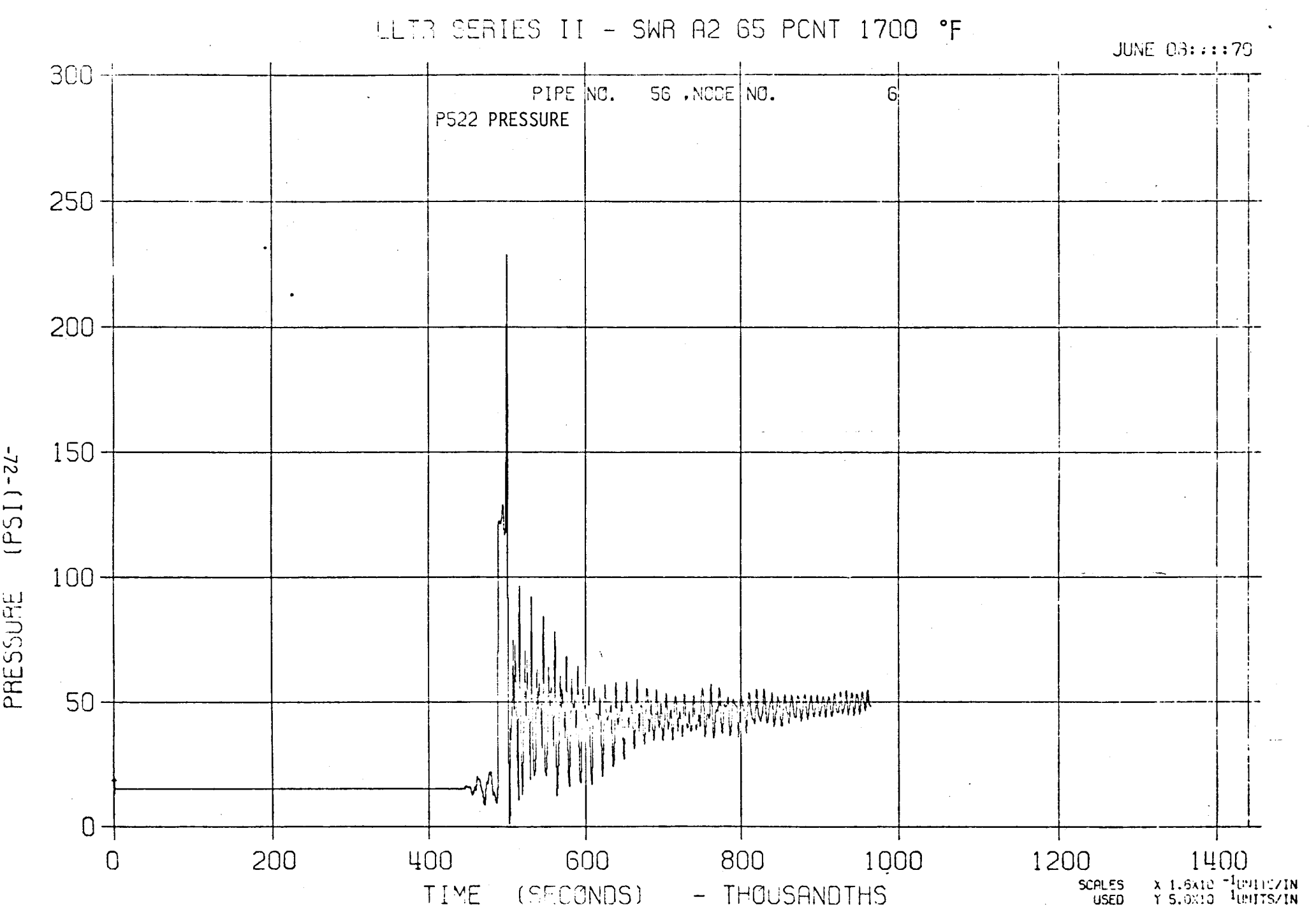

33-L

FIGURE 33-L

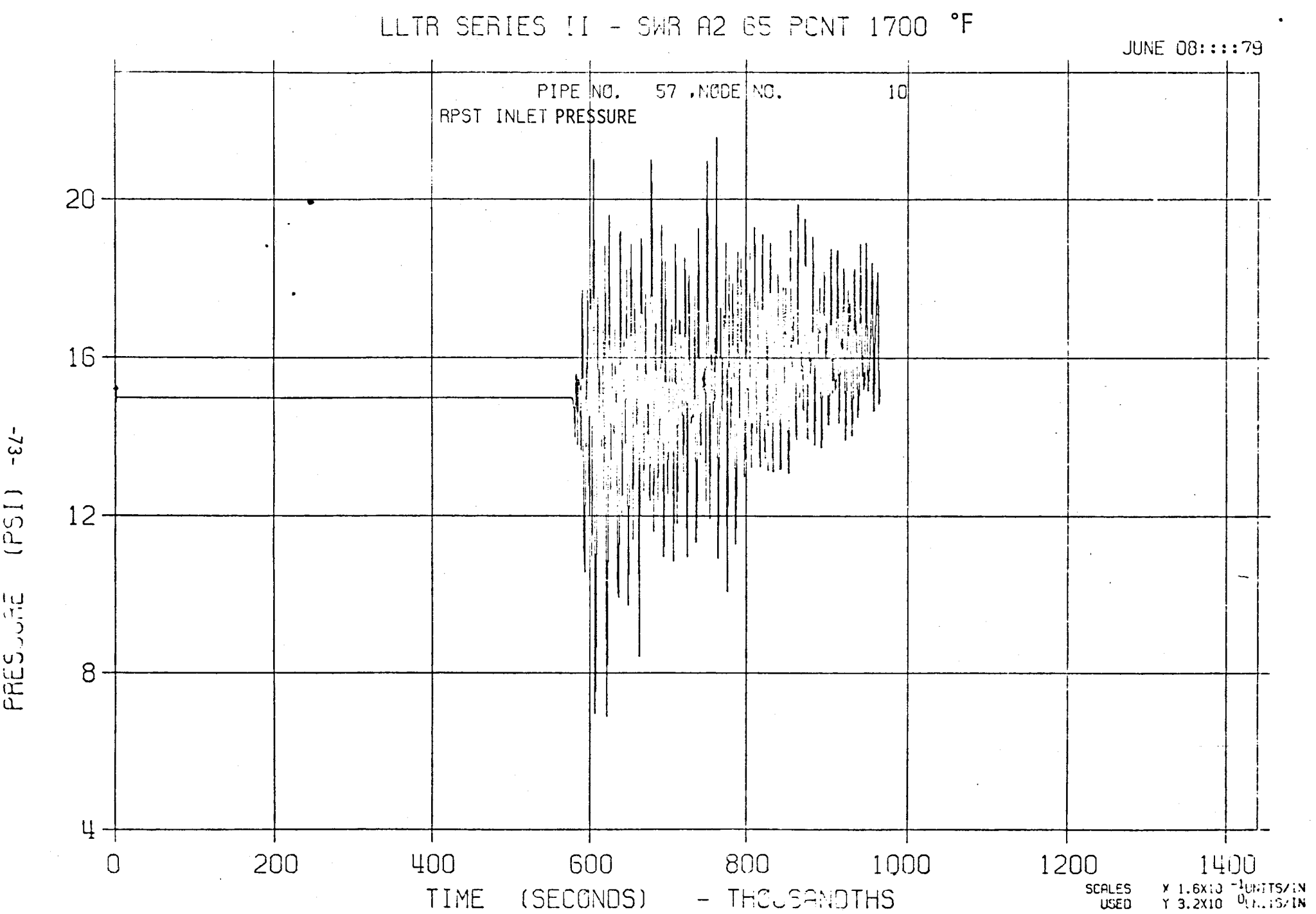

34-L

FIGURE 34-L

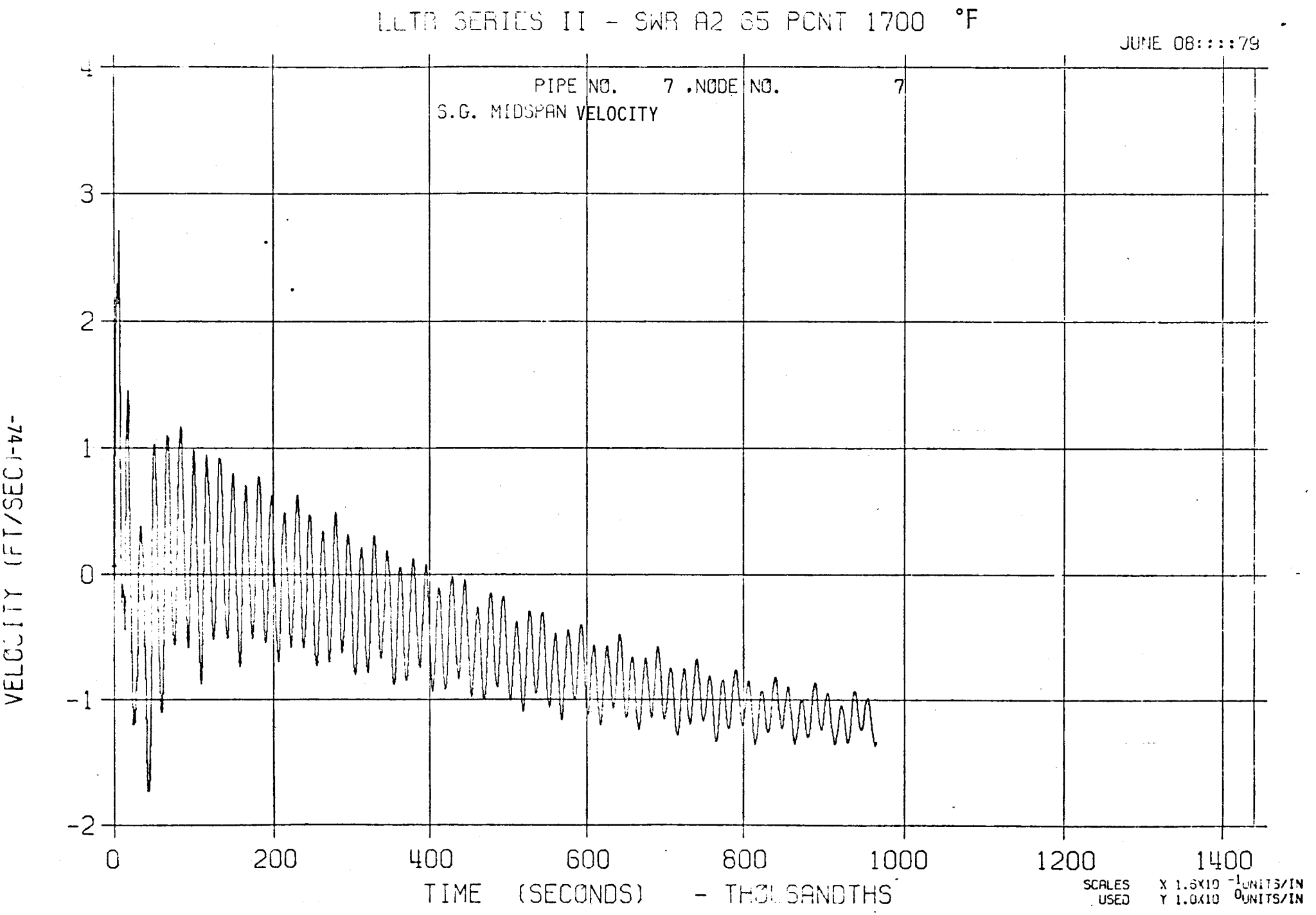

34-S

FIGURE 34-S

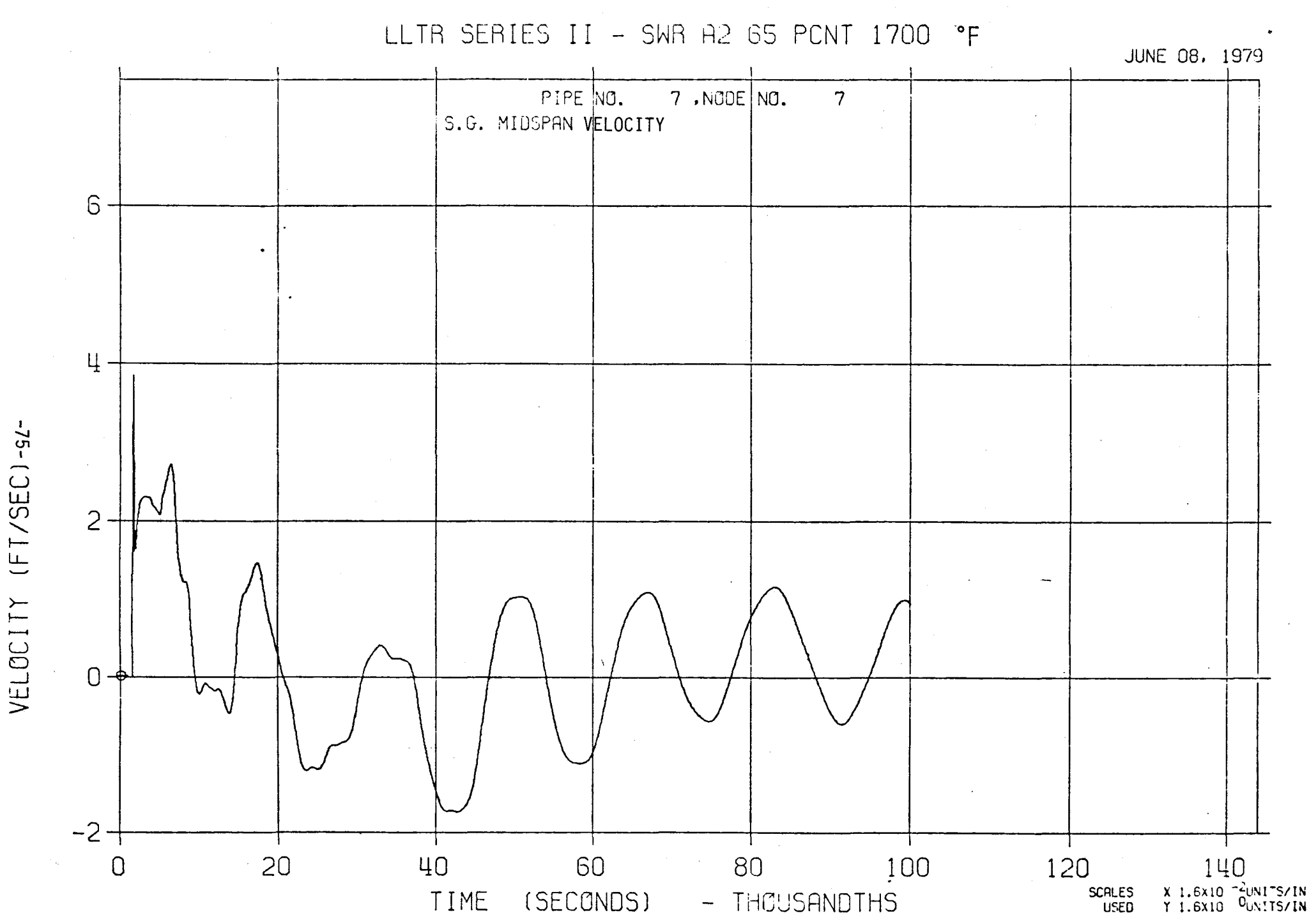

35-L

FIGURE 35-L

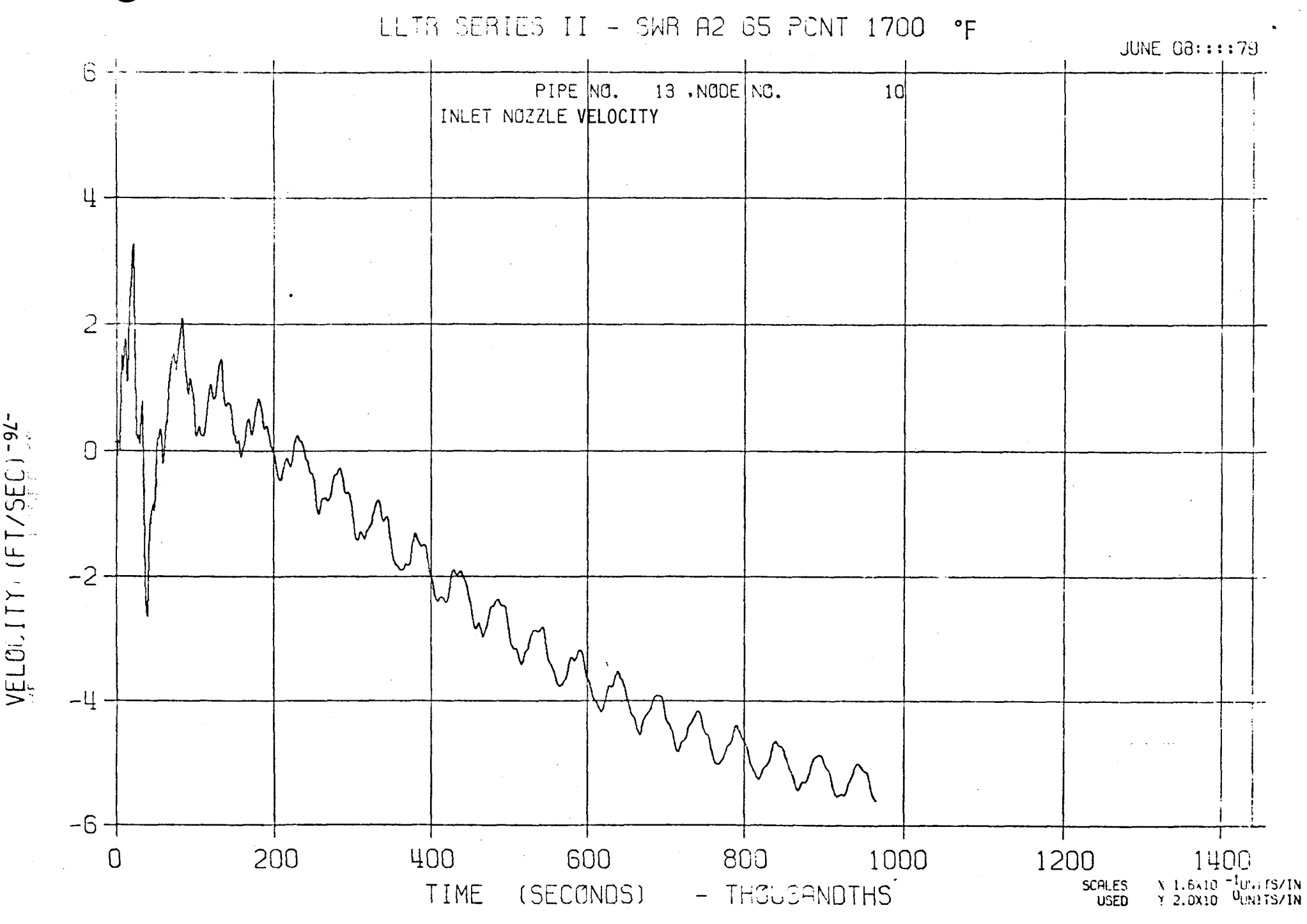

35-S

FIGURE 35-S

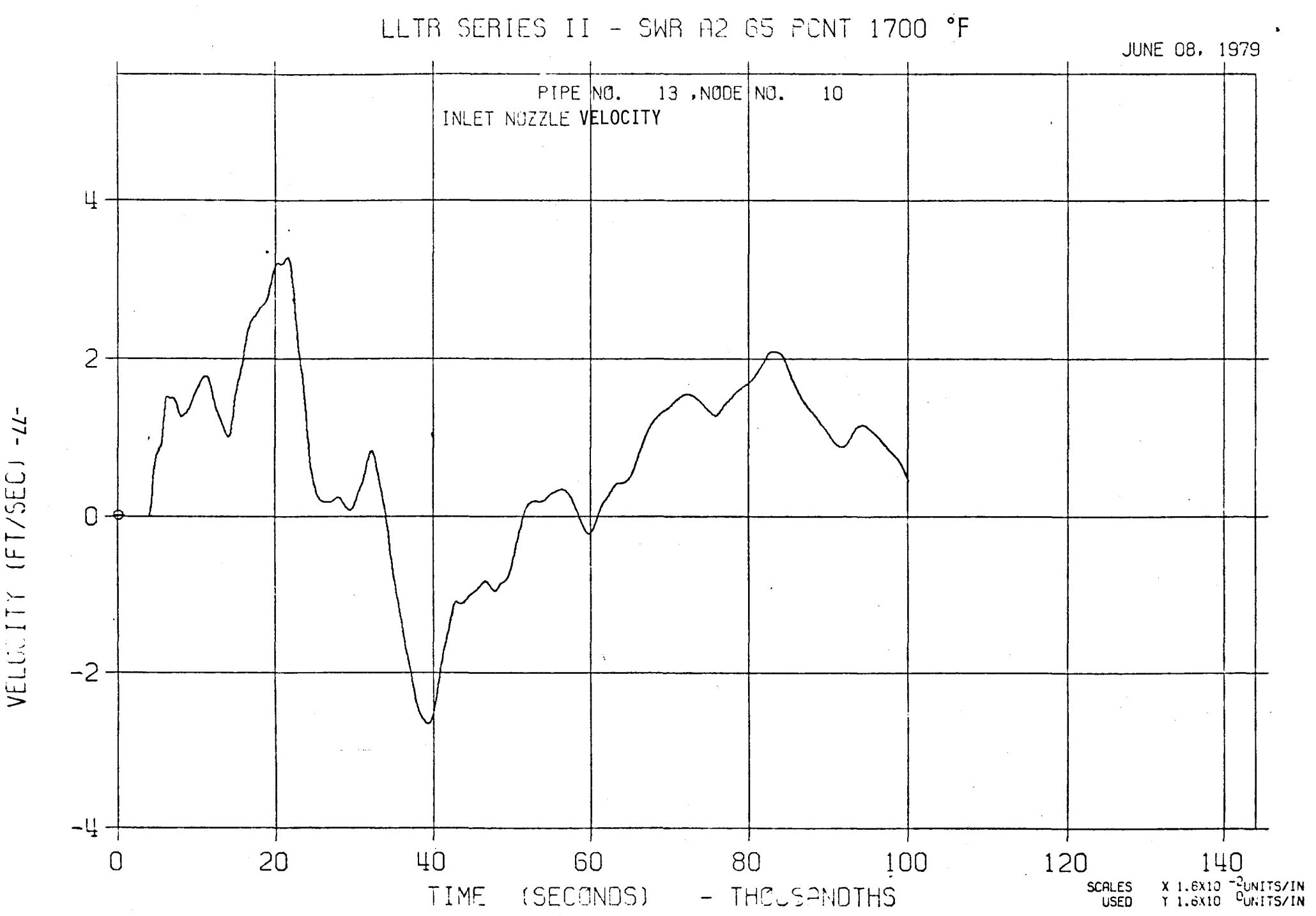

36-C

FIGURE 36-L

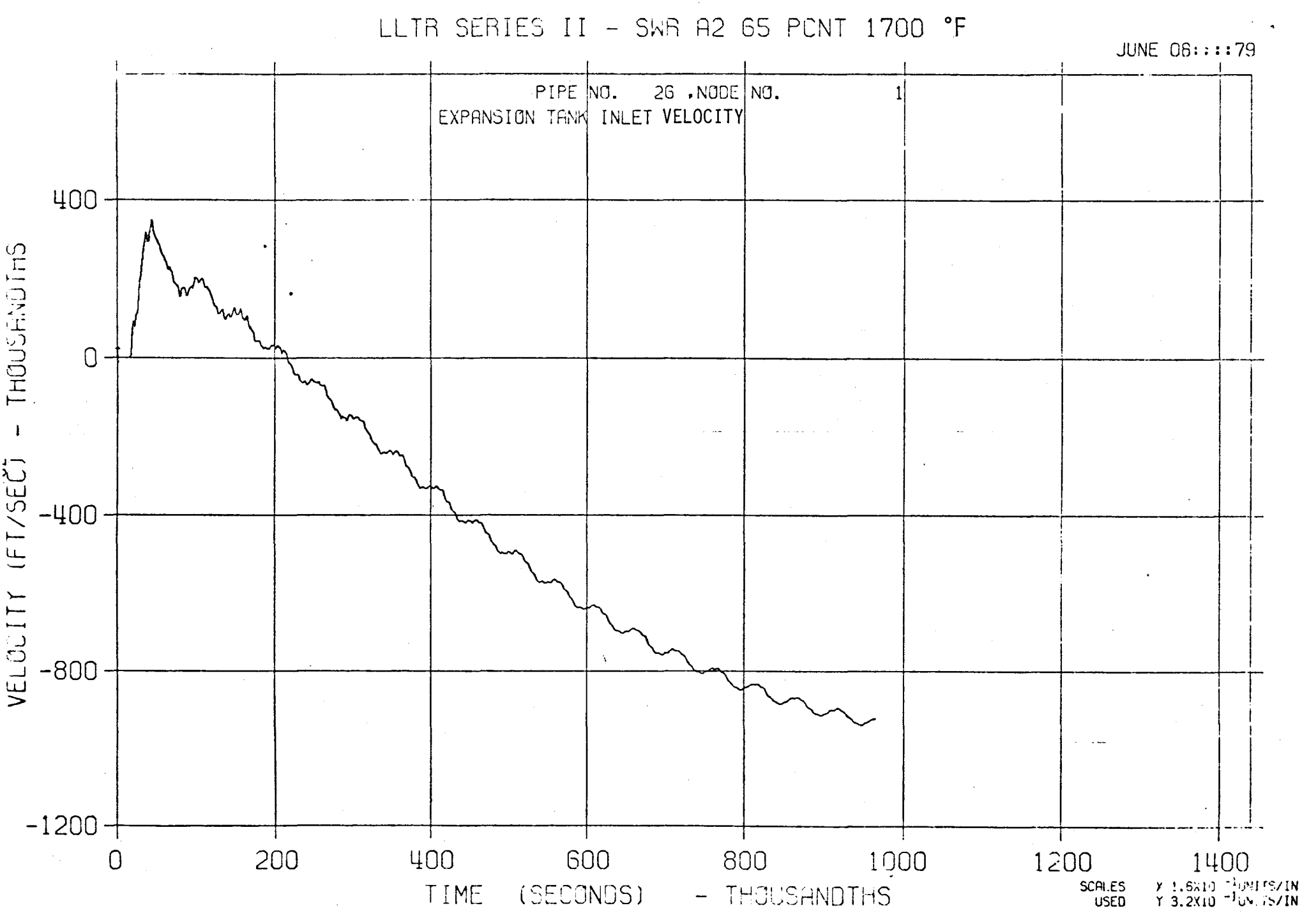

FIGURE 36-S

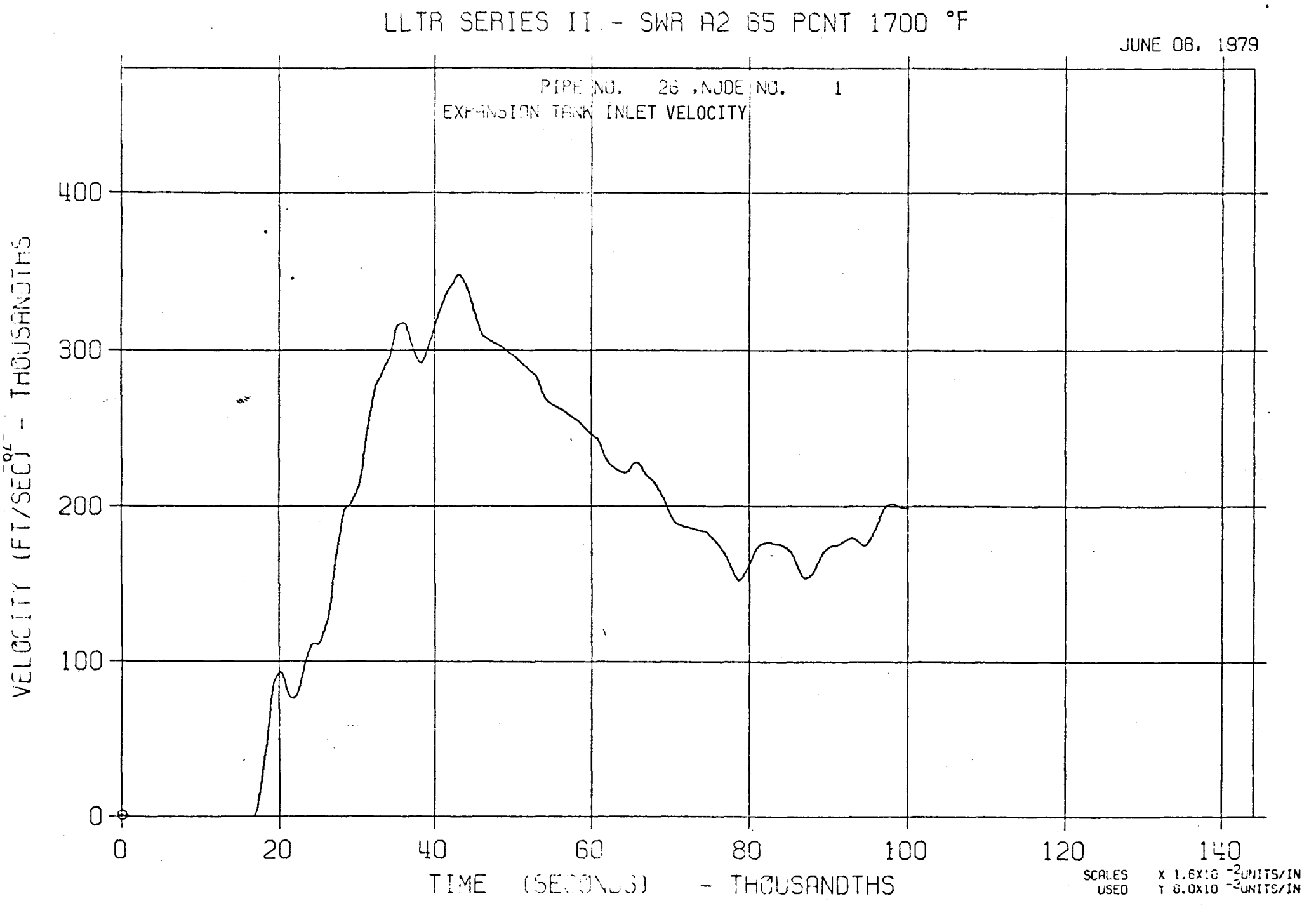
LLTR SERIES II - SWR A2 65 PCNT 1700 °F
JUNE 08, 1979
PIPE NO. 26 ,NODE NO. 1
EXPANSION TANK INLET VELOCITY
VELOCITY (FT/SEC) - THOUSANDTHS
400
300
200
100
0
0
20
40
60
80
100
120
140
TIME (SECONDS) - THOUSANDTHS
SCALES USED
X 1.6X10 -2 UNITS/IN
Y 8.0X10 -2 UNITS/IN

37-C

FIGURE 37-L

LLTR SERIES II - SWR A2 65 PCNT 1700 °F

JUNE 08::::79

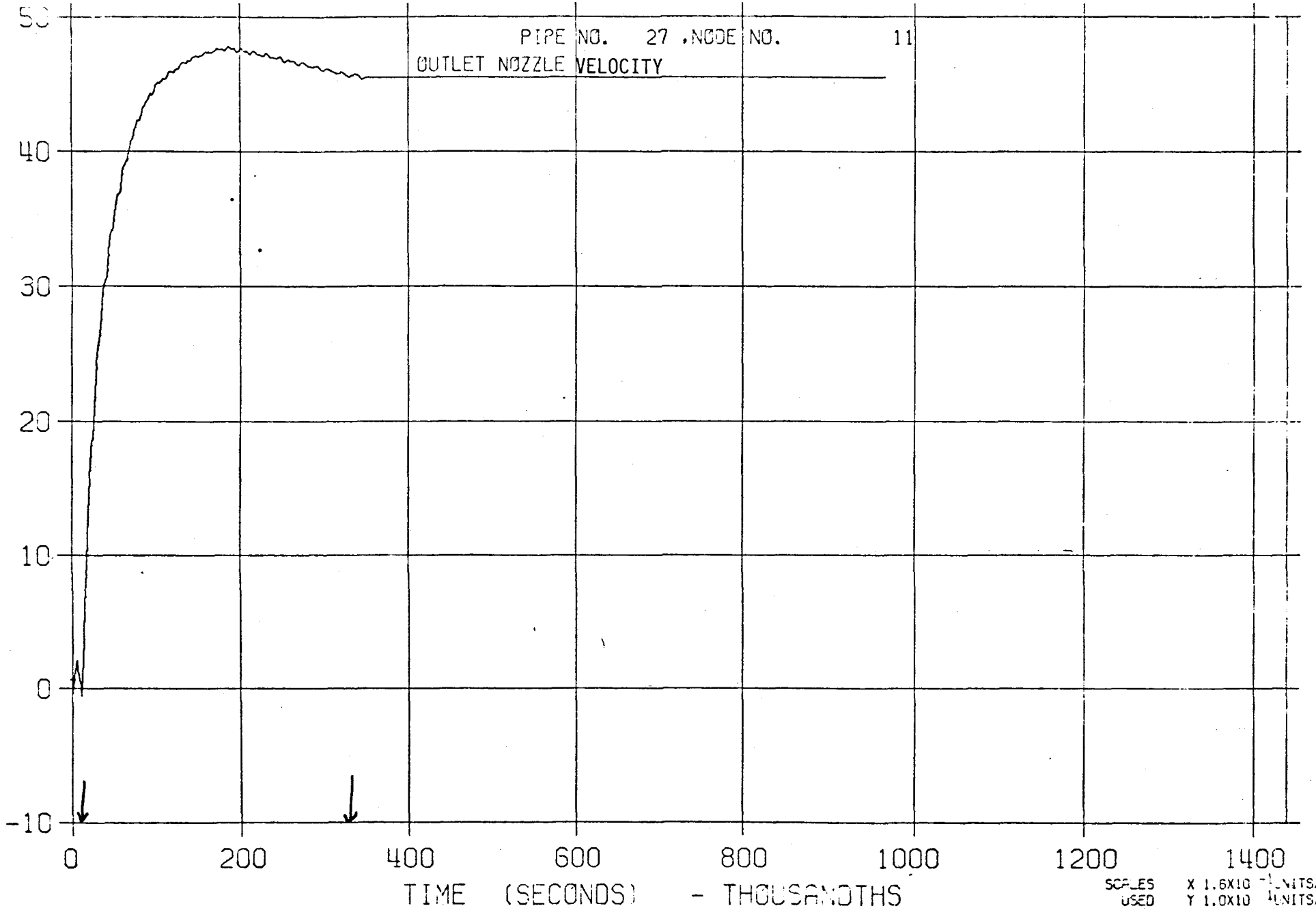

37-S

FIGURE 37-S

LLTR SERIES II - SWR A2 65 PCNT 1700 °F

JUNE 08, 1979

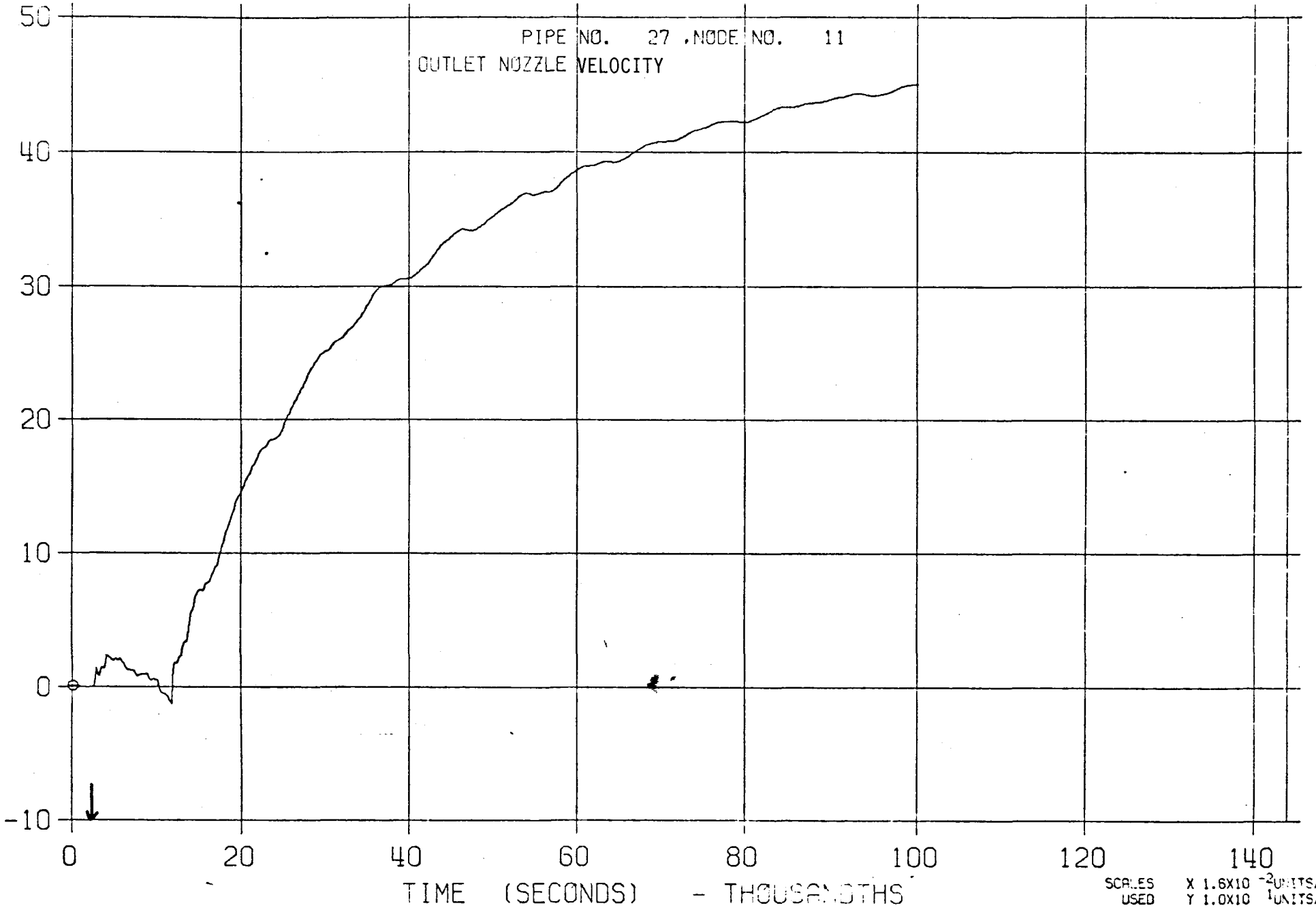

VELOCITY (FT/SEC)

38-L

FIGURE 38-L

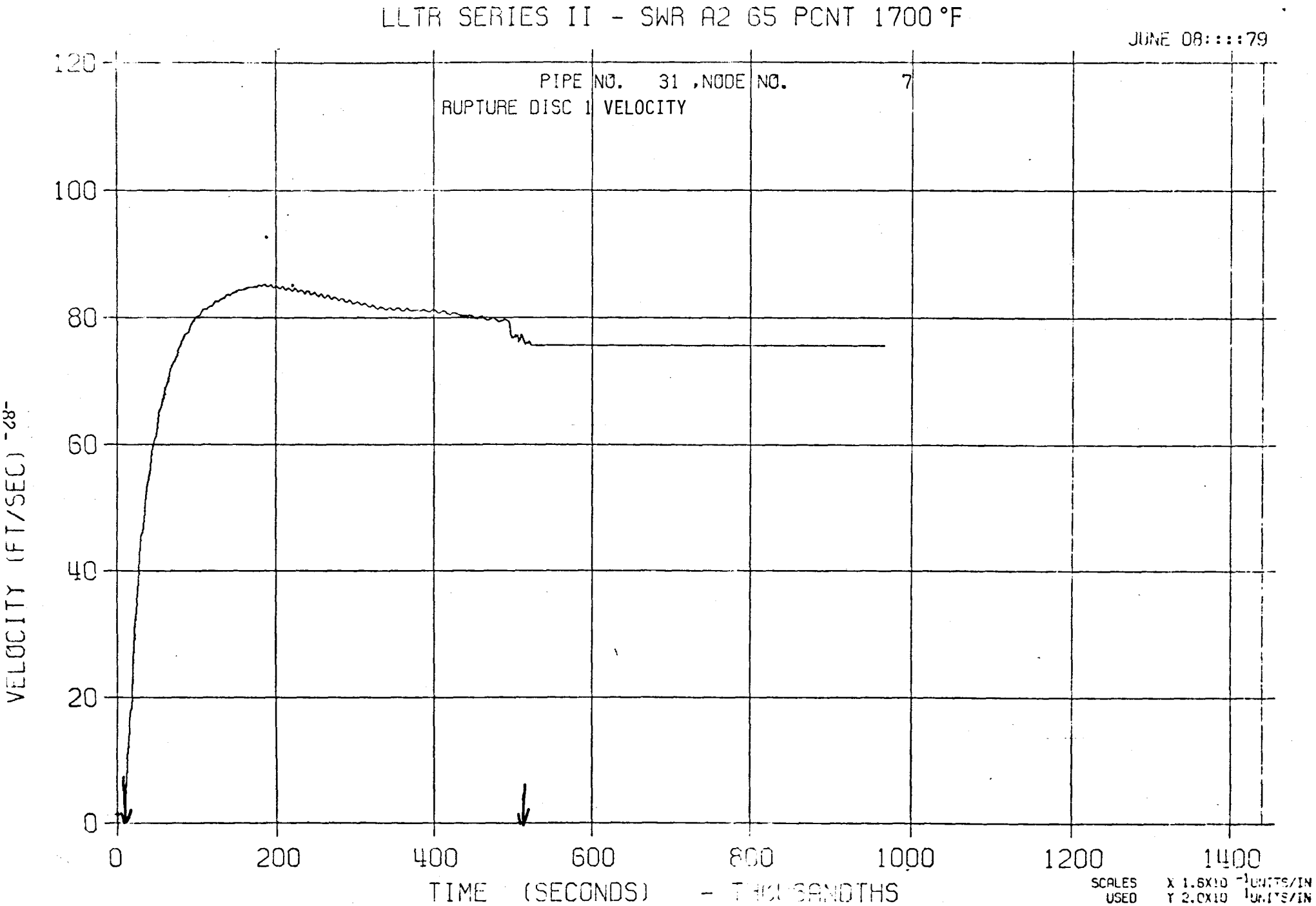

38-S

FIGURE 38-S

LLTR SERIES II - SWR A2 65 PCNT 1700 °F

JUNE 08, 1979

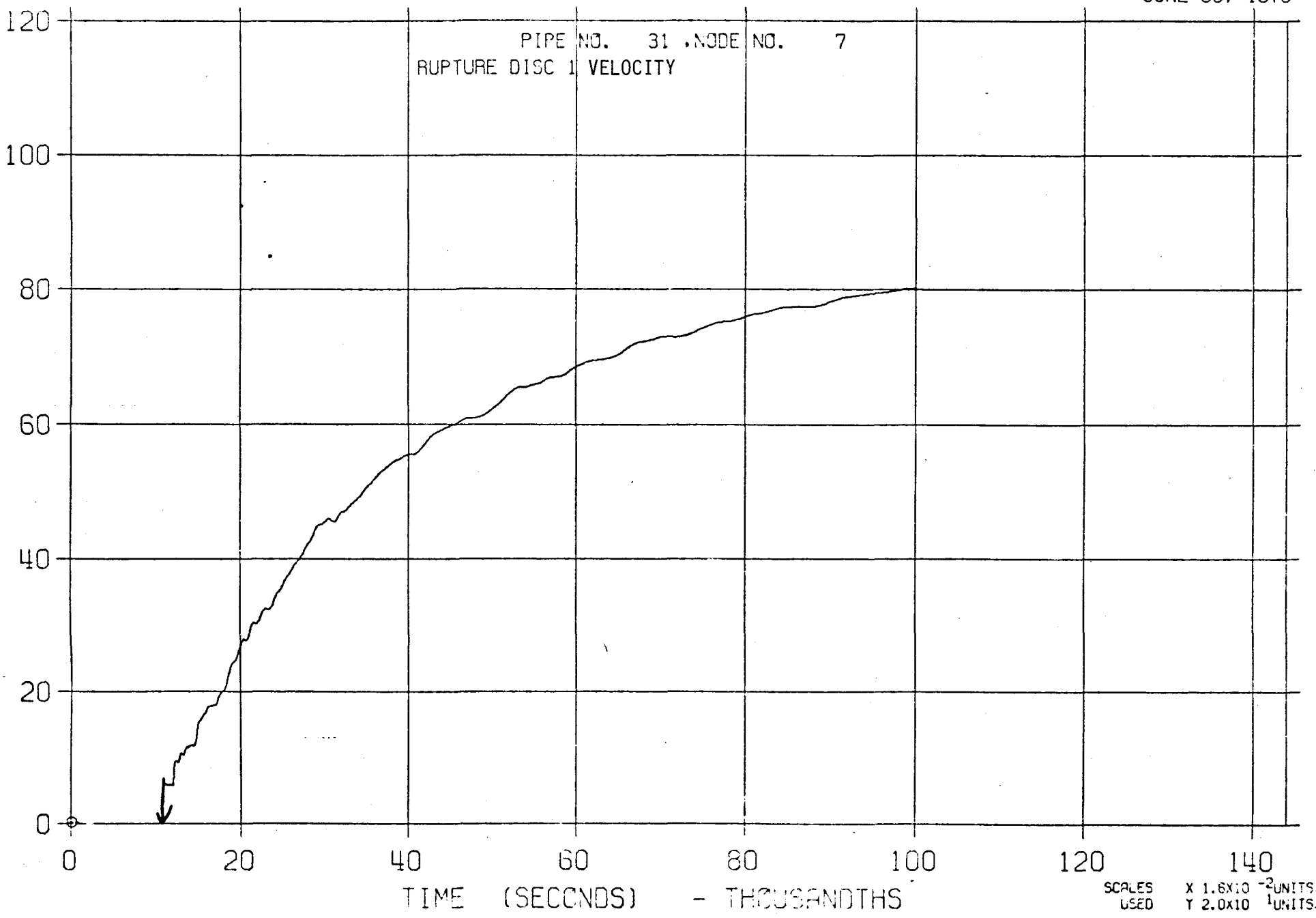

1

39-L

FIGURE 39-L

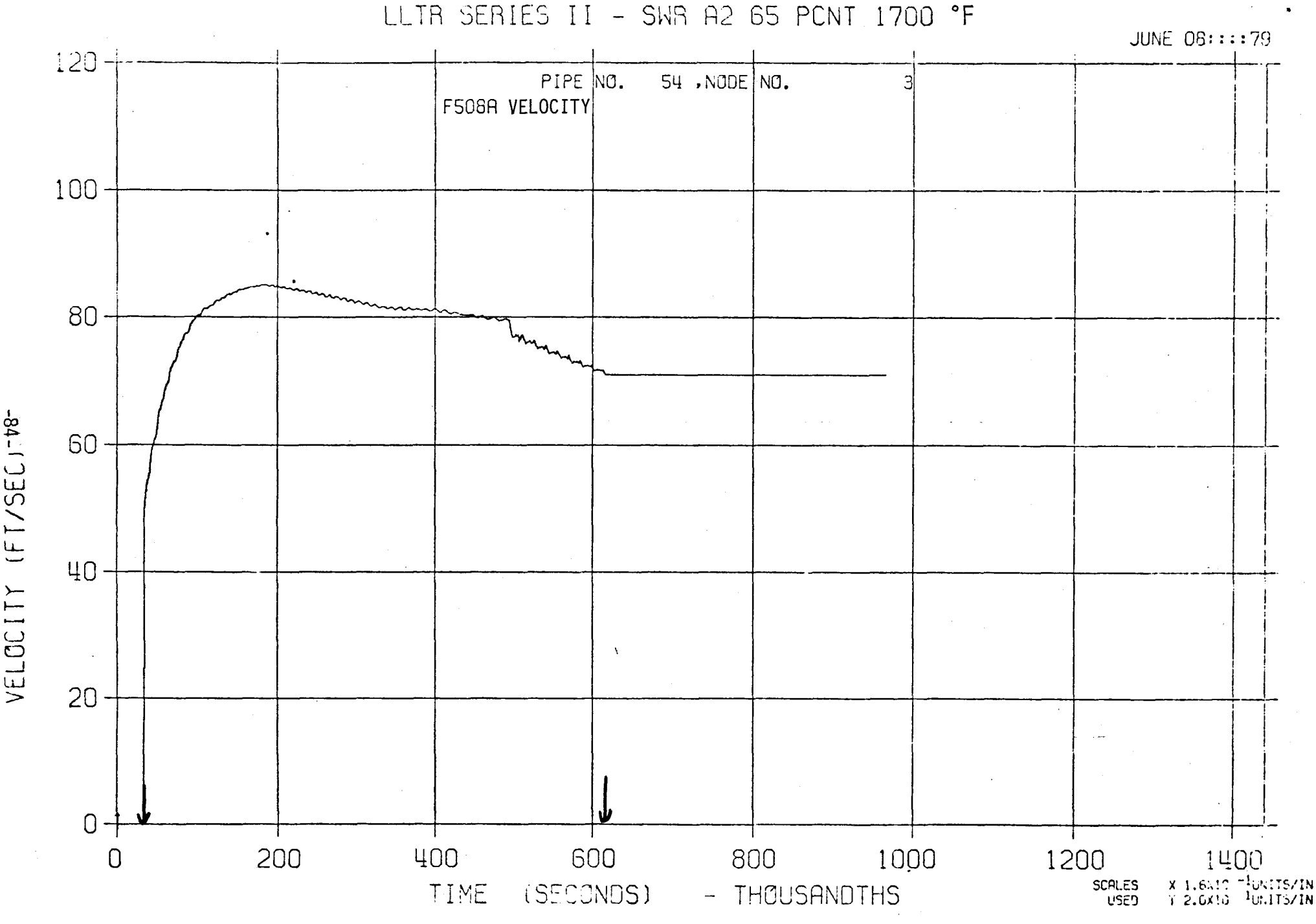

37-S

FIGURE 39-S

LLTR SERIES II - SNR A2 65 PCNT 1700 °F

JUNE 08, 1979

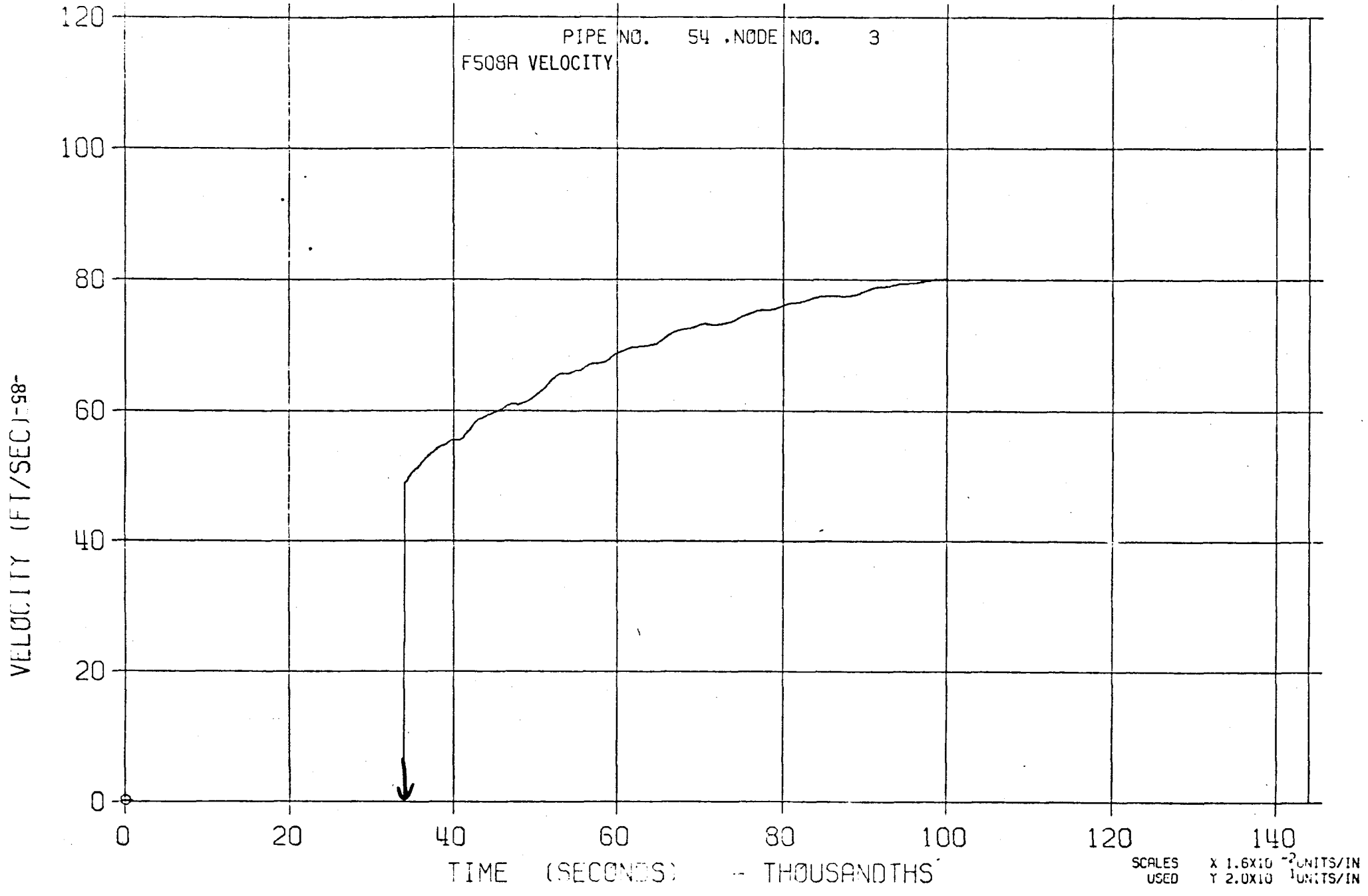

40-L

FIGURE 40-L

LLTR SERIES II - SWR A2 65 PCNT 1700 °F

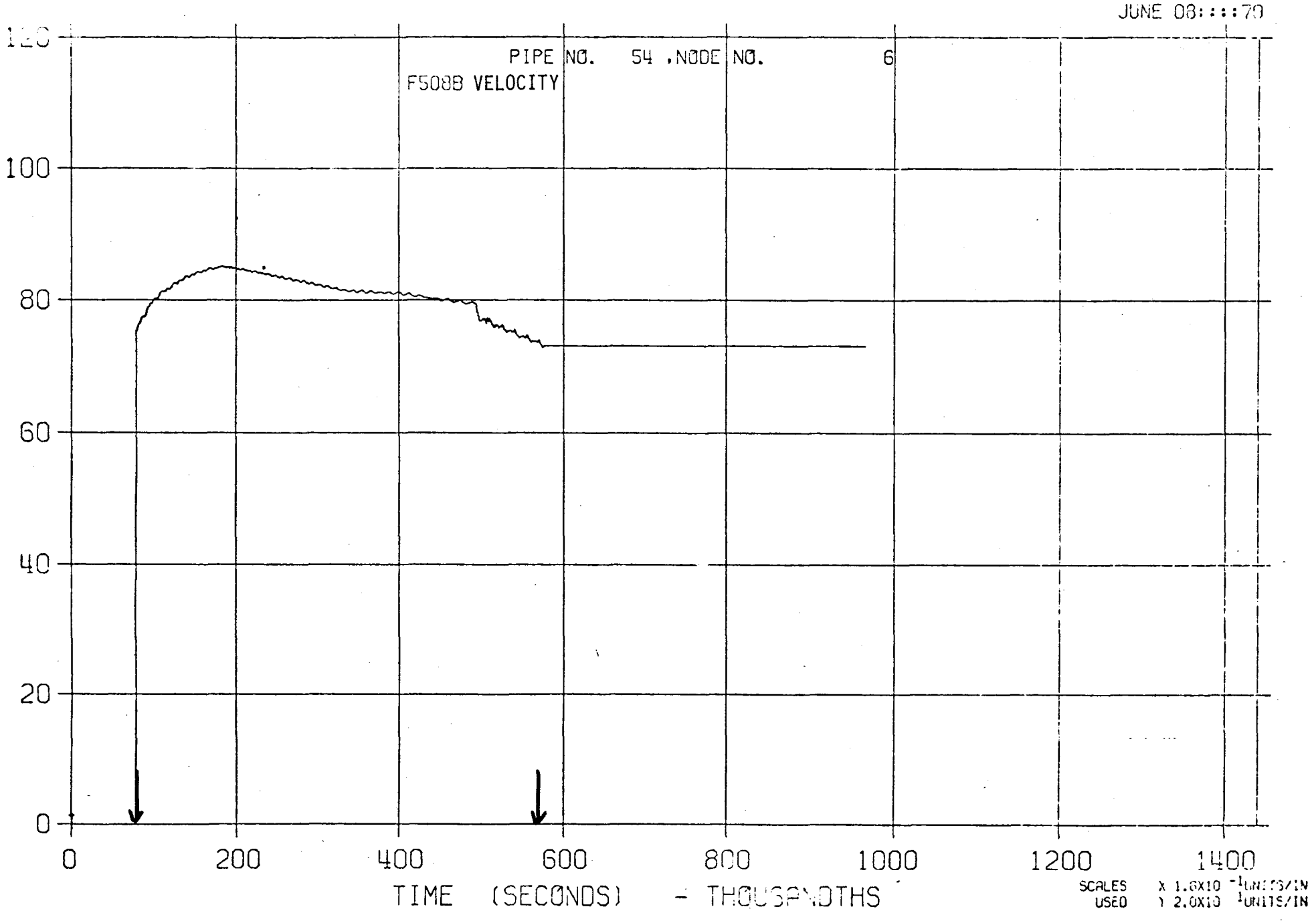

40-S

FIGURE 40-S

LLTR SERIES II - SWR A2 65 PCNT 1700 °F

JUNE 08, 1979

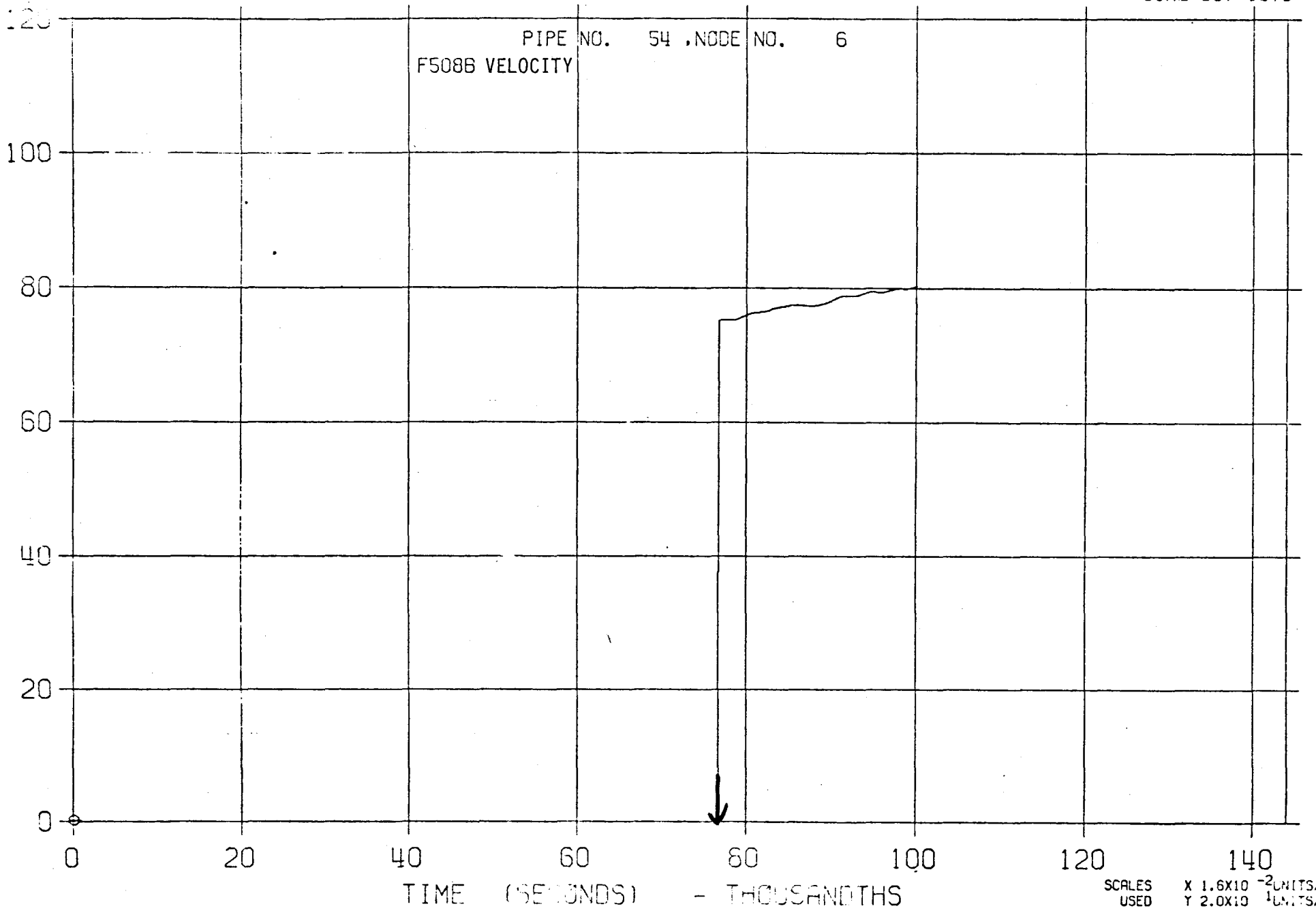

41-L

FIGURE 41-L

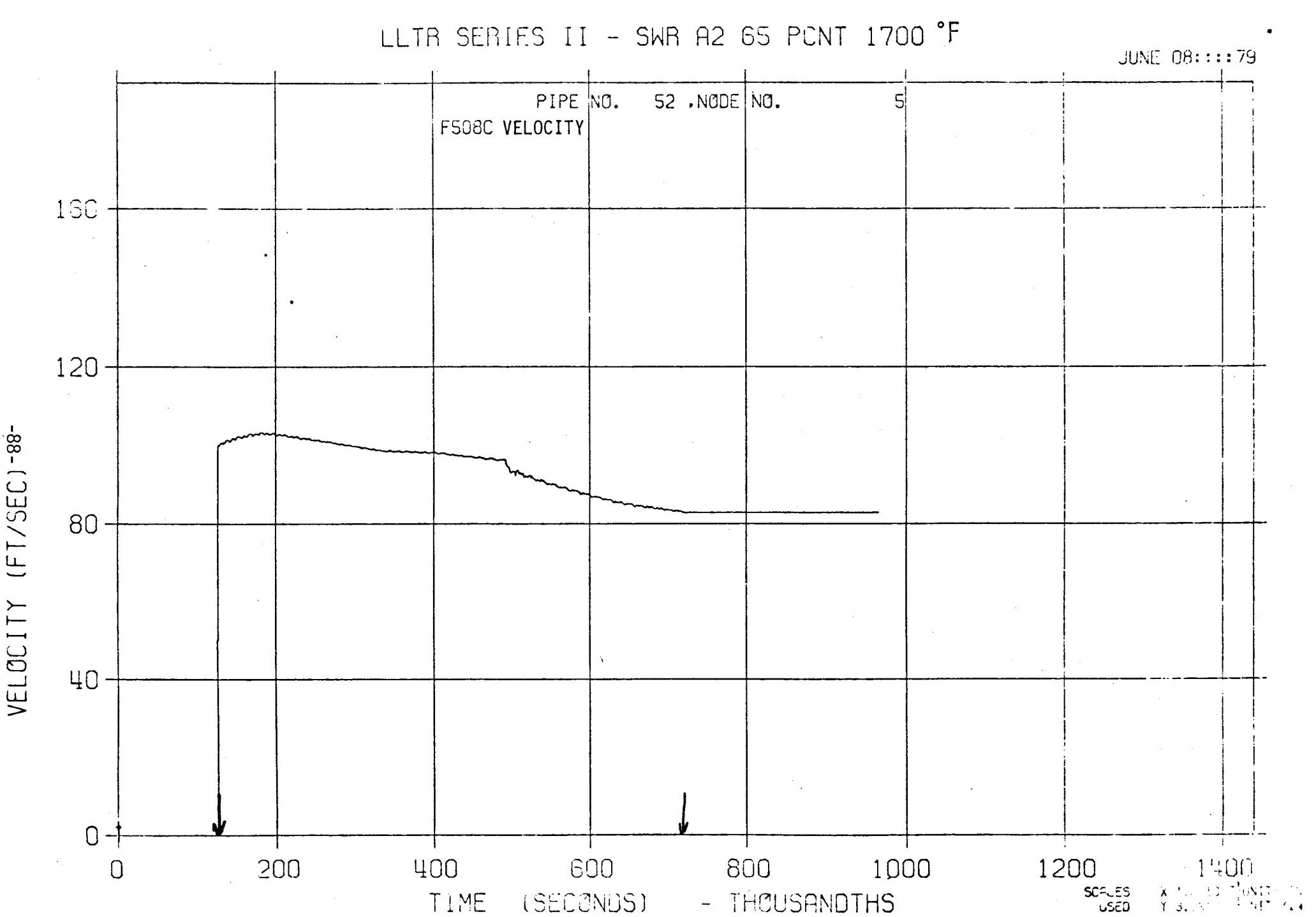

42-L

FIGURE 42-L

LLTR SERIES II - SWR A2 65 PCNT 1700 °F

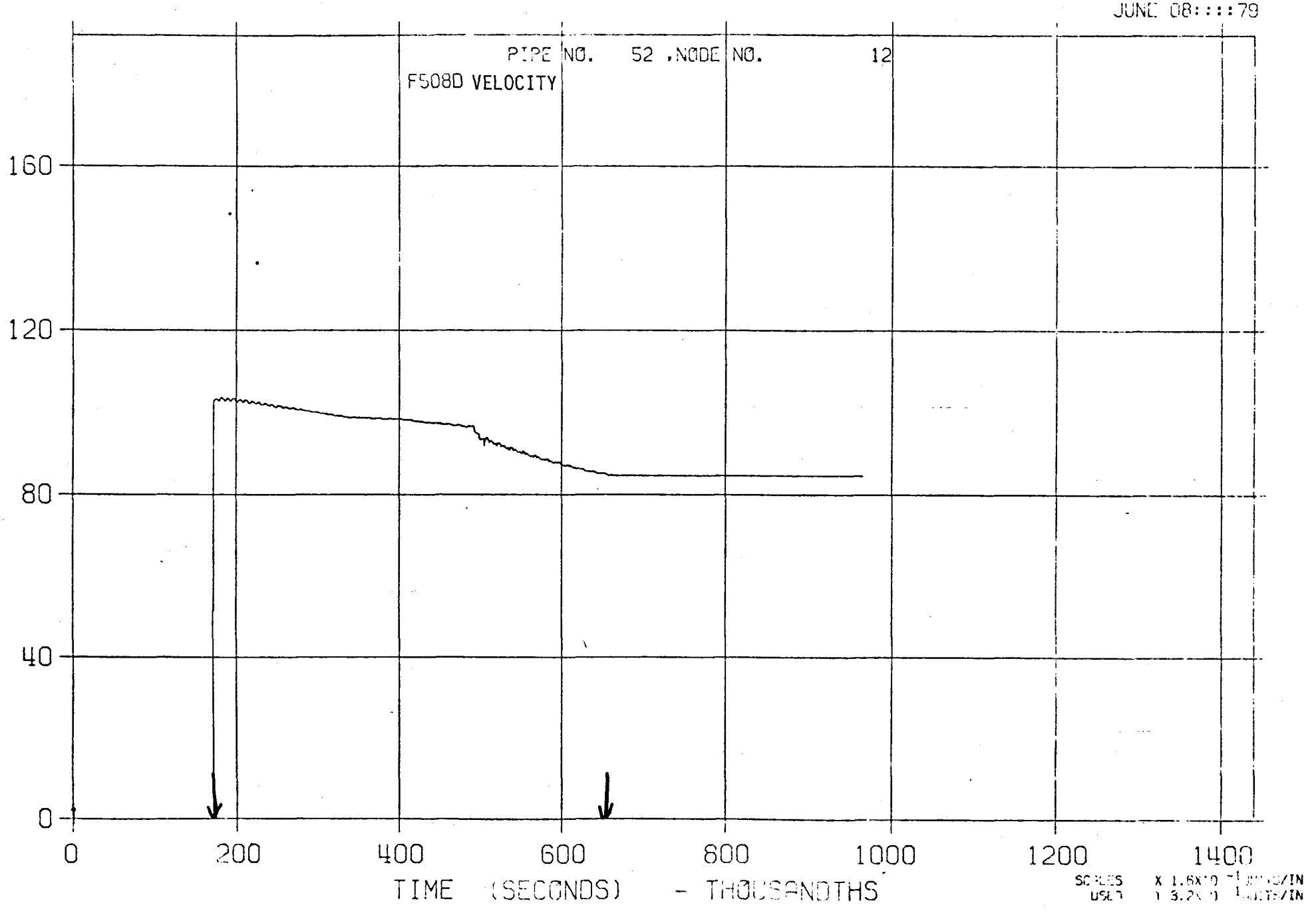

43-L

FIGURE 43-L

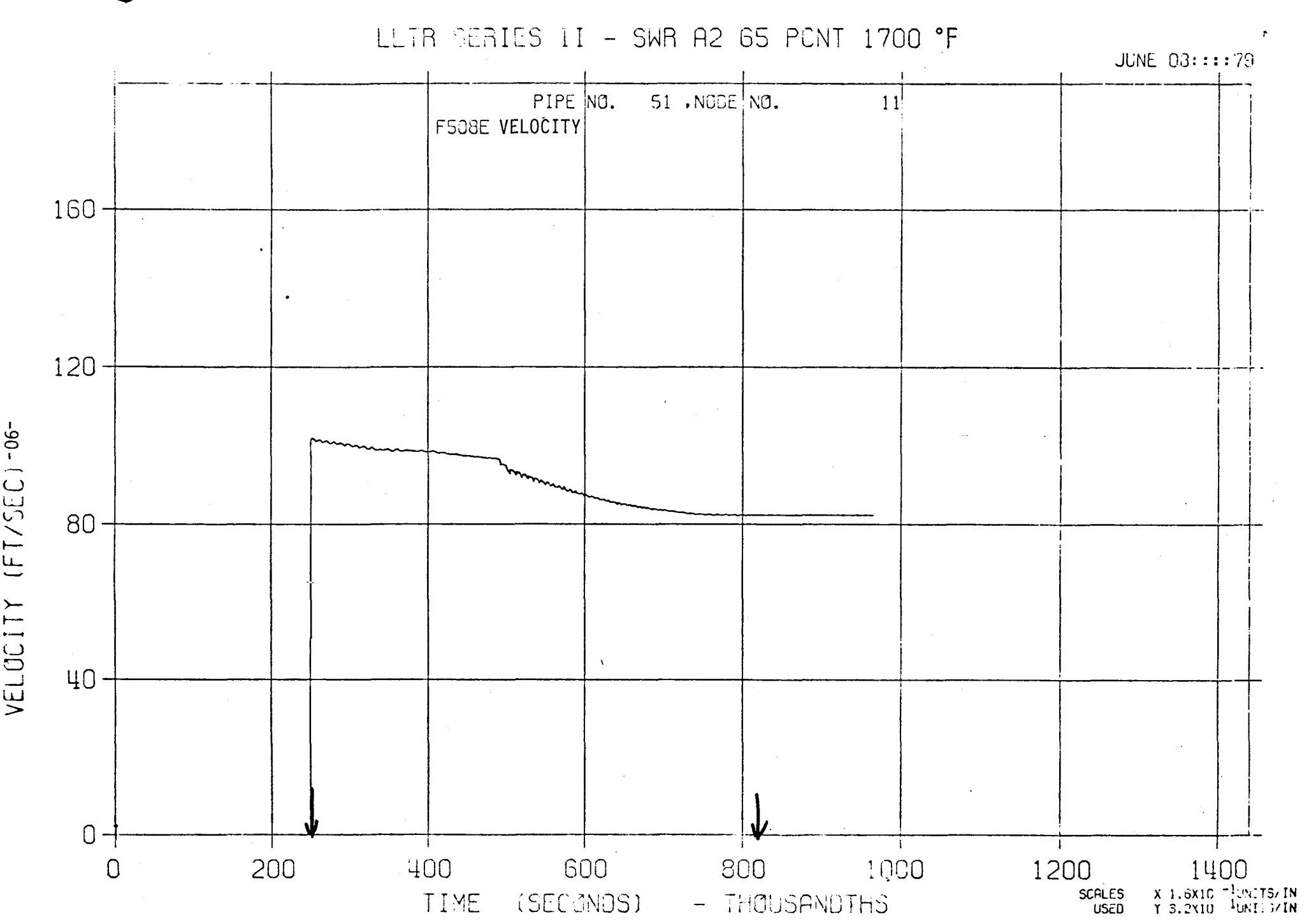

44-L

FIGURE 44-L

LLTR SERIES II - SWR A2 65 PCNT 1700 °F

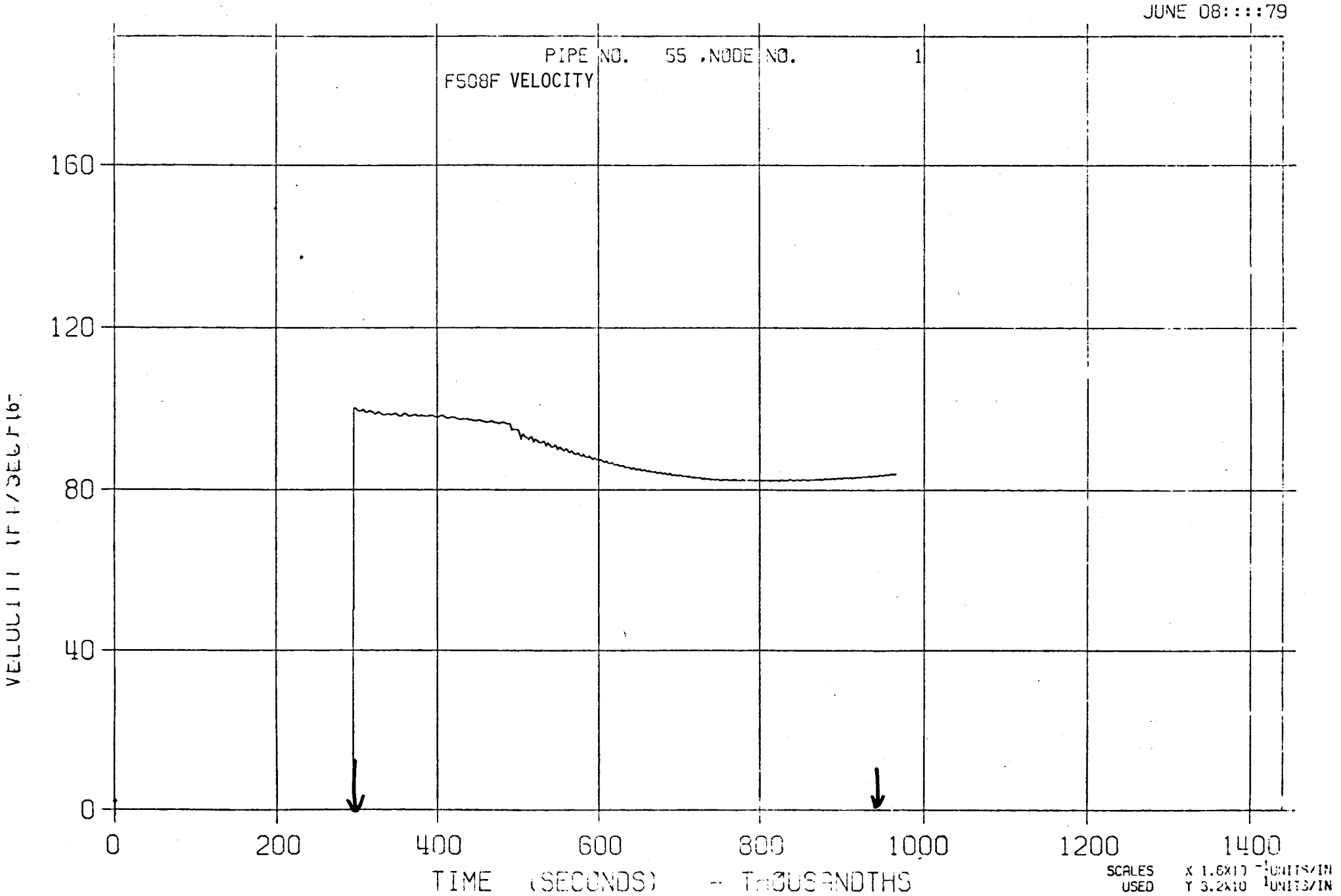

45-L

FIGURE 45-L

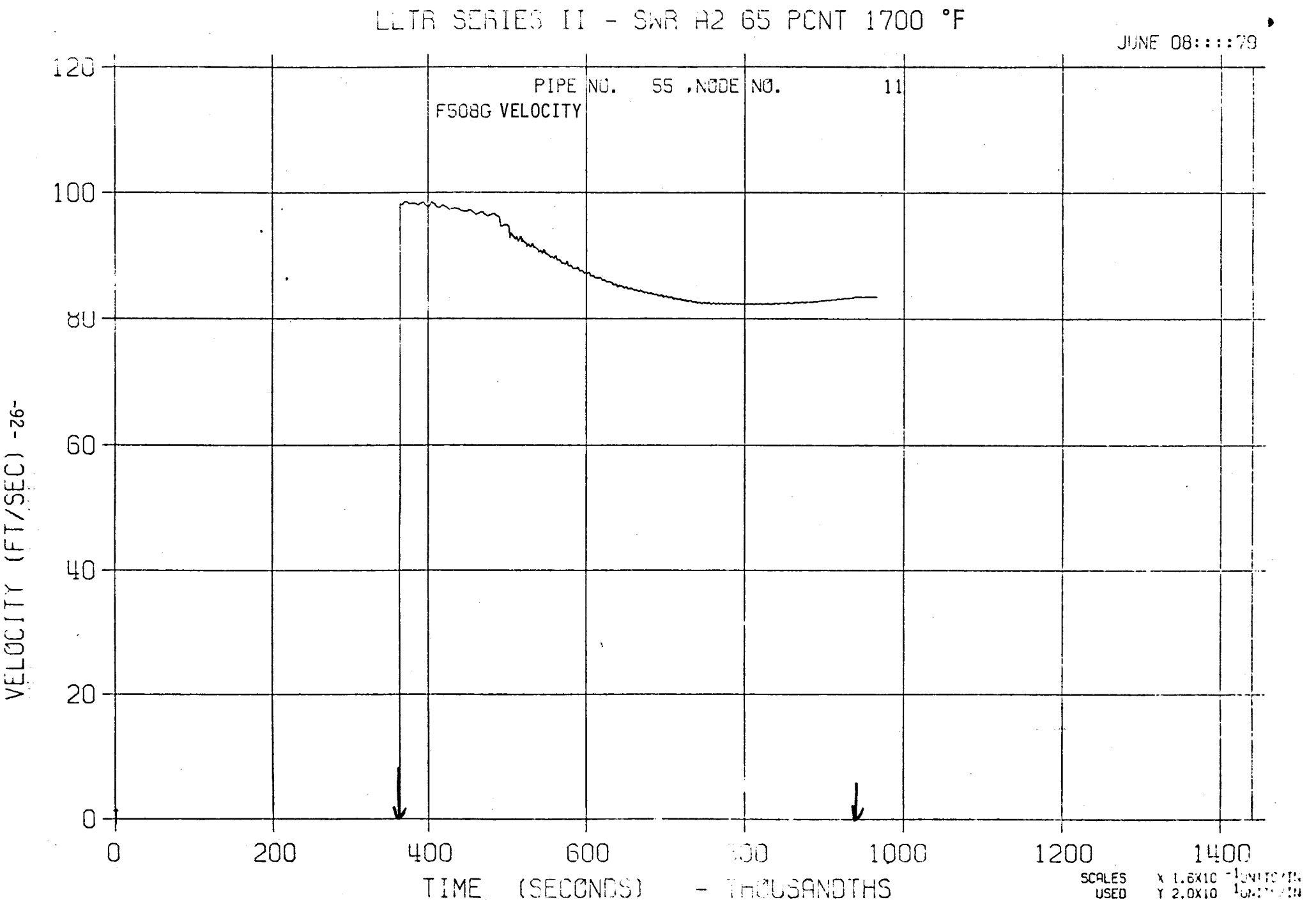

46-L

FIGURE 46-L